METHODOLOGIES FOR THE OPTIMAL DESIGN OF FIBRE-REINFORCED COMPOSITE STRUCTURES

RYAN ELLIOT SMITH

A THESIS SUBMITTED IN COMPLIANCE WITH THE REQUIREMENTS FOR THE MASTERS DEGREE IN TECHNOLOGY TO THE DEPARTMENT OF MECHANICAL ENGINEERING AT THE DURBAN INSTITUTE OF TECHNOLOGY

APPROVED FOR FINAL SUBMISSION

PROFESSOR MARK WALKER
SUPERVISOR

25/03/2003
DATE

DURBAN, SOUTH AFRICA
MARCH 2003

Declaration

I declare that this thesis is my own unaided work except where due acknowledgment is made to others. This thesis is being submitted for the Masters Degree in Technology to the Department of Mechanical Engineering at the Durban Institute of Technology, and has not been submitted previously for any other degree or examination.

Ryan Elliot Smith

25/03/2003
Date

Acknowledgments

I would like to thank Professor Mark Walker for the opportunity to study towards the qualification of Masters Degree in Technology. I am extremely grateful for his help and guidance during the course of this research. I would also like to thank David Jonson for his assistance in many aspects during this time, Pavel Tabakov for the informative discussions about genetic algorithms, and Marino Kekana for his help and advice.

Abstract

Composites have become important engineering materials, especially in the fields of automotive, aerospace and marine engineering. This is due to the high specific strength and stiffness properties they offer. At present, fibre-reinforced plastic (FRP) laminates are some of the most common types of composite used. They are produced in various forms with different structural properties. As with all engineering materials, there is the existence of both advantages and disadvantages. One of the main disadvantages is the expense involved in producing both the material and the finished product. The design time is also costly as the material has to be designed concurrently with the structure.

An advantage of using composite materials is that their properties can be tailored by varying the ply orientations. By optimising these angles, the ply thicknesses can often be minimised, thus lowering the mass of the structure. The effectiveness can also be increased in many applications by using these materials as facings in conjunction with low density core materials to form sandwich laminates. Sandwich constructions provide more tailoring opportunities than monolithics, and thus greater chance of satisfying design constraints.

To simplify the fabrication process, discrete ply angles are often used, although continuous ply angles are occasionally employed. Structures composed of composite materials often contain components which may be modelled as rectangular plates or cylindrical shells, for example. Modelling of components such as plates and shells can be useful as it is a means of simplifying elements of structures.

The work presented in this thesis focuses on methodologies for optimally designing fibre-reinforced laminated composite structures for minimum mass, deflection and cost, or maximum load-bearing capacity. Both discrete and continuous ply angles are considered. Search routines have been combined with different techniques (like the *Finite Element Method* in some cases) to assess fitness and produce powerful optimisation methodologies. The FEM is a powerful numerical method that has become synonymous with composite design and analysis due to the complex nature of the mathematics involved in modelling these materials.

This thesis discusses six new procedures for the optimisation of composite structures. The first four techniques are independent of structure, whereas the fifth and sixth procedures are specific to rectangular sandwich plates (in the fifth case) and cylindrical sandwich shells (in the sixth case). Examples are presented in each case, which demonstrate the technique.

Problem 1 is titled: *Design of fibre-reinforced laminated composite structures for a maximum combination of torque and inplane load.* It describes a procedure to select the optimal fibre orientations and determine the maximum load carrying capacity of symmetrically laminated fibre-reinforced composite structures. Cylindrical shells subject to combinations of torque and inplane forces are used to illustrate the methodology and are optimally designed for maximum strength. The finite element method, based on Mindlin plate and shell theory, is used in this application in conjunction with an optimisation routine in order to obtain the optimal designs. The methodology consists of two stages; the objective of the first is to maximise the strength of the cylindrical shells by determining the fibre orientations optimally while the objective of the second stage is to maximise the inplane compression loading subject to a failure criterion. The effect of different shell aspect ratios, wall thickness, layer numbers and boundary conditions on the results is investigated.

Problem 2 is titled: *The optimisation of laminated composite structures for minimum mass using the finite element method and genetic algorithms.* A method is described that combines genetic algorithms together with finite element analysis to design for manufacture and minimise the mass of fibre-reinforced symmetrically laminated structures with several design variables. The design constraint implemented here is based on the Tsai-Wu failure criterion. Composite rectangular plates with eight layers are used to demonstrate the technique. Thus, the four fibre orientations and laminae thicknesses are to be determined optimally. In addition, the fibre orientations and layer thicknesses must be selected from a set of discrete (and commercially available) values. Also, variations of the technique which enhance efficiency are mentioned.

Problem 3 is titled: *The multiobjective optimisation of laminated composite structures for both minimum mass and deflection using the finite element method and genetic algorithms.* It describes a methodology for using genetic algorithms with the finite element method

to minimise a weighted sum of the mass and deflection of fibre-reinforced structures with several design variables. The design constraint implemented here is based on the Tsai-Wu failure criterion. Symmetrically laminated composite rectangular plates with eight layers are used to demonstrate the technique. Thus, the four fibre orientations and laminae thicknesses are to be determined optimally by defining a design index comprising a weighted average of the objective functions and determining the minimum. In addition, the fibre orientations and layer thicknesses must be selected from a set of discrete values. Results are presented for different load distributions, and various combinations of clamped, simply supported and free boundary conditions. The effect of aspect ratio on the results is also investigated.

Problem 4 is titled: *A simple self-design methodology for laminated composite structures for minimum mass* and describes a simple procedure, based on the finite element method, for the self-design of laminated composite structures. The objective is to minimise the mass, and the design constraint implemented is based on the Tsai-Wu failure criterion. Suitable elements from the finite element model of the structure are deleted until all the elements that can be deleted without affecting the structural (or mesh) integrity have been. In addition, because the present study adopts a numerical approach, the effects of bending-twisting coupling are included. The finite element formulation used is based on Mindlin theory. Simple composite rectangular plates with one and eight layers are used to demonstrate the technique.

Problem 5 is titled: *The optimal design of composite sandwich panels for minimum cost via the selection of the best material combinations.* A procedure is described to select the best material combination and optimally design sandwich laminates with fibre-reinforced skins and low density cores for minimum cost. The objective of this optimisation is to minimise the laminate cost by selecting the skin and core material combination, layer thicknesses and skin fibre angles optimally, subject to load and mass constraints. As the optimisation problem contains a number of continuous (ply angles and thicknesses) and discrete (material combinations) design variables, a sequential solution procedure is devised in which the optimal variables are computed in different stages.

Problem 6 is titled: *The optimal design of composite sandwich cylindrical shells for minimum mass via selection of the best material combinations.* It described a methodology to select the best material combination and optimally design composite sandwich cylinders having fibre-reinforced skins and low density cores for minimum mass. The objective of this optimisation is to minimise the laminate mass by selecting the skin and core material combination, layer thicknesses and skin fibre angles optimally, subject to load and cost constraints. As the optimisation problem contains a number of continuous (ply angles and thicknesses) and discrete (material combinations) design variables, a sequential solution procedure is devised in which the optimal variables are computed in different stages.

List of Figures

List of Tables

Contents

Chapter 1

Introduction

1.1 Fibre-reinforced composites

A composite comprises two or more materials having characteristics that are derived from the individual constituents [1]. Depending on how these constituents are combined, the resulting composite may have the combined characteristics of the constituents or substantially different properties to the individual constituents. Occasionally the properties of the composite exceed those of the individual constituents themselves.

Fibre-reinforced composite materials are the most commonly used form of these constituent combinations. The *fibres* of such composites are usually strong and stiff and serve as the primary load-carrying constituent. The *matrix*, being a softer material that supports the fibres, serves to distribute the loads evenly across the fibres. The matrix also redistributes the loads from a broken fibre to the adjacent fibres in the material when fibres start failing under excessive loads. This property of the matrix contributes to one of the most important characteristics of fibrous composites; improved strength compared to the individual constituents.

A form of fibre-reinforced plastic composite comprises thin layers (or plies) of material completely bonded together to form composite *laminates*. The plies of a laminated composite material may be different single materials and may be composites themselves. These

fibrous composite layers can be placed so that the different layers have different characteristics. This type of composite is the most commonly encountered laminated material used in the design of high-performance structures.

1.1.1 Properties of laminated composites

Material orthotropy

Laminate properties (ie. strength, stiffness, thermal, etc.) depend on the form of the reinforcement [1]. The directional nature of the fibres introduce directional dependence to most of the properties. Materials whose properties are independent of direction are called *isotropic* materials. Conversely, those materials with different properties in different directions are called *anisotropic*. A special case of anisotropy is the existence of two mutually perpendicular planes of symmetry in the material properties. Such materials are referred to as *orthotropic*. Continuous fibre composites are orthotropic in nature and their properties are defined in the plane of the layer in two directions; the direction along the fibres and the direction perpendicular to the fibre orientation.

Stiffness is an example of an orthotropic material property of unidirectional fibre-reinforced laminates. Both the matrix and fibres are generally isotropic. However, when combined, the properties become anisotropic. Consider the fibre-reinforced material shown in Figure 1-1, loaded along either the fibre direction, x_1, or transverse to the fibre direction, x_2. When the material is loaded along the fibre direction, the deformation is small compared to the deformation under a load of the same magnitude applied in a direction perpendicular to the fibre. Since the amount of deformation under a specified load reflects the stiffness of a material, the unidirectional composite has different stiffness properties along these two mutually perpendicular directions. The stiffness of the laminate in the fibre direction is much closer to that of the fibre stiffness, E_f, and the stiffness perpendicular to the fibre direction is governed mostly by the properties of the matrix, E_m, G_m, and ν_m. Directions that are along the fibre and perpendicular to the fibre directions are commonly referred to as the *principal material directions* or *principal axes* of the material.

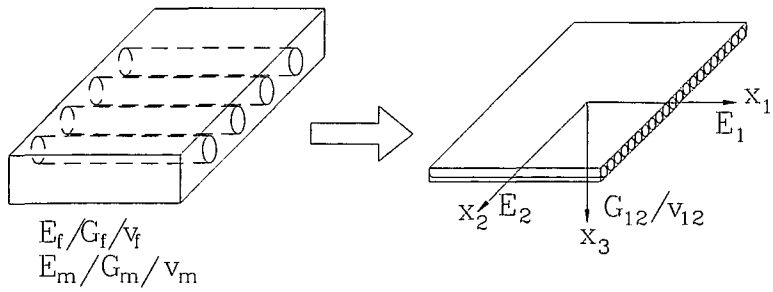

Figure 1-1: Elastic properties of a unidirectional fibre-reinforced composite layer

Four elastic stiffness properties, commonly referred to as the engineering constants, describe the mechanical properties of an orthotropic layer in its plane. These are two Young's moduli, E_1 and E_2, along the fibre and transverse to the fibre directions, respectively, and the shear modulus G_{12} and Poisson's ratio ν_{12} in the plane of the layer. These properties are related to the amount of fibre present in the composite layer. A quantity, V_f, referred to as the *fibre volume fraction*, is commonly used to measure the amount of fibre in a composite material. Typical stiffness properties of various unidirectional composite materials are given in Table 1.1, along with the fibre volume fraction. The properties are for cured laminates made up of T300/5208 Graphite/Epoxy, S-2 Glass/Epoxy and Kevlar 49/Epoxy [2], [4]. The Balsa and PVC properties are used as core materials.

Typical strength properties for T300/5208, S-2 Glass and Kevlar 49 (all with Epoxy), unidirectional laminae are given in Table 1.2.

Material	P_i	ρ (kg/m^3)	E_1 (GPa)	E_2 (GPa)	G_{12} (GPa)	ν	V_f
T300/5208	5	1600	181	10.34	7.17	0.28	0.70
S-2 Glass	1	2000	43.5	11.5	3.45	0.27	0.60
Kevlar 49	3.5	1460	76	5.5	2.3	0.34	0.60
D-100 Balsa	0.6	150	3.4	3.4	0.159	0.4	-
B-2.5 PVC	2.5	40	0.028	0.028	0.013	0.3	-

Table 1.1: Properties of the skin and core materials

Material	Longitudinal tensile X	Longitudinal compression X'	Transverse tensile Y	Transverse compression Y'	Shear
T300/5208	1500	1500	40	246	68
S-2 Glass	1062	610	31	118	72
Kevlar 49	1400	235	12	53	34

Table 1.2: Strengths of various unidirectional composites (MPa)

Laminate definition

The laminae discussed thus far are described according to a standard notation called the *stacking sequence* [1], which lists fibre orientations as being measured from the laminate reference axis. If the orientation is counterclockwise from the reference direction, it is considered positive. The standard stacking sequence lists orientations of the different layers, starting from the top of the laminate to the bottom. A laminate with N layers is represented as $[\theta_1/\theta_2/.../\theta_N]$ and is *symmetric* when the fibre orientations of the bottom half of the laminate are mirror images of the fibre orientations above the midplane of the laminate; for example, $[-45/30/0/45/45/0/30/-45]$. Symmetric laminates with an even number of layers are represented by the portion of the stacking sequence above the laminate midplane followed by the subscript 's' after the closing bracket, $[-45/30/0/45]_s$. If the layers within the brackets are repeated, the number of repetitions can also be placed after the bracket before the subscript 's'. That is the laminate [45/0/45/0/0/45/0/45] can be represented as $[45/0]_{2s}$. A laminate is said to be *anti-symmetric* if the magnitude of the ply orientation angle below the laminate midplane is a mirror image of the ply orientations above the midplane with the signs reversed. For example, $[45/-45/45/-45]$ is an anti-symmetric laminate. It can be desirable to place a negative θ orientation for every positive θ orientation. These laminates are called *balanced laminates.* Pairs of positive and negative orientations do not have to be placed adjacent to one another.

Several unique cases of laminate stacking sequence definitions can also be used. Laminates that have alternating orientations of 0^o and 90^o plies are known as *cross-ply laminates.* Examples of cross-ply laminates include [0/90], $[0/90]_s$, and $[0_3/90]_s$. Laminates consisting of an equal number of equal-thickness layers at $+\theta$ and $-\theta$ fibre orientations are known as *angle-ply laminates.* For example, a 30^o symmetric angle-ply laminate could be $[30/-$

$30/30/-30]_s$. All the layers of an angle-ply laminate have the same fibre orientation angle, say $\theta = \alpha$, with an alternating sign. A very important and common class of laminates is called *quasi-isotropic* because the inplane effective elastic response of this class of laminates is isotropic. All symmetric laminates with $2N$ equal-thickness layers ($N \geq 3$) and N equal angles between fibre orientations (Figure 1-2) are quasi-isotropic. For N equal angles of $\Delta\theta$ between fibre orientations:

$$\Delta\theta = \frac{\pi}{N} \tag{1.1}$$

Examples of quasi-isotropic laminates are those with angles $\Delta\theta$ between fibres of 60^o ($\pi/3$), 45^o ($\pi/4$), 36^o ($\pi/5$), 30^o ($\pi/6$), etc.

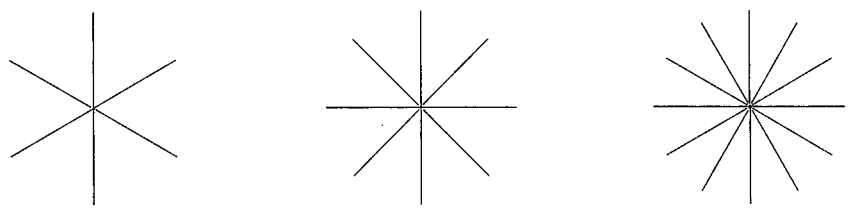

Figure 1-2: Quasi-isotropic fibre orientations

1.1.2 Mechanics of laminated composite materials

To design a structure that will meet the requirements of certain response quantities such as displacements, stresses or buckling loads, the response for a specific loading must be determined. Elastic properties form the relation between stresses and strains and are the fundamental quantities that govern the material response. Quantities such as deformations, stresses and buckling loads depend on elastic properties such as the elastic modulus, shear modulus and Poisson's ratio. In designing structures made up of monolithic materials these properties are normally given and are not included among the set of parameters that

the designer varies in order to improve the performance of the structure. For composite materials, part of the effort is to design the elastic properties of the laminate.

Thin structures made from thin layers of material can carry loads through two different types of mechanisms. The first involves stretching or compressing the layers in their own plane and is referred to as *membrane action*. The second mechanism involves bending of the layers.

Orthotropic layers

Individual layers have directional properties with planes of symmetry that are not necessarily oriented along the x - y axes of the laminate [1]. For a unidirectional fibre-reinforced lamina there are two perpendicular planes of symmetry that define two principal axes of material properties (see Figure 1-3). These principal axes correspond to the direction of the fibres and a direction transverse to the fibres and are denoted by subscripts '1' and '2', respectively. Such layers are referred to as orthotropic and the $1-2$ axes are the principle axes of orthotropy. When the principal axes of orthotropy are oriented at an angle, θ, with respect to the axes of the laminate (an off-axis layer), the laminar behaviour will appear to have the characteristics of an anisotropic material.

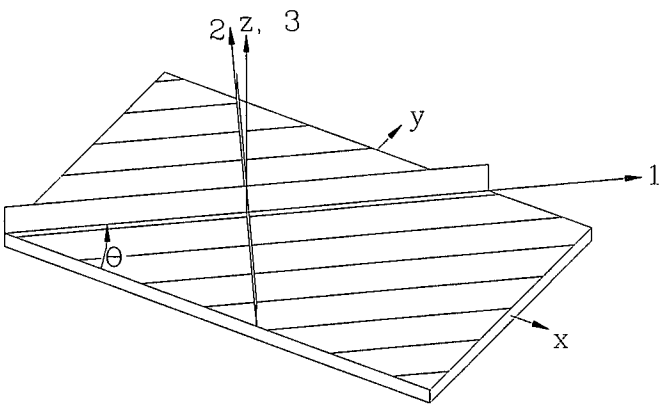

Figure 1-3: Planes of material symmetry for an orthotropic layer

The equations that govern fibre-reinforced laminates are as follows:

$$\begin{aligned} Q_{11} &= \frac{E_1}{1-\nu_{12}\nu_{21}}, \quad Q_{22} = \frac{E_2}{1-\nu_{12}\nu_{21}} \\ Q_{12} &= \frac{\nu_{12}E_2}{1-\nu_{12}\nu_{21}} = \frac{\nu_{21}E_1}{1-\nu_{12}\nu_{21}} \\ Q_{66} &= G_{12} \end{aligned} \tag{1.2}$$

and the Poisson's ratios are:

$$\frac{\nu_{21}}{E_2} = \frac{\nu_{12}}{E_1} \tag{1.3}$$

After much mathematical manipulation, a material stiffness matrix can be found (Eqn. 1.4):

$$\begin{Bmatrix} \sigma_1 \\ \sigma_2 \\ \tau_{12} \end{Bmatrix} = \begin{bmatrix} Q_{11} & Q_{12} & 0 \\ Q_{21} & Q_{22} & 0 \\ 0 & 0 & Q_{66} \end{bmatrix} \begin{Bmatrix} \varepsilon_1 \\ \varepsilon_2 \\ \gamma_{12} \end{Bmatrix} \tag{1.4}$$

In matrix notation Eqn. 1.4 can be represented as:

$$\sigma = Q\varepsilon \tag{1.5}$$

where the matrix Q is commonly referred to as the *reduced material stiffness matrix.* The transformed reduced stiffnesses $\overline{Q}_{ij}$ are related to the Q_{ij} by

$$\begin{aligned} \overline{Q}_{11} &= Q_{11}\cos^4\theta + 2(Q_{12}+2Q_{66})\sin^2\theta\cos^2\theta + Q_{22}\sin^4\theta \\ \overline{Q}_{12} &= (Q_{11}+Q_{22}-4Q_{66})\cos^2\theta\sin^2\theta + Q_{12}(\sin^4\theta+\cos^4\theta) \\ \overline{Q}_{22} &= Q_{11}\sin^4\theta + 2(Q_{12}+2Q_{66})\sin^2\theta\cos^2\theta + Q_{22}\cos^4\theta \end{aligned} \tag{1.6}$$

$$
\begin{aligned}
\overline{Q}_{16} &= (Q_{11} - Q_{12} - 2Q_{66}) \sin\theta \cos^3\theta + (Q_{12} - Q_{22} + 2Q_{66}) \sin^3\theta \cos\theta \\
\overline{Q}_{26} &= (Q_{11} - Q_{12} - 2Q_{66}) \sin^3\theta \cos\theta + (Q_{12} - Q_{22} + 2Q_{66}) \sin\theta \cos^3\theta \\
\overline{Q}_{66} &= (Q_{11} + Q_{22} - 2Q_{12} - 2Q_{66}) \sin^2\theta \cos^2\theta + Q_{66}(\sin^4\theta + \cos^4\theta)
\end{aligned}
$$

These equations can be put into a simpler form by using trigonometric identities to replace the terms with powers of sines and cosines of the fibre orientation angle θ with the sine and cosine of multiple angles 2θ and 4θ. Tsai and Pagano [5] defined the following material properties:

$$
\begin{aligned}
U_1 &= \frac{1}{8}(3Q_{11} + 3Q_{22} + 2Q_{12} + 4Q_{66}) \\
U_2 &= \frac{1}{2}(Q_{11} - Q_{22}) \\
U_3 &= \frac{1}{8}(Q_{11} + Q_{22} - 2Q_{12} - 4Q_{66}) \\
U_4 &= \frac{1}{8}(Q_{11} + Q_{22} + 6Q_{12} - 4Q_{66}) \\
U_5 &= \frac{1}{8}(Q_{11} + Q_{22} - 2Q_{12} + 4Q_{66})
\end{aligned}
\tag{1.7}
$$

which yield a simpler form of the transformed reduced material stiffness matrix as

$$
\begin{aligned}
\overline{Q}_{11} &= U_1 + U_2 \cos 2\theta + U_3 \cos 4\theta \\
\overline{Q}_{12} &= U_4 - U_3 \cos 4\theta \\
\overline{Q}_{22} &= U_1 - U_2 \cos 2\theta + U_3 \cos 4\theta \\
\overline{Q}_{16} &= \frac{1}{2}U_2 \sin 2\theta + U_3 \sin 4\theta \\
\overline{Q}_{26} &= \frac{1}{2}U_2 \sin 2\theta - U_3 \sin 4\theta \\
\overline{Q}_{66} &= U_5 - U_3 \cos 4\theta
\end{aligned}
\tag{1.8}
$$

Both the U's and the Q's are independent of the ply orientation, but the $\overline{Q}$'s are dependent on ply orientation for orthotropic materials. An advantage of the form of the reduced

stiffnesses in Eqn. 1.8 is the constant parts of $\overline{Q}_{11}$, $\overline{Q}_{12}$, $\overline{Q}_{22}$, and $\overline{Q}_{66}$ given in terms of the U_1, U_4, and U_5 which do not depend on the ply orientation. Based on this feature, the U's are sometimes called the *material invariants*.

1.1.3 Laminate theories for monolithic laminates

Classical Laminate Theory

A monolithic laminate is one in which no core material exists. Classical Laminate Theory (CLT) provides a simple and direct technique for calculating stresses and strains in laminates. It is not very accurate, though, as it does not satisfy elasticity equations at every point. It applies to a section of plate over which both forces and moments are assumed constant, and in which through-thickness shear strain is ignored [6]. Therefore, only in-plane direct and shear stresses are considered. CLT is equivalent to beam theory, which only considers a pure moment loading, which results in a direct stress acting parallel to the beam's longitudinal axis. Shear strains are ignored.

In practice, beams are usually subjected to bending moments which vary along their length. The resultant direct stresses cause shear stresses, and can be calculated from equilibrium equations. Even in these circumstances shear strains can usually be ignored as they only have a significant effect on beam deflections when the beam is considered short. For a laminate, such shear stresses are referred to as interlaminar shear, and can give rise to interlaminar failure or delamination.

Plate equations can be modified to include varying moments and through-thickness shear strains. The plate constitutive equations are modified to account for the through-thickness shear resultants by including two additional terms in the **A** matrix.

The inclusion of shear strains is appropriate for thick isotropic plates, and also for thick composite plates. The latter will generally have a low through-thickness shear modulus, thus making the inclusion of such shear strains advisable for typical composites, even if of moderate thickness.

Edges The limitations of CLT imply that the plate is infinitely long and wide (ie. the theory ignores edges). In many practical situations, laminates, such as test coupons, have edges. The stresses acting at a plate edge can be seen in Figure 1-4. A simple example is the free edge of a cross-ply laminate. Due to the mismatch in ply Poisson's ratio $(90^o/0^o)_s$ is preferred to $(0^o/90^o)_s$ as the latter produces tensile through-thickness stresses. A problem in analysing these situations is that the high stresses occur within one or two plate thicknesses from the edge. Solutions can also indicate singularities in finite element models.

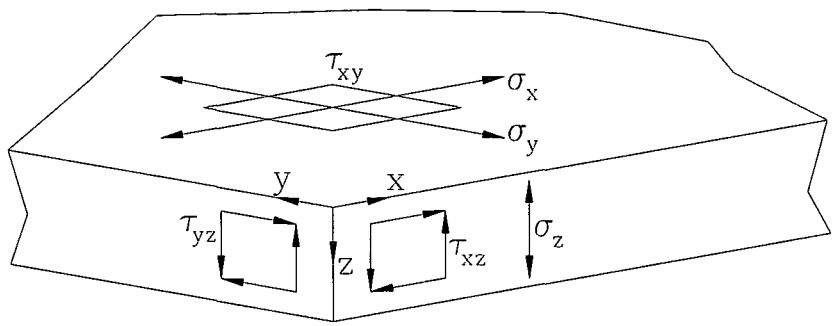

Figure 1-4: Stresses at laminate edge in the z-direction

Assumptions of Lamination Theory The following assumptions are fundamental to laminate theory [4]:

1. The laminae are perfectly bonded.

2. Each layer is a homogenous material with known effective properties.

3. Individual layer properties can be isotropic, orthotropic or transversely isotropic.

4. Each layer is in a state of plane stress.

5. The laminate deforms according to the following Kirchhoff assumptions for bending and stretching of thin plates:

5a. Normals to the midplane remain straight and normal to the deformed midplane after deformation.

5b. Normals to the midplane do not change length.

Laminates of orthotropic plies CLT assumes that N orthotropic layers are perfectly bonded together with an infinitely thin bond-line and the inplane deformations across the bond-line are continuous [1]. The mechanical behaviour of laminated plates is characterised by the following relationship:

$$\left\{ \begin{array}{c} N \\ M \end{array} \right\} = \left[\begin{array}{cc} A & B \\ B & D \end{array} \right] \left\{ \begin{array}{c} \varepsilon^o \\ K \end{array} \right\} \tag{1.9}$$

where $N^T = (N_x, N_y, N_{xy})$ is the vector of inplane force resultants; $M^T = (M_x, M_y, M_{xy})$ is the vector of moment resultants; $\varepsilon^o = \left(\varepsilon^o_x, \varepsilon^o_y, \varepsilon^o_{xy}\right)$ and $K = (K_x, K_y, K_{xy})$ are the midplane strains and plate curvatures, respectively. Using CLT u, v and w being the midplane displacements in the x, y and z directions:

$$\begin{array}{ll} \varepsilon^o_x = u_{,x} & K = -w_{,xx} \\ \varepsilon^o_y = v_{,y} & K_y = -w_{,yy} \\ \varepsilon^o_{xy} = u_{,y} + v_{,x} & K_{xy} = -2w_{,xy} \end{array} \tag{1.10}$$

Equation 1.11 represents the *inplane stiffness matrix*, Eqn. 1.12 the *coupling* or *bending-extension stiffness matrix*, and Eqn. 1.13 represents the *material flexural stiffness matrix.*

$$A_{ij} = \sum_{k=1}^{N} \left(\overline{Q}_{ij}\right)_{(k)} (z_k - z_{k-1}) \tag{1.11}$$

$$B_{ij} = \frac{1}{2} \sum_{k=1}^{N} \left(\overline{Q}_{ij}\right)_{(k)} \left(z_k^2 - z_{k-1}^2\right) \tag{1.12}$$

$$D_{ij} = \frac{1}{3} \sum_{k=1}^{N} \left(\overline{Q}_{ij}\right)_{(k)} \left(z_k^3 - z_{k-1}^3\right) \tag{1.13}$$

with $i = 1, 2, 6$ and $j = 1, 2, 6$ and where the $\overline{Q}^{ij}|_k$ are the elements of the reduced stiffness

matrix of layer k and z_k the coordinates of the interface between ply k and ply $k+1$.

In applications where symmetric laminates are used, the B matrix representing the bending-extension coupling vanishes and:

$$\{N\} = [A]\{\varepsilon^o\} \tag{1.14}$$

$$\{M\} = [D]\{K\} \tag{1.15}$$

Elastic properties of composite laminates The inplane, bending and coupling stiffness matrices are sufficient to describe the elastic response characteristics of a laminate under combined inplane and bending loads [1]. Due to the complex couplings that exist between the different deformation modes for laminates, it is not possible to associate the stiffness properties of a laminate with quantities that are similar to the classical elastic material properties.

Unless the lamination sequence is symmetric with respect to the laminate midplane, there exists a coupling ($B \neq 0$) between inplane and bending deformations. A more intricate coupling is due to the B_{16} and B_{26} terms. These terms may induce twisting deformations in laminates even if there is no applied twisting action. Laminates loaded by inplane loads inducing uniform inplane stress states will experience twisting curvatures. The B_{16} and B_{26} terms are often referred to as the *extension-twisting coupling* terms and are caused by the existence of off-axis layers that are not symmetric with respect to the laminate midplane.

When restricted to symmetric stacking sequences, vanishing of the **B** matrix eliminates coupling between the inplane and out-of-plane responses of a laminate. In this case, the midplane strains are only related to the inplane stress resultants and the curvatures to the moment resultants.

For the bending stiffness matrix, the stiffness terms D_{16} and D_{26} couple the moment resultants M_x and M_y with the twisting curvature. The resulting effect is the tendency of the

laminate to curl under applied uniform bending moments. Thus, the D_{16} and D_{26} terms are referred to as the *bending-twisting coupling* terms. These terms exist for all laminates that have layers with off-axis orientations. Their relative magnitude compared to the other bending stiffness terms may be made small by manipulating the stacking sequence, but unless the off-axis layers are removed from the laminate they will have a finite value.

Similarly, the existence of the A_{16} and A_{26} terms in the inplane stiffness matrix yields a coupling behaviour termed *shear-extension coupling.* The net effect of these terms on the laminate response is the induction of shearing deformation under inplane normal stress resultants N_x and N_y. Although the primary reason for the existence of these terms is the presence of layers with off-axis fibre orientations, unlike the bending-twisting terms, these terms may be eliminated quite easily by enforcing a balanced condition of the off-axis layers. Balanced laminates have to be placed adjacent to each other, but can be at separate through-thickness locations. However, the distance between them has a direct influence on the D_{16} and D_{26} terms. Balanced laminates with adjacent layers of plus and minus θ orientations will have smaller bending-twisting terms compared to ones that have layers with the same orientations grouped together and separated from the layers with negative angles.

In cross-ply laminates the D_{16} and D_{26} terms are zero since the $\overline{Q}_{16}$ and $\overline{Q}_{26}$ terms are zero. The A_{16} and A_{26} terms are zero for angle ply laminates.

Mindlin Plate theory

To account for transverse shear deformation, the assumption that right angles in a cross-section are preserved must be abandoned [7]. This means that planes initially normal to the midsurface may experience rotations different from rotations of the midsurface itself. Thus the differential element in Figure 1-5 has the deformations depicted in Figure 1-6, where θ_x and θ_y are rotation components of a line initially normal to the midsurface.

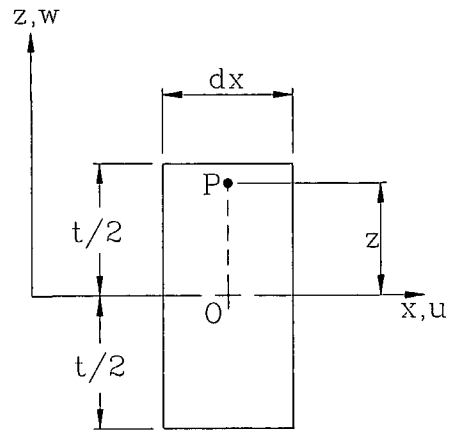

Figure 1-5: Differential slice of a plate of thickness t before loading

Combining these displacements with Eqns 1.16

$$\varepsilon_x = \frac{\partial u}{\partial x} \qquad \varepsilon_y = \frac{\partial v}{\partial y} \qquad \gamma_{xy} = \frac{\partial u}{\partial y} + \frac{\partial v}{\partial x} \tag{1.16}$$

Eqns 1.17 are obtained

$$\begin{array}{llll} u = z\theta_y & \varepsilon_x = z\frac{\partial \theta_y}{\partial x} & \gamma_{xy} = z\left(\frac{\partial \theta_y}{\partial y} - \frac{\partial \theta_x}{\partial x}\right) \\ v = -z\theta_x & \varepsilon_y = -z\frac{\partial \theta_x}{\partial y} & \gamma_{yz} = \frac{\partial w}{\partial y} - \theta_x \\ & & \gamma_{zx} = \frac{\partial w}{\partial x} + \theta_y \end{array} \tag{1.17}$$

instead of Eqns 1.18.

$$\varepsilon_x = -z\frac{\partial^2 w}{\partial x^2} \qquad \varepsilon_y = -z\frac{\partial^2 w}{\partial y^2} \qquad \gamma_{xy} = -2z\frac{\partial^2 w}{\partial x \partial y} \tag{1.18}$$

Equations 1.17 are the main equations of Mindlin Plate Theory. If $\theta_x = \partial w/\partial y$ and $\theta_y = -\partial w/\partial x$, transverse shear deformation vanishes and Eqns 1.17 reduce to Eqns 1.18.

Loads and supports Loads in the z-direction, either distributed or concentrated, may be applied to lateral surfaces $z = \pm t/2$ or to edges of a plate. Such loads are called *lateral*

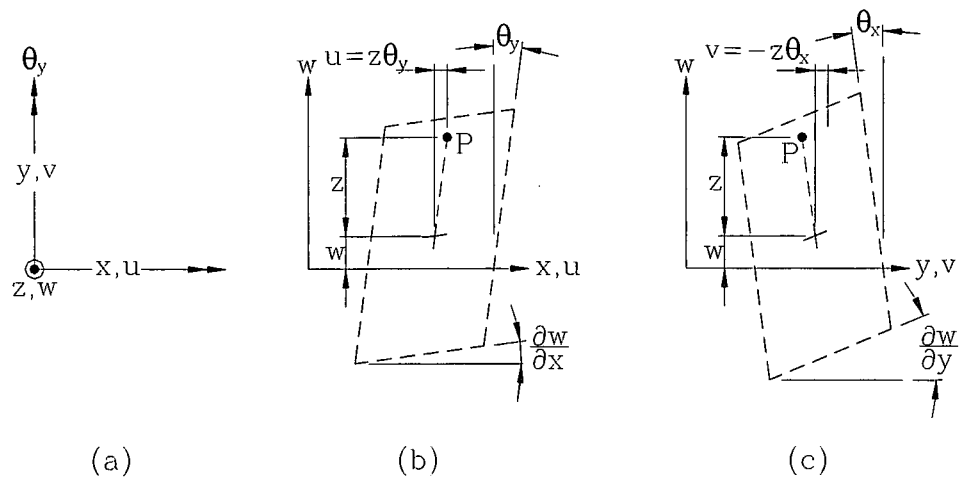

Figure 1-6: (a) Displacements and positive directions for rotations θ_x and θ_y, viewed normal to the xy plane. (b) Mindlin theory displacements in an xz-parallel cross-section. (c) Mindlin theory displacments in a yz-parallel cross-section.

loads. Distributed load has dimensions [force/length^2] on a lateral surface or [force/length] on an edge. A plate edge may also be loaded by a bending moment whose vector is tangent to the edge. The same kinds of edge loads may be applied to the plate by supports.

At the point where a concentrated lateral (z-direction) force is applied, Mindlin theory predicts infinite bending moments and infinite displacement. In reality no force can be truly concentrated, and in plate theory the infinities disappear if the *concentrated* load is applied over a small area instead [7].

1.1.4 Sandwich laminates

In order to minimise the mass and deflection capabilities of composite plates, sandwich panels are often used. Sandwich panels are found in many applications, such as in aerospace, marine and automotive structures. These plates will invariably undergo various loads and it is thus important to optimise them. In many applications, numerous different materials can be successfully used. The cross-section through a sandwich panel can be seen in Figure 1-7.

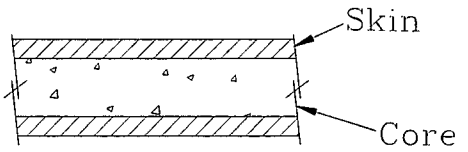

Figure 1-7: Cross-section through sandwich panel

Core materials

The deflection of a beam under a given load depends on its geometry and the modulus of the material. The easiest way to make a beam more rigid is to make it thicker (the deflection is increased as the cube of the length and decreased as the cube of the thickness). The deflection can be halved if the thickness is increased by a quarter.

Where mass is critical, it is preferable to use a sandwich construction where the outside surfaces, or *skins*, in which the highest tensile and compressive stresses occur, are separated by a *core* of much lighter material. There are different types of commonly used cores, which include honeycombs, balsa wood and plastic foams.

The skins are chosen from a material that gives enough strength and stiffness, abrasive and corrosion resistance, desired appearance and ease of production. The core is chosen from criteria such as; design of the construction, ease of application, mechanical properties (static and dynamic), design temperature, and bond properties.

The minimum strength of the bond must satisfy the requirements of the core material. A loss of strength in the bond gives the result that the shearing forces cannot be transferred from the skins to the core. The shear stiffness and strength of the core are of vital importance in determining critical deflections and loads. Too low a core density gives intolerable deflections and perhaps shear fracture. The same discussion holds for the risk of local buckling (ie. wrinkling and face dimpling).

Advantages of using sandwich laminates

One of the advantages of using fibre-reinforced laminated composites is that they possess low densities. In the aerospace industry low mass structures are critical in order to improve efficiency (ie. better fuel consumption, better maneuverability, etc.).

The use of sandwich construction combining thin strong skins over thick lightweight cores suggests possibilities of deriving constructions that achieve a minimum mass for a given stiffness or load. The minimum-mass constructions derived may not be practical due to unusually thin skins which are not commercially available, or some other detail such as unusual lightweight core of great thickness.

1.1.5 Buckling of fibre-reinforced composites

Fibre-reinforced laminates can fail by a phenomenon known as buckling when subjected to compressive or shear loads [8]. This is especially true if the laminates are thin. The characteristic of buckling is that the panel retains its original configuration until the initial buckling load is reached, at which point large out-of-plane displacements occur. The magnitude of the load is determined by the stiffness of the laminate, together with the geometry and edge supports.

Most structures can continue to sustain load over and above the initial buckling strength. Final failure will be determined by the strength of the laminate and it is usual for the design load to be equal to, or less than the initial buckling load. In only a few situations is it possible to use closed-form solutions to calculate initial buckling loads.

Buckling of flat plates

Consider a rectangular plate in the Cartesian x - y plane with dimensions of length a, width b, thickness t and fibre angle θ_s. The coordinate system x,y,z is located in the midplane, and the plate is subjected to compressive forces N_x in the x direction and N_y in the y direction with the load-ratio defined as $\lambda = N_y/N_x$. The laminae are symmetric with respect to the

midplane and the plate is simply supported at all edges.

It may be shown that the buckling load is given by [8]:

$$N(m,n) = \frac{n^2\pi^2}{b^2(1+\lambda\alpha_{mn}^2)} \left[\begin{array}{l} D_{11}\alpha_{mn}^{-2} + 2(D_{12}+ \\ + 2D_{66}) + D_{22}\alpha_{mn}^2 \end{array} \right] \tag{1.19}$$

where m and n represent the half wave numbers, $\alpha_{mn} = na/mb$ and D_{ij} are the bending stiffnesses. The critical load is obtained by minimising $N(m,n)$ over the integer parameters m and n. Thus the *critical buckling load* is given by

$$N = \min_{m,n} N(m,n) \tag{1.20}$$

In Eqn. 1.19, the terms involving bending-twisting coupling stiffnesses D_{16} and D_{26} have been omitted. Their effect on the buckling load becomes negligible provided the following conditions are satisfied

$$D_{16}/(D_{11}D_{12}^3)^{1/4} \leq 0.2, \; D_{26}/(D_{22}D_{12}^3)^{1/4} \leq 0.2 \tag{1.21}$$

This result and further discussion of the subject are given in Ref. [9].

Buckling of laminated cylindrical shells

A common structural element is the hollow cylinder or tube. Tubes are used in a wide variety of fabricated applications such as hoses, pipes, drive shafts, structural members and space trusses. Fibrous composites can be fabricated accurately and efficiently to specifications as laminated tubes using filament winding, pultrusion, or other fabrication methods. The opportunity to create an optimised configuration in terms of materials selection, fibre orientations and layer thicknesses is ever present.

Consider a symmetrically laminated cylindrical shell with orthotropic FRC layers. The shell lies in the x,y,z coordinate system, where x is the longitudinal, y is the circumferential, and

z is the radial direction. It has dimensions of length l, mean radius R and wall thickness t. The displacement components of the midplane are given by u, v and w in the x, y and z directions, respectively. The fibre angle is defined as the angle between the fibre direction and the longitudinal (x) axis and is given by θ_s. The fibre orientations are symmetric with respect to the midplane of the shell and are given by $\theta_k = (-1)^{k+1}\theta$ for $k \leq K_T/2$ and $\theta_k = (-1)^k\theta$ for $k \geq K_T/2 + 1$, where $k = 1, ..., K_T$ with k being the layer number. The buckling of a symmetric cylindrical shell under an axial load N_x is governed by the system of equations [11]:

$$\begin{aligned} &A_{11}u_{xx} + A_{12}\left(v_{,xy} + w_{,x}/R\right) + A_{66}\left(v_{,xy} + u_{,xy}\right) = 0 \\ &A_{66}\left(v_{,xx} + u_{,xy}\right) + A_{12}u_{,xy} + A_{22}\left(v_{,yy} + w_{,y}/R\right) = 0 \\ &D_{11}w_{,xxxx} + 2\left(D_{12} + 2D_{66}\right)w_{,xxyy} + D_{22}w_{,yyyy} + \\ &\left[A_{12}u_{,x} + A_{22}\left(v_{,y} + w/R\right)\right]/R = N_x w_{,xx} \end{aligned} \tag{1.22}$$

where A_{ij} and D_{ij} are the extensional and bending stiffnesses, respectively. Due to the mid-surface symmetry of the shell, the bending-extension coupling matrix does not appear in Eqn. 1.22. For a simply supported shell, the boundary conditions are given as:

$$w = 0,\ v = 0 \text{ at } x = 0,\ L \tag{1.23}$$

The solution to the system of Eqns 1.22 which satisfies the boundary conditions (Eqns 1.23) is obtained by taking the displacements in the form:

$$\begin{aligned} u &= u_{mn}\cos\left(\frac{m\pi}{L}x\right)\sin\left(\frac{n}{R}y\right) \\ v &= v_{mn}\sin\left(\frac{m\pi}{L}x\right)\sin\left(\frac{m\pi}{L}y\right) \\ w &= w_{mn}\sin\left(\frac{m\pi}{L}x\right)\sin\left(\frac{n}{R}\right) \end{aligned} \tag{1.24}$$

where u_{mn}, v_{mn} and w_{mn} are the amplitudes of the displacement components, and m and n represent the half-wave numbers in the axial and circumferential directions, respectively. The buckling load N_x corresponding to these wave numbers is obtained as an eigenvalue of the linear system of equations by substituting Eqns 1.24 into Eqns 1.22. The following

expression results from this computation:

$$N(m,n,\theta) = \left(\frac{L}{m\pi}\right)^2 \frac{\begin{vmatrix} C_{11} & C_{12} & C_{13} \\ C_{21} & C_{22} & C_{23} \\ C_{31} & C_{32} & C_{33} \end{vmatrix}}{\begin{vmatrix} C_{11} & C_{12} \\ C_{21} & C_{22} \end{vmatrix}} \tag{1.25}$$

$$\begin{aligned}
C_{11} &= A_{11}\left(\frac{m\pi}{L}\right)^2 + A_{66}\left(\frac{n}{R}\right)^2 \\
C_{22} &= A_{22}\left(\frac{n}{R}\right)^2 + A_{66}\left(\frac{m\pi}{L}\right)^2 \\
C_{33} &= D_{11}\left(\frac{m\pi}{L}\right)^4 + 2\left(D_{12}+2D_{66}\right)\left(\frac{m\pi}{L}\right)^2\left(\frac{n}{R}\right)^2 + D_{22}\left(\frac{n}{R}\right)^4 + \frac{A_{22}}{R^2} \\
C_{12} &= C_{21} = \left(A_{12}+A_{66}\right)\left(\frac{m\pi}{L}\right)\left(\frac{n}{R}\right) \\
C_{13} &= C_{31} = \frac{A_{12}}{R}\left(\frac{m\pi}{L}\right) \\
C_{23} &= C_{32} = \frac{A_{22}}{R}\left(\frac{n}{R}\right)
\end{aligned} \tag{1.26}$$

The critical load is obtained by minimising $N(m,n)$ over the integer parameters m and n. Thus the critical buckling load is given by:

$$N_b = \min_{m,n} N(m,n) \tag{1.27}$$

In Eqns 1.26, the terms involving bending-twisting coupling stiffnesses A_{16}, A_{26}, D_{16} and D_{26} have been omitted. Their effect on the buckling load becomes negligible provided the following conditions are satisfied,

$$D_{16}/(D_{11}D_{12}^3)^{1/4} \leq 0.2,\ D_{26}/(D_{22}D_{12}^3)^{1/4} \leq 0.2 \tag{1.28}$$

This result and further discussion of the subject are given in Ref. [9].

1.1.6 Combined torque and inplane compression of cylindrical shells

Consider a symmetrically laminated cylindrical shell of length l, diameter d and wall thickness H under combined loadings of torque T and inplane compression load P as shown in Figure 1-8. The shell is located in the x, ϕ, r coordinate system and is constructed of an arbitrary number K of orthotropic layers of equal thickness h_k and fibre orientation θ_k where $k = 1, 2, ..., K$.

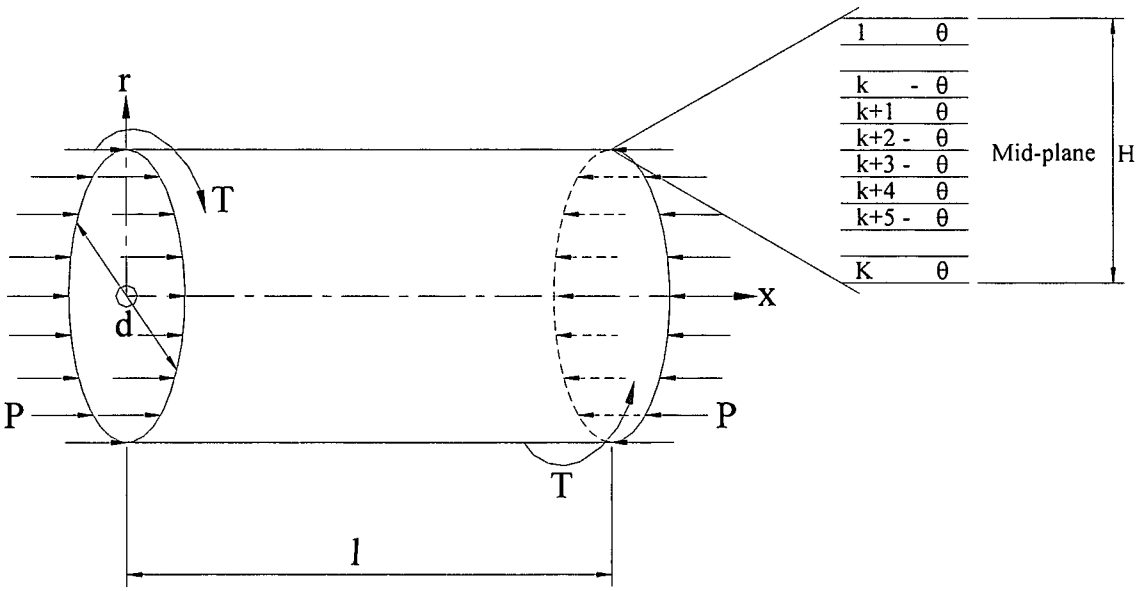

Figure 1-8: Geometry and loading of cylindrical shell

The axial (x) direction of the cylinder is the 90^o fibre direction. If the inside radius is R_i and the outside radius R_o, then the expression for P is given as [4]:

$$P = \int_{R_i}^{R_o} 2\pi\sigma_x r \, dr = 2\pi \sum_{k=1}^{K} \int_{r_{k-1}}^{r_k} \sigma_x^{(k)}(r) r \, dr \tag{1.29}$$

where σ_x is the resulting inplane stress.

Similarly, the torque T is given as:

$$T = 2\pi \int_{R_i}^{R_o} \tau_{x\phi} r^2 \, dr = 2\pi \sum_{k=1}^{K} \int_{r_{k-1}}^{r_k} \tau_{x\phi}^{(k)}(r) r^2 \, dr \tag{1.30}$$

where τ_{ϕ} is the shear stress moment.

Due to the symmetry of the laminate, the force resultants in the geometric coordinate axes are given by

$$[N] = [A][\varepsilon] \tag{1.31}$$

where

$$[N] = \begin{bmatrix} N_x \\ N_\phi \\ N_{x\phi} \end{bmatrix}, \; [A] = \begin{bmatrix} A_{11} & A_{12} & A_{16} \\ A_{12} & A_{22} & A_{26} \\ A_{16} & A_{26} & A_{66} \end{bmatrix}, \; [\varepsilon] = \begin{bmatrix} \varepsilon_x \\ \varepsilon_\phi \\ \gamma_{x\phi} \end{bmatrix} \tag{1.32}$$

In Eqn. 1.32, A_{ij} are the extensional stiffnesses given by $A_{ij} = H\bar{Q}_{ij}(\phi)$ for $i,j = 1,2$ and $i,j = 6$ and $A_{i6} = 0$ for balanced laminates with $i = 1,2$. Also in Eqn. 1.32, $\varepsilon_x, \varepsilon_\phi, \gamma_{x\phi}$ denote the normal and shear strains. Here $\bar{Q}_{ij}(\phi)$ is the transformed reduced stiffness component.

The stress-strain equations for the k^{th} orthotropic layer are given by

$$[s^{(k)}] = [\bar{Q}_{ij}^{(k)}][\varepsilon] \tag{1.33}$$

where $[\varepsilon] = [A]^{-1}[N]$ from Eqn. 1.31, and $[s^{(k)}] = [\sigma_x^{(k)} \; \sigma_\phi^{(k)} \; \tau_{x\phi}^{(k)}]^T$ denotes the stress vector in the $x\phi$ coordinate system. The stress vector in the material coordinate system, denoted by $[\sigma^{(k)}] = [\sigma_1^{(k)} \; \sigma_2^{(k)} \; \tau_{12}^{(k)}]^T$, is obtained from the geometric stress vector $[s^{(k)}]$ via the matrix transformation $[\sigma^{(k)}] = [T^k][s^{(k)}]$ where $[T^{(k)}] = [T(\phi_k)]$ denotes the transformation matrix for the k^{th} layer. From these equations it follows that $[\sigma^{(k)}] = [T^k][\bar{Q}_{ij}^{(k)}][\varepsilon]$.

1.1.7 Flexural response of fibre-reinforced composites

The major difference between designing for inplane response and flexural response is in the importance of the stacking sequence. For inplane response, only the total thickness of the layers of a given orientation matters, whereas for flexural response, the order of the layers with different orientations is as important as their total thickness. Layers that are located on the outside of the laminate contribute much more to the overall flexural stiffness

than identical layers that are located near the midplane. Unlike inplane response, flexural stiffness response often depends not only on the thickness of the laminate but also on its other dimensions.

Consider a symmetrically laminated rectangular plate of length a, width b and thickness h under a transverse bending load $q(x,y)$, as shown in Figure 1-9. The plate is located in the x,y,z plane and constructed of an arbitrary number K of orthotropic layers of thickness h_k and fibre orientation θ_k where $k = 1, 2, ..., K$. The displacement of a point (x^0, y^0, z^0) on the reference surface is denoted by (u^0, v^0, w^0).

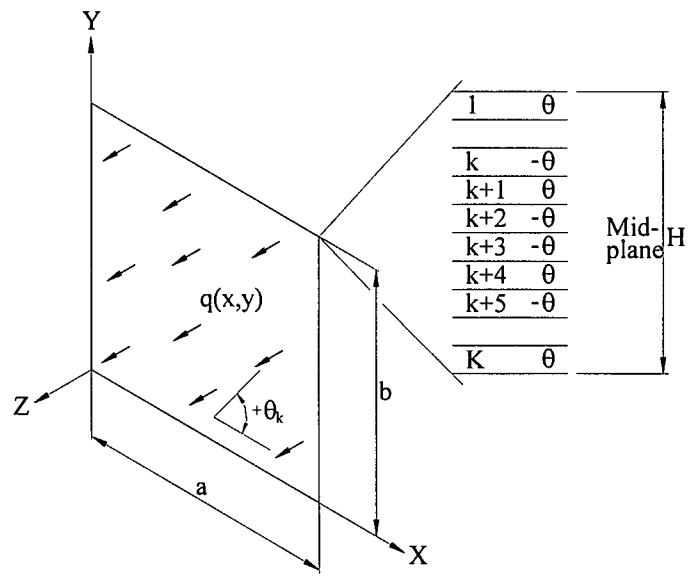

Figure 1-9: Geometry and loading of plate

The governing equation for the deflection w in the z direction under a transverse load q is given by [10]:

$$D_{11}w_{,xxxx} + 4D_{16}w_{,xxxy} + 2(D_{12} + 2D_{66})w_{,xxyy} + 4D_{26}w_{,xyyy} + D_{22}w_{,yyyy} = q \qquad (1.34)$$

where variables after the comma denote differentiation with respect to that variable.

As no simplifications are assumed on the elements of the $[D]$ matrix, Eqn. 1.34 includes bending-twisting coupling as exhibited by virtue of $D_{16} \neq 0, D_{26} \neq 0$.

1.1.8 Failure Criteria

To predict the failure of structures, the stresses are usually compared to the material strength limits [1]. The fundamental stress-strain relations, equilibrium equations and boundary conditions for a specific laminate configuration can be used to determine the stresses or strains under prescribed loads. Determining the strength of a laminate presents several difficulties. The first is that there is no sound analytical foundation for the determination of strength. This is also true for isotropic materials where the strength properties are determined empirically from tension and compression coupon test data.

The second difficulty is caused by through-thickness variation of stresses within the laminate. For monolithic isotropic materials, stress concentrations are likely to cause localised failures. For brittle materials, local failures generally lead to complete fracture and a total loss of load-carrying capability, whereas for ductile materials local failure is in the form of yielding that remains localised. High-performance unidirectional composite materials generally behave in a brittle manner.

There is an additional level of complication when dealing with laminates, which is the result of stacking together several layers with different orientations and material properties. As both the stresses and strengths may vary across different layers, it is possible that the stresses in one or more of the layers would reach their limiting strength earlier than other layers as the loading increases. It is, thus, likely that the laminate would suffer damage in the form of local (and most probably brittle) failures in those layers before ultimate structural failure is reached. In some applications first-failure of any layer is not acceptable as it degrades the strength and stiffness of the laminate. Failure prediction based on first-failure is commonly referred to as the *first-ply-failure* criterion. In other applications the laminate is considered to be unfailed as long as it stably carries a portion of the first-ply-failure load. In this case, failure progresses from one layer to others as the load is increased, leading to what is referred to as *progressive failure*

Using unidirectional laminates with orthotropic properties brings in additional complexities to failure prediction. At the macroscopic level the elastic properties change as a function of layer orientation. Therefore, the strength of unidirectional plies is direction dependent. The strength in the fibre direction is generally high, whereas the strength in a direction perpendicular to the fibre is controlled by the matrix material and is usually an order of magnitude lower than the fibre direction strength. Therefore, a load applied to a laminate along the fibre direction may be carried safely, whereas the same load may cause failure when applied perpendicularly to the fibres. It is also possible that, for a lamina restrained in a direction transverse to the fibres, application of loads along the fibre direction may induce failure transverse to the fibres due to Poisson's effect.

Axial compressive strength

Compressive failure of unidirectional composites loaded in the fibre direction is usually considered to be a microbuckling problem (sometimes called *shear crippling* or *fibre kinking*). As such, it is influenced by many factors, including fibre size and shape, fibre waviness, fibre/matrix bond strength, fibre and matrix stiffness, and fibre and matrix compressive strength. Composites using small-diameter fibres such as carbon, glass, and Kevlar are more susceptible to fibre buckling than those made with larger diameter fibres such as boron.

Tsai-Wu Failure Criterion

A general form of the failure criterion for orthotropic materials under plane stress assumption is known as the *Tsai-Wu failure criterion* [2], [3], which stipulates that the condition for non-failure for any particular ply is:

$$F(\theta) = F_{11}\sigma_1^{(k)}\sigma_1^{(k)} + F_{22}\sigma_2^{(k)}\sigma_2^{(k)} + F_{66}\tau_{12}^{(k)}\tau_{12}^{(k)} + 2F_{12}\sigma_1^{(k)}\sigma_2^{(k)} + F_1\sigma_1^{(k)} + F_2\sigma_2^{(k)} \leq 1 \quad (1.35)$$

where the strength parameters $F_{11}, F_{22}, F_{66}, F_1, F_2$ and F_{12} are given by

$$\begin{array}{lll} F_{11} = 1/(X_t X_c) & F_{22} = 1/(Y_t Y_c) & F_{66} = 1/G^2 \\ F_1 = 1/X_t - 1/X_c & F_2 = 1/Y_t - 1/Y_c & F_{12} = -\frac{1}{2}\sqrt{F_{11}F_{22}} \end{array} \tag{1.36}$$

and X_t, X_c, Y_t, Y_c are the tensile and compressive strengths of the composite material in the fibre and transverse directions, and G is the inplane shear strength.

1.2 Design optimisation procedures

Researchers and designers use various optimisation techniques to create new methodologies or to design structures. With the advent of fibre-reinforced laminated composites, these optimisation techniques have helped engineers minimise the calculation time and simplify complexity to produce optimal structures. Three of these optimisation techniques are briefly discussed below.

1.2.1 Minimisation or maximisation of functions

Consider a function f that depends on one or more independent variables [12]. The value of those variables where f takes on a maximum or a minimum value must then be found. The value of f that achieves the maximum or minimum can then be calculated. The computational requirements are to perform the computation quickly and economically and to use as little memory as possible. Often the computational effort is dominated by the cost of evaluating f. In such cases it is necessary to evaluate f as few times as possible.

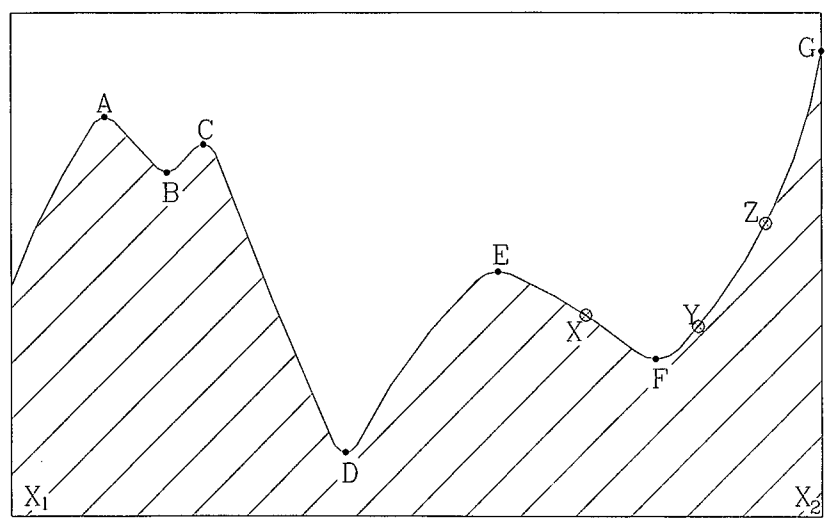

Figure 1-10: Extrema of a function in an interval. Points A, C, and E are local maxima. Points B and F are local minima. The global maximum occurs at G, while the global minimum is at D. Points X, Y, and Z are said to "bracket" the minimum F, since Y is less than both X and Z.

An extremum can be either global or local (see Figure 1-10). Finding a global extremum is often very difficult and two standard heuristics are often used. The first is to find the local extrema by starting from widely varying values of the independent variables (perhaps chosen quasi-randomly), and then pick the most extreme of these. The second is to perturb a local extremum by taking a finite amplitude step away from it, and see if the routine returns to a better point, or returns to the original point.

1.2.2 Examples of search routines

There are various techniques for finding maxima or minima, including *Simulated Annealing*, *Linear Programming*, *Monte Carlo* and the *Golden Section* method. Simulated Annealing is a relatively new optimisation routine and has solved problems previously thought to be unsolvable. This routine directly addresses the problem of finding global extrema in the presence of large numbers of undesired local extrema. Linear Programming is a well developed area of *Constrained Optimisation* where both the function to be optimised and the constraints happen to be linear functions of the independent variables.

The Golden Section method

The Golden Section method is a simple one-dimensional search routine that works as follows [12]: The root is bracketed in an interval (a_p, b_p). The function is then evaluated at an intermediate point x_p and a new, smaller bracketing interval, either (a_p, x_p) or (x_p, b_p) is obtained. This process continues until the bracketing interval is acceptably small. It is optimal to choose x_p to be the midpoint of (a_p, b_p) so that the decrease in the interval length is maximised when the function is as uncooperative as it can be. The position of x_p is found by manipulation and the end result is:

$$w = \frac{3 - \sqrt{5}}{2} = 0.38197$$

There is a precise translation of these considerations to the minimisation problem. To bracket a minimum involves bracketing a pair of points, a_p and b_p, when the function has opposite sign at these two points, which gives the root of a function. A minimum, by contrast, is known to be bracketed only when there is a *triplet* of points, $a_p < b_p < c_p$ (or $c_p < b_p < a_p$), such that $f(b_p)$ is less than both $f(a_p)$ and $f(c_p)$. In this case it is known that the function (if it is nonsingular) has a minimum in the interval (a_p, c_p).

The analog of bisection is to choose a new point x_p, either between a_p and b_p or between b_p and c_p. If the latter choice is made, then $f(x_p)$ is evaluated. If $f(b_p) < f(x_p)$, then the new bracketing triplet of points is (a_p, b_p, x_p); if $f(b_p) > f(x_p)$, then the new bracketing triplet is (b_p, x_p, c_p). In all cases the middle point of the new triplet is the abscissa whose ordinate is the best minimum achieved thus far. The process is continued until the distance between the two outer points of the triplet is tolerably small.

Genetic Algorithms

Many optimisation problems from the engineering world are very complex in nature and difficult to solve using conventional optimisation techniques. Since the 1960's, there has been an increasing interest in imitating living beings to solve such kinds of difficult optimisation problems. Simulating the natural evolutionary process of nature results in stochastic optimisation techniques called *evolutionary algorithms,* which can often outperform conventional optimisation techniques when applied to difficult real-world problems. There are currently three main avenues of this research: *genetic algorithms* (GAs), *evolutionary programming* (EP), and *evolution strategies* (ESs). Among them, genetic algorithms are perhaps the most widely known type of evolutionary algorithms.

Recently, genetic algorithms have received considerable attention regarding their potential as an optimisation technique for complex problems, including those relating to the design of fibre-reinforced composite structures [13].

General structure of genetic algorithms The usual form of genetic algorithms was described by Goldberg [14]. GAs are stochastic search techniques based on the mechanism

of natural selection and natural genetics [13]. Differing from conventional search techniques, GAs begin with an initial set of random solutions called a *population.* Each individual in the population is called a *chromosome*, representing a solution to the problem at hand, and is made up of a string of symbols. The chromosomes evolve through successive iterations, call *generations.* During each generation, the chromosomes are evaluated using some measure of fitness. To create the next generation, new chromosomes, called *offspring*, are formed by either i) merging two chromosomes from the current generation using a *crossover* operator or ii) modifying a chromosome using a *mutation* operator. A new generation is formed by i) selecting, according to the fitness values, some of the parents and offspring and ii) rejecting others so as to keep the population size constant. Fitter chromosomes have higher probabilities of being selected. After several generations, the algorithms converge to the best chromosome, which should represent the optimal or suboptimal solution to the problem.

There are only two kinds of operations in genetic algorithms:

i) *Genetic operations*: crossover & mutation

ii) *Evolution operation*: selection

The genetic operations mimic the process of heredity of genes to create new offspring at each generation. The evolution operation mimics the process of *Darwinian evolution* to create populations from generation to generation.

Crossover is the main genetic operator. It operates on two chromosomes at a time and generates offspring by combining both chromosomes' features. A simple way to achieve crossover would be to choose a random cut-point and generate the offspring by combining the segment of one parent to the left of the cut-point with the segment of the other parent to the right of the cut-point. The performance of genetic algorithms depends, to a real extent, on the performance of the crossover operator used.

The crossover rate is defined as the ratio of the number of offspring produced in each generation to the population size. This ratio controls the expected number of chromosomes to undergo the crossover operation. A higher crossover rate allows exploration of more of

the solution space and reduces the chances of settling for a false optimum; but if this rate is too high, it results in the wastage of a lot of computation time in exploring unpromising regions of the solution space.

Mutation is a background operator which produces spontaneous random changes in various chromosomes. A simple way to achieve mutation would be to alter one or more genes. In genetic algorithms, mutation serves the crucial role of either i) replacing the genes lost from the population during the selection process so that they can be tried in a new context or ii) providing the genes that were not present in the initial population.

The mutation rate is defined as the percentage of the total number of genes in the population. The mutation rate controls the rate at which new genes are introduced into the population for trial. If it is too low, many genes that would have been useful are never tried out; but if it is too high, there will be much random perturbation, the offspring will start losing their resemblance to the parents, and the algorithm will lose the ability to learn from the history of the search.

Genetic algorithms differ from conventional optimisation and search procedures in several fundamental ways. They can be summarised as follows:

i. Genetic algorithms work with a coding of solution set, not the solutions themselves.

ii. Genetic algorithms search from a population of solutions, not a single solution.

iii. Genetic algorithms use payoff information (fitness function), not derivatives or other auxiliary knowledge.

iv. Genetic algorithms use probabilistic transition rules, not deterministic rules.

Genetic operators Basic operators used to create successive improved populations include selection, crossover, mutation, and interchange. Typically, two designs selected from a population are mated to create child designs. In order to ensure that good designs propagate to the child populations, a higher chance to be selected as parents is given to those designs that are better (viz. have a higher fitness) than the rest of the population. Selection

is the part of the algorithm that provides better opportunity to good designs by implementing, for example, a roulette wheel which is divided into slices representing different designs. Those designs with better characteristics are given a proportionally larger slice of the wheel. When the wheel is spun (simulated by using a random number generator between 0 and 1, where the circumference of the wheel is normalized to be 1), those designs that occupy larger slices of the wheel have a better chance to be chosen as parent designs.

When maximizing the fitness, this is ideal but minimisation requires inversion of the fitness parameter.

Crossover operator: Once a pair of parents are selected, the mating of the pair also involves a random process called crossover. For example, by splicing together the left part of the string of one parent with the right part of the string of the other parent (ensuring to keep the orientations and thicknesses separate), two child strings are generated.

Mutation operator: Mutation is implemented by changing, at random and with small probability, the value of a gene and serves the purposes of avoiding premature loss of diversity in the designs. Since inferior designs may have some good traits that can get lost in the gene pool when these designs are not selected as parents, by introducing occasional mutations, different portions of the design space can be investigated for valuable information.

1.2.3 Multiobjective optimisation

In order to formulate an optimal design when there are several design objectives can pose a problem. If the objectives oppose each other then the problem becomes one of determining the ideal design that satisfies the opposing objectives. An optimal design must then be solved for, taking the multiple objectives and constraints into account. This type of problem is known as *multiobjective* optimisation.

By way of example, an engineer may be required to design a beam for minimum deflection and mass. This is a multiobjective problem with two opposing objectives. That is, an increase in mass would cause a reduction in deflection [15].

Problem formulation

A multiobjective design problem is solved in a similar manner to a single-objective problem. In a single-objective problem the idea is to find a set of values for the design variables that, when subject to a number of constraints, yield an optimum value of the objective function. In multiobjective problems, the values for the design variables that simultaneously optimise the objective functions are to be found. In this manner the solution is chosen from a so-called *Pareto* optimal set. For multiobjective problems the optimal solutions obtained by individual optimisation of the objectives (i.e. single-objective optimisation) is not a feasible solution to the multiobjective problem.

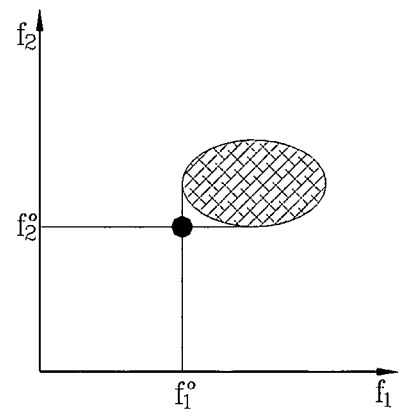

Figure 1-11: Ideal solution (f_1^0, f_2^0), obtained via individual minimisation of each function is not within the feasible region

In a multiobjective problem, a set of values for the design variables which optimise a set of objective functions is to be found. The set of variables that produces the optimal solution is designated as the optimal set and is denoted by $\bar{x}^*$. The optimal set is referred to as the Pareto optimal set and yields a set of possible results from which the desired values of the design variables are chosen.

Definitions

The initial step in the optimisation process is to formulate the problem. A mathematical model must be developed that, for all possible situations, will mimic the behavior of the system.

Design variables are identified as x_i $(i = 1, 2, ..., n)$. For example, for the optimisation of a structure for minimum mass and minimum deflection, the design variables will be as follows:

x_1 = mass

x_2 = deflection

The design variables may be modified in order to simplify the problem. These modified quantities are classified as parameters. In general, the vector of n design variables will be represented as

$$\bar{x} = \begin{bmatrix} x_1 \\ \vdots \\ x_2 \end{bmatrix} \tag{1.37}$$

The next step in the formulation of the problem is to identify the *constraints*. Constraints are conditions which must occur in order for the design to function as intended. For example, a beam is required to sustain a certain load without failing. Constraints can be either inequalities, equalities, or both.

Inequality constraints are specified as $\bar{g}\ (\bar{x}) \leq \bar{0}$ (where $\bar{g}$ is a vector representing the constraints g_j, $j = 1, ..., J$). The standard form of an inequality constraint is

$$g_j\ (\bar{x}) \leq 0 \quad \text{for } j = 1, ..., J \tag{1.38}$$

Equality constraints are specified as $\bar{h}\,(\bar{x}) = \bar{0}$. In scalar form they can be written as

$$h_k\,(\bar{x}) = 0 \quad \text{for } k = 1, ..., K \tag{1.39}$$

The final step in the problem statement is to define the *objective functions*. These are the quantities to be optimised and are designated by

$$\bar{f}\,(\bar{x}) \tag{1.40}$$

The functions may be defined so that they are all minimised. This can be done by multiplying any objective function which is to be maximised by -1, ie.

$$\max f_i(\bar{x}) = -\min(-f_i(\bar{x})) \tag{1.41}$$

The problem, when written in the standard form, appears as

$$\min_{\bar{x} \in \Re^n} \{\bar{f}\,(\bar{x}) : \quad \bar{h}\,(\bar{x}) = \bar{0}, \quad \bar{g}\,(\bar{x}) \leq \bar{0}\} \tag{1.42}$$

The above notation reads thus: Find the real values of the design variables (ie., they belong to $\Re^n$) that result in the smallest values of the objective functions subject to both inequality and equality constraints.

Definition of a Pareto Optimum

A set of points is said to be Pareto optimal if, in moving from point **A** to point **B** in the set, any improvement in one of the objective functions from its current value causes at least one other objective function to deteriorate from its current value. From this definition, point **C** is not Pareto optimal in Figure 1-12.

The Pareto optimal set yields an infinite set of solutions, from which the desired solution can be selected. In most cases, the Pareto optimal set is on the boundary of the feasible region.

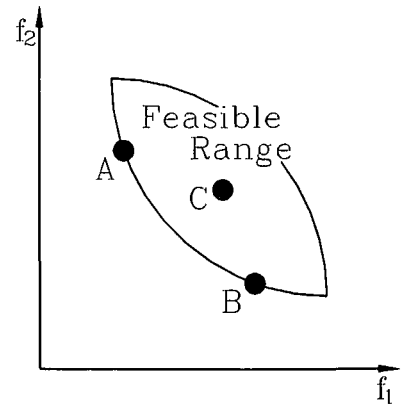

Figure 1-12: Graphical determination of the Pareto optimal

Weighting objectives method

This method takes each objective function and multiplies it by a fraction of one. This *weighting coefficient* is represented by (w_i) . The summation of the modified functions create a single cost function, which can be solved using any single objective method. Mathematically, the new function can be written as

$$f(\bar{x}) = \sum_{j=1}^{k} w_j f_j(\bar{x}) \tag{1.43}$$

where $0 \leq w_j \leq 1$ and $\sum_{j=1}^{k} w_j = 1$.

With this method, the weighting coefficients are assumed beforehand. The coefficients are then varied to yield a set of feasible optima, known as the Pareto optimal set. The values of the variables are then chosen from this set of solutions. If the problem is convex, then a complete set of Pareto solutions can be found. However, if the problem is not convex, there is no guarantee that the method will yield the entire Pareto set.

Geometrical interpretation of the weighting functions method

Consider the convex space of objective functions for a two-objective optimisation problem. The problem is as follows

$$\min f_1 \tag{1.44}$$

$$\min f_2 \tag{1.45}$$

Upon transformation to a weighting objective problem, the above problem becomes

$$\min f = w_1 f_1 + w_2 f_2 \tag{1.46}$$

1.2.4 Self-Design optimisation

Self-design research programmes generally deal with two and three-dimensional topological optimisation issues [16]. Most combine a methodology with finite element analysis, with the aim usually of adding material where stresses are high, and removing material where they are low, and work in an iterative manner. Generally, after each iteration, remeshing of the remaining geometry occurs, in order to ensure the accuracy of the finite element model and so that the shape becomes clear. All of the studies discussed in the literature deal with the optimisation of structures composed of isotropic materials, and trials have shown that large amounts of material can be removed without the structure failing.

The application of self-design methodologies to laminated composite structures is problematic, due to the orthotropic nature of these materials. The best approach would be to determine the optimal fibre orientations and laminae thicknesses at each iteration, so that the directional properties of these materials are optimally utilised, particularly as the shape (and thus load path) changes. This is difficult when there are several layers and thus many extra design variables.

Bull & Pitouras [16] presented a review of the self-design approach on the optimisation of engineering structures. Other authors discussed issues such as product optimisation [17], evolutionary material translation as a tool for the design of low mass, low stress structures [18]. They also discussed the low stress design of welded plates [19] and through depth plate profiling for reduced stress concentrations [20]. Other research includes that by Reynolds *et al* [21] who discussed reverse adaptivity for structural optimisation.

1.3 The Finite Element Method

1.3.1 Introduction

The finite element method is based on a theory whereby an original body is viewed as an assembly of discrete building blocks [22]. The application of the method involves dividing the body into an optimum number of blocks, called *elements* and using them as basis for computations. These blocks are considered to be severed from each other and joined only at specific points, called *nodes*, forming a network. The number of elements is determined by two factors: The capabilities of the computer being used, and the desired accuracy of the results.

The elements that compose the object are of finite size and hence the name of the method (FEM). The smaller the size, the smaller the errors, and as a result, the solution obtained comes closer to the true solution. In essence, the finite element method translates a complex design problem into a system of linear algebraic equations.

Today, the finite element method is indispensable in aircraft, automotive, and other industries.

Compatibility

Although the basic approach of separating a body into finite elements has been explained, the continuity of the body's response must not be forgotten. To prove continuity, a body, being seen as an assembly of separate elements, contains an assumed existence of forces acting on the elements through interconnecting joints. To obtain a workable solution, the following two requirements must be fulfilled:

i. Elements joined by a particular node must have the same displacement at that node.

ii. The interface between two elements is subject to displacements that are functions of the nodes on the interface, and those nodes only.

These two requirements are called the *compatibility conditions* of the finite element model and provide the mathematical justification of the polynomial relationship, called the *shape function* [22].

1.3.2 Convergence requirements

As the finite element method is a numerical technique, a sequence of approximate solutions is obtained as the element size is successively reduced [23]. This sequence will converge to the exact solution if the interpolation polynomial satisfies the following convergence requirements:

i. The field variable must be continuous within the elements. This requirement is easily satisfied if continuous functions are chosen as interpolation models. Since polynomials are inherently continuous, they easily satisfy this requirement.

ii. All uniform states of the field variable ϕ and its partial derivatives up to the highest order appearing in the functional $I(\phi)$ must have representation in the interpolation polynomial when, in the limit, the element size reduces to zero.

iii. The field variable ϕ and its partial derivatives up to one order less than the highest order derivative appearing in the functional $I(\phi)$ must be continuous at element boundaries or interfaces.

The elements whose interpolation polynomials satisfy the requirements (i) and (iii) are called *compatible* or *conforming* elements and those satisfying condition (ii) are called *complete* elements. If the r^{th} derivative of the field variable ϕ is continuous, then ϕ is said to have C^r continuity. In terms of this notation, the completeness requirement implies that ϕ must have C^r continuity within an element, while the compatibility requirement implies that ϕ must have C^{r-1} continuity at element interfaces.

In the case of general solid and structural mechanics problems, this requirement implies that the element must deform without causing openings, overlaps or discontinuities between adjacent elements. In the case of beam, plate and shell elements, the first derivatives of the

displacement across interelement boundaries must also be continuous.

If the interpolation polynomial satisfies all three requirements, the approximate solution converges to the correct solution when the mesh is refined and an increasing number of smaller elements are used. In order to prove the convergence mathematically, the mesh refinement has to be made in a regular fashion so as to satisfy the following conditions:

i. All previous (coarse) meshes must be contained in the refined meshes;

ii. The elements must be made smaller in such a way that every point of the solution region can always be within an element, and

iii. The form of the interpolation polynomial must remain unchanged during the process of mesh refinement.

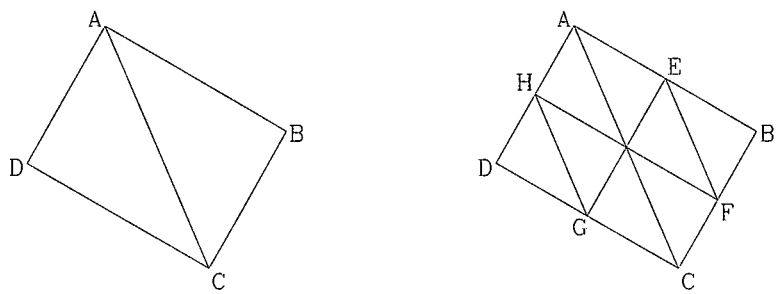

(a) Idealisation with 2 elements (b) Idealisation with 8 elements

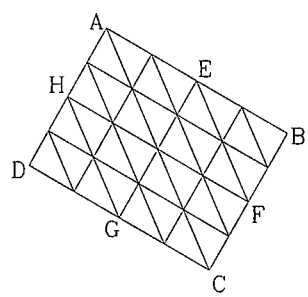

(c) Idealisation with 32 elements

Figure 1-13: All previous meshes contained in refined meshes

Conditions (i) and (ii) are illustrated in Figure 1-13, where a two-dimensional region is discretised with increasing number of triangular elements. From Figure 1-14, where the

solution region is assumed to have a curved boundary, it can be seen that conditions (i) and (ii) are not satisfied if elements with straight boundaries are used. In structural problems, interpolation polynomials satisfying all the convergence requirements always lead to the convergence of the displacement solution from below, while nonconforming elements may converge either from below or from above.

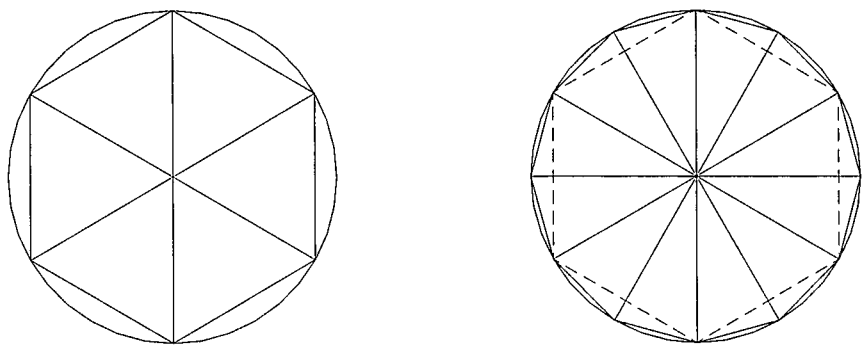

(a) Idealisation with 6 elements (b) Idealisation with 12 elements

Figure 1-14: Previous mesh is not contained in the refined mesh

1.3.3 Two-dimensional (Quadrilateral) element

Natural coordinates

For the local r, s (natural) coordinate system (Figure 1-15), the origin is taken as the intersection of lines joining the midpoints of opposite sides and the sides are defined by $r = \pm 1$ and $s = \pm 1$. The natural and Cartesian coordinates are related by the following equation [23]:

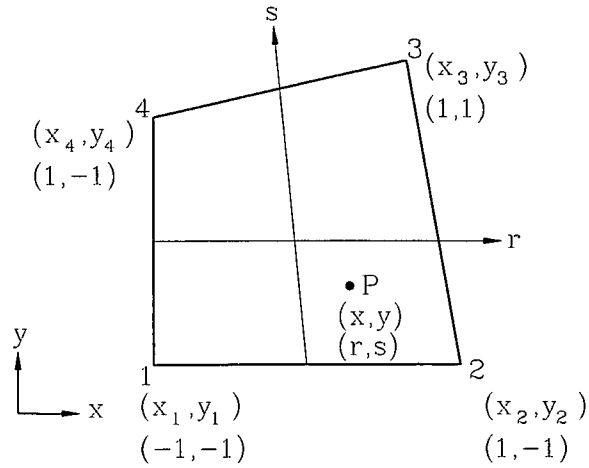

Figure 1-15: Natural coordinates for a quadrilateral element

$$\begin{Bmatrix} x \\ y \end{Bmatrix} = \begin{bmatrix} N_1 & N_2 & N_3 & N_4 & 0 & 0 & 0 & 0 \\ 0 & 0 & 0 & 0 & N_1 & N_2 & N_3 & N_4 \end{bmatrix} \begin{Bmatrix} x_1 \\ x_2 \\ x_3 \\ x_4 \\ y_1 \\ y_2 \\ y_3 \\ y_4 \end{Bmatrix} \tag{1.47}$$

where (x_i, y_i) are the (x, y) coordinates of node i $(i = 1, 2, 3, 4)$,

$$N_i = \frac{1}{4}(1 + rr_i)(1 + ss_i); \qquad i = 1, 2, 3, 4 \tag{1.48}$$

and the natural coordinates of the four nodes of the quadrilateral are given by:

$$\begin{aligned} (r_1, s_1) &= (-1, -1) \quad (r_2, s_2) = (1, -1) \\ (r_3, s_3) &= (1, 1) \qquad (r_4, s_4) = (-1, 1) \end{aligned} \tag{1.49}$$

If ϕ is a function of the natural coordinates r and s, its derivatives with respect to x and y

can be obtained as:

$$\begin{Bmatrix} \frac{\partial \phi}{\partial x} \\ \frac{\partial \phi}{\partial y} \end{Bmatrix} = [J]^{-1} \begin{Bmatrix} \frac{\partial \phi}{\partial r} \\ \frac{\partial \phi}{\partial s} \end{Bmatrix} \tag{1.50}$$

where $[J]$ is a 2 x 2 matrix, called the *Jacobian* matrix, given by:

$$\begin{aligned} [J] &= \begin{bmatrix} \frac{\partial x}{\partial r} & \frac{\partial y}{\partial r} \\ \frac{\partial x}{\partial s} & \frac{\partial y}{\partial s} \end{bmatrix} \\ &= \frac{1}{4} \begin{bmatrix} -(1-s) & (1-s) & (1+s) & -(1+s) \\ -(1-r) & -(1+r) & (1+r) & (1-r) \end{bmatrix} \end{aligned} \tag{1.51}$$

The integration of functions of r and s has to be performed numerically with:

$$dA = dx\ dy = \det [J] \cdot dr\ ds \tag{1.52}$$

and the limits of both r and s will be -1 and 1.

Linear element

For a quadrilateral element, it is not possible to have linear variation of the field variable (in terms of two independent coordinates) if one degree of freedom is chosen at each of the corner nodes. Hence the interpolation model is taken as:

$$\phi(x,y) = [N] \vec{\Phi}^{(e)} = [N_1\ N_2\ N_3\ N_4] \vec{\Phi}^{(e)} \tag{1.53}$$

where

$$N_i = (1 + rr_i)(1 + ss_i)/4, \qquad i = 1,2,3,4 \tag{1.54}$$

and

$$\vec{\Phi}^{(e)} = \left\{ \begin{array}{c} \Phi_1 \\ \Phi_2 \\ \Phi_3 \\ \Phi_4 \end{array} \right\}^{(e)} = \left\{ \begin{array}{c} \phi(x_1, y_1) \\ \phi(x_2, y_2) \\ \phi(x_3, y_3) \\ \phi(x_4, y_4) \end{array} \right\}^{(e)} \equiv \left\{ \begin{array}{c} \phi(\text{at } r = -1,\ s = -1) \\ \phi(\text{at } r = 1,\ s = -1) \\ \phi(\text{at } r = 1,\ s = 1) \\ \phi(\text{at } r = -1,\ s = 1) \end{array} \right\}^{(e)} \tag{1.55}$$

The nodal shape functions represented by Eqn. (1.54) are shown in Figure 1-16. It can be seen that the variation of the field variable along the edges of the quadrilateral is linear. This element is called a *linear element.*

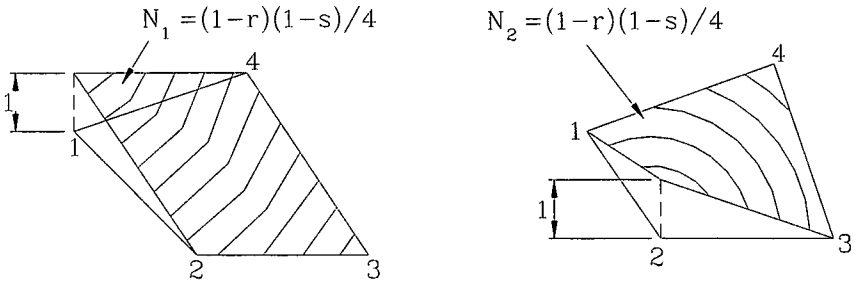

Figure 1-16: Linear interpolation functions (4 nodes) for a quadrilateral element

1.3.4 Two-dimensional (Rectangular) elements using classical interpolation polynomials

Using Lagrange interpolation polynomials

The Lagrange interpolation polynomials defined in Eqn. (1.56) for one-dimensional problems can be used to construct interpolation functions for two or higher dimensional problems [23]:

$$L_k(x) = \prod_{i=0, i\neq k}^{n} \frac{(x - x_i)}{(x_k - x_i)} = \frac{(x - x_o)(x - x_1)\cdots(x - x_{k-1})(x - x_{k+1})\cdots(x - x_n)}{(x_k - x_o)(x_k - x_1)\cdots(x_k - x_{k-1})(x_k - x_{k+1})\cdots(x_k - x_n)} \tag{1.56}$$

For example, in two-dimensions, the product of Lagrange interpolation polynomials in x and y directions can be used to represent the interpolation functions of a rectangular element as (see Figure 1-17):

$$\phi(r,s) = [N]\ \vec{\Phi}^{(e)}\ [N_1\ N_2\ N_3\ N_4]\ \vec{\Phi}^{(e)} \tag{1.57}$$

where

$$N_i(r,s) = L_i(r) \cdot L_i(s)\,; \qquad i = 1,2,3,4 \tag{1.58}$$

and

$$\vec{\Phi}^{(e)} = \left\{ \begin{array}{c} \Phi_1 \\ \Phi_2 \\ \Phi_3 \\ \Phi_4 \end{array} \right\}^{(e)} = \left\{ \begin{array}{l} \phi(r=-1, s=-1) \\ \phi(r=1, s=-1) \\ \phi(r=1, s=1) \\ \phi(r=-1, s=1) \end{array} \right\}^{(e)} \tag{1.59}$$

$L_i(r)$ and $L_i(s)$ denote interpolation polynomials in r and s directions corresponding to node i and are defined, with reference to Figure 1-17, as:

$$\begin{aligned} L_1(r) &= \frac{r-r_2}{r_1-r_2},\ L_2(r) = \frac{r-r_1}{r_2-r_1},\ L_3(r) = \frac{r-r_4}{r_3-r_4},\ L_4(r) = \frac{r-r_3}{r_4-r_3} \\ L_1(s) &= \frac{s-s_4}{s_1-s_4},\ L_2(s) = \frac{s-s_3}{s_2-s_3},\ L_3(s) = \frac{s-s_2}{s_3-s_2},\ L_4(s) = \frac{s-s_1}{s_4-s_1} \end{aligned} \tag{1.60}$$

The nodal interpolation functions N_i given by Eqn. (1.58) are called *bilinear* since they are defined as products of two linear functions.

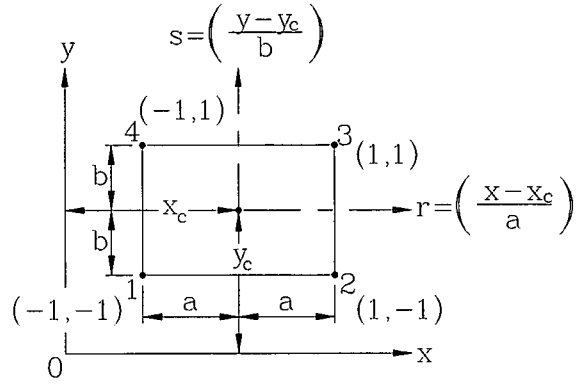

Figure 1-17: Location of nodes in rectangular elements

1.3.5 Continuity conditions

The interpolation model assumed for the field variable ϕ has to satisfy the following conditions [23]:

i. It has to be continuous inside and between the elements up to order $r-1$ where r is the order of the highest derivative in the functional I. For example, if the governing differential equation is quasi-harmonic, ϕ has to be continuous (i.e. C^o continuity is required). On the other hand, if the governing differential equation is biharmonic $\left(\nabla^4\phi = 0\right)$, ϕ as well as its derivative $(\partial\phi/\partial n)$ has to be continuous inside and between elements (i.e. C^1 continuity is required). The continuity of the higher order derivatives associated with the free or natural boundary conditions need not be imposed as their eventual satisfaction is implied in the variational statement of the problem.

ii. As the size of the elements decreases, the derivatives appearing in the functional of the variational statement will tend to have constant values. Thus, it is necessary to include terms which represent these conditions in the interpolation model of ϕ.

For elements requiring C^o continuity (i.e. continuity of only the field variable ϕ at element interfaces), the nodal values of ϕ are taken only as the degrees of freedom. To satisfy the interelement continuity condition, the number of nodes along the side of the element (and hence the number of nodal values of ϕ) are taken to be sufficient to determine the variation

of ϕ along that side uniquely. Thus if a cubic interpolation model is assumed within the element and retains its cubic behaviour along the element sides, then four nodes are taken along each side.

It can be observed that the number of elements capable of satisfying C^o continuity is infinite. This is because nodes and degrees of freedom to the elements can be added to form ever increasing higher order elements. All such elements will satisfy the C^o continuity. In general, higher order elements can be derived by increasing the number of nodes and hence the nodal degrees of freedom and assuming a higher order interpolation model for the field variable ϕ. Due to this, a smaller number of higher order elements yield more accurate results compared to larger number of simpler elements for the same overall effort.

Elements with C^o continuity

The above quadrilateral element considers only the nodal values of ϕ as the degrees of freedom and satisfy C^o continuity. If the nodal interpolation functions for rectangular elements are defined by products of Lagrange interpolation polynomials, then the C^o continuity is satisfied.

Elements with C^1 continuity

The construction of elements that satisfy C^1 continuity of the field variable ϕ is much more difficult than constructing elements for C^o continuity. To satisfy the C^1 continuity, the continuity of ϕ as well as its normal derivative $\partial\phi/\partial n$ along the element boundaries must be ensured.

For two-dimensional elements, it must be ensured that ϕ and $\partial\phi/\partial n$ are specified uniquely along an element boundary by the nodal degrees of freedom associated with the nodes of that particular boundary. The rectangular element considered in Figure 1-18 considers ϕ, $\partial\phi/\partial x$, $\partial\phi/\partial y$, and $\partial^2\phi/\partial x\partial y$ as nodal degrees of freedom and satisfies the C^1 continuity.

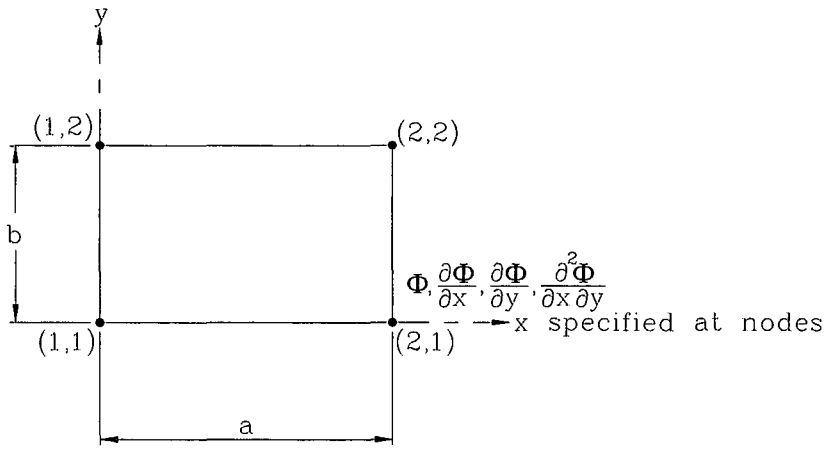

Figure 1-18: Rectangular element with 16 degrees of freedom

1.3.6 Finite elements for plates and shells

A plate is a thin solid and might be modelled using 3D elements (see Figure 1-19(a)) [6]. But a solid element is wasteful of d.o.f., as it computes transverse normal stress and transverse shear stresses, all of which are considered negligible in a thin plate. Also, thin 3D elements invite troubles produced by ill-conditioning because stiffness associated with thickness-direction ε_z is very much larger than other stiffnesses. The plate element in Figure 1-19(b) has half as many d.o.f. as the comparable solid element and omits ε_z from its formulation. In sketches, thickness t may appear to be zero (Figure 1-19(b)), but the physically correct value is used in formulating element stiffness matrices.

A *plane* element must be able to display states of constant σ_x, σ_y and τ_{xy} if it is to pass patch tests. A plate element must be able to display these states in each z = constant layer, which means that a valid plate element must pass patch tests for states of constant M_x, M_y, and M_{xy}. Figure 1-20 depicts a patch test for constant M_x, which requires constant $\partial\theta_y/\partial x$ in Mindlin theory if the test is to be passed. If $v \neq 0$, rotations about the x axis must be prevented at nodes 1, 3, 4, 6, and 7 in Figure 1-20.

Although Cartesian coordinates are used in this discussion, this is not a limitation of plate theory or of FE theory. Classical plate theory uses polar coordinates for circular plates.

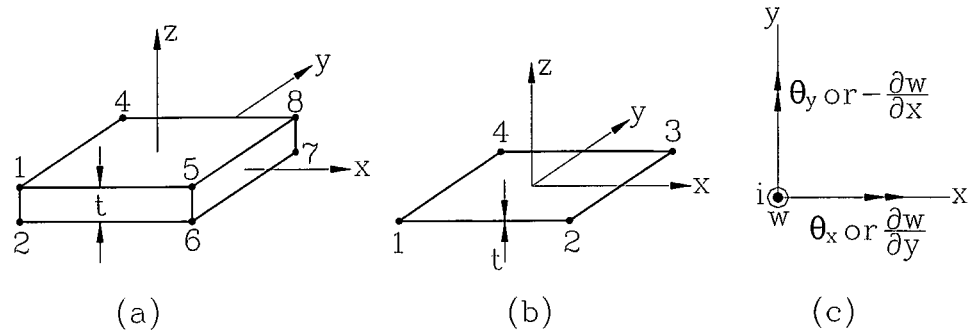

Figure 1-19: (a) A 3D solid element. (b) The comparable plate element. (c) Plate d.o.f. at a typical node i, viewed normal to the xy plane

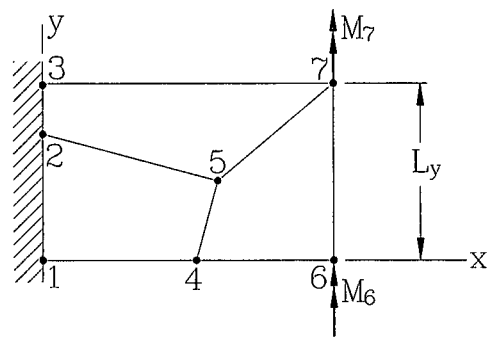

Figure 1-20: A patch test for constant curvature (or for constant M_x). Nodal moment loads are $M_6 = M_7 = M_x L_y/2$.

In FE analysis, a circular plate can be modelled by shell of revolution elements, simply by making shell elements flat rather than cylindrical or conical. Each such element is thus a flat annular ring, joined to adjacent annular elements at its inner and outer radii.

1.3.7 Mindlin plate elements

A Mindlin element is based on three fields [6]: $w = w(x,y)$, $\theta_x = \theta_x(x,y)$, and $\theta_y = \theta_y(x,y)$. Each is interpolated from nodal values. If all interpolations use the same polynomial, then for an element of n nodes,

$$\begin{Bmatrix} w \\ \theta_x \\ \theta_y \end{Bmatrix} = \sum_{i=1}^{n} \begin{bmatrix} N_i & 0 & 0 \\ 0 & N_i & 0 \\ 0 & 0 & N_i \end{bmatrix} \begin{Bmatrix} w_i \\ \theta_{xi} \\ \theta_{yi} \end{Bmatrix} = \mathbf{Nd} \tag{1.61}$$

$$\begin{aligned} N_1 &= \frac{1}{4}(1-\xi)(1-\eta) \quad N_2 = \frac{1}{4}(1+\xi)(1-\eta) \\ N_3 &= \frac{1}{4}(1+\xi)(1+\eta) \quad N_4 = \frac{1}{4}(1-\xi)(1+\eta) \end{aligned} \tag{1.62}$$

From Eqns 1.17 and 1.61 a strain-displacement matrix $\mathbf{B}$ can be formed. In the stiffness matrix formula, $k = \int \mathbf{B}^T \mathbf{E} \mathbf{B} dv$, $\mathbf{E}$ is a 5 by 5 matrix that includes the 3 by 3 $\mathbf{E}$ of plane stress and also shear moduli associated with the two transverse shear strains. Integration of $\mathbf{B}^T\mathbf{E}\mathbf{B}$ with respect to z is done explicitly. Integration in the plane of the element is done numerically if the element is isoparametric.

The N_i are given by Eqn. 1.62 for a four-node quadrilateral element. In any z = constant layer, strains vary in the same way as in the corresponding plane element provided that all terms of the integrand are integrated by the same quadratic rule. This is not usually done, for reasons discussed below.

Consider the bending mode shown in Figure 1-21. Element strains ε_x are independent of x, therefore, any order of quadrature will report the same strain energy for pure bending. However, this element displays spurious shear strain. If a/t is large, transverse shear strain γ_{zx} becomes large and the element is too stiff in bending, unless γ_{zx} is evaluated at $x = 0$, where γ_{zx} vanishes. But one-point quadrature for all strains would introduce four instability modes. This observation suggests "selective" integration, in which one-point quadrature is applied to bending terms. Then two instability modes remain. They may be controlled by "stabilisation" matrices. Calculated stresses are usually most accurate at Gauss points.

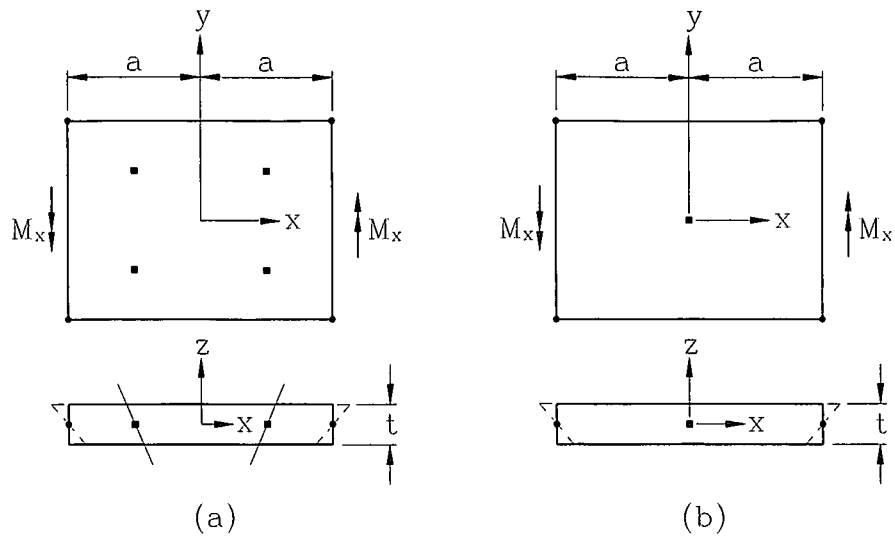

Figure 1-21: A bending deformation in a four-node Mindlin plate element. (a) Four-point integration rule. (b) One-point integration rule.

1.3.8 Elements used for composite laminate analysis

The layered nature of laminates means that only certain types of elements can be used efficiently within the FEM. It would, in theory, be possible to stack three-dimensional solid elements with one layer of solids representing a laminate ply. This is impractical for two reasons. It would be expensive to run such a model if the layup had more than a few plies and a real structure was being represented. In addition, layering solid elements through the thickness of relatively thin plates leads to ill-conditioned sets of equations. For these reasons solids tend to be used either where the layup is very thick or the geometry is more solid than plate-like, or where there is a three-dimensional field in the material, as can occur at the free edges of plates. In the latter case the 3D nature of the stress field is only significant over a short length, typically 3-5 thicknesses, and a small 3D sub-model of the region can be used [6].

Figure (1-22) shows a typical four node quadrilateral flat plate element with only inplane displacements. Such elements are widely used in composite analysis for modelling the inplane behaviour of flat plates. However, care must be taken to ensure that both the

stresses and the displacements are zero out of the element's plane, otherwise the model is not valid. With layered composites this depends upon the orientation of the plies. If the layup is not balanced then this 2D element cannot be used.

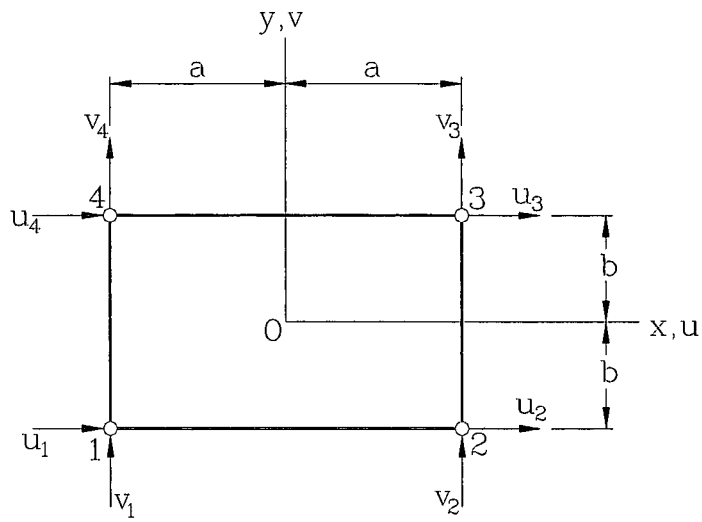

Figure 1-22: A bilinear quadrilateral and its eight nodal degrees of freedom

In practice it is more usual to employ a plate or shell element. The shell is modelled in terms of its mid-surface plane rather than the complete volume. The standard bending theory assumption that the strains only have a combination of constant and linear variation through the thickness of the shell is then used. This means that the deformation of the shell can then be defined by stretching (for the constant strain components) and rotation (for the linear strain components) of the shell's mid-thickness surface.

Both the two-dimensional solid and the general plate element can occur as quadrilaterals or triangles. They all have nodes at the corners of the element.

Provided that the shell is thin, then shell theory gives a good description of its behaviour. It is assumed that there is no stress or strain in the direction normal to the plane of the mid-surface. With this idealised behaviour it is only necessary to define displacements and rotations as the degrees of freedom on the element mid-surface plane. However, if Kirchhoff thin shell theory is used it is found to be very difficult to derive finite elements for other than very simple (rectangular) geometries. This arises from the need to differentiate

the transverse displacements twice to derive the bending strains. Definition of the shape functions and determination of the Jacobian matrix for arbitrary shaped elements has not proven to be simple in such cases. Instead, other shell theories have been used, typically the Mindlin theory [6]. These allow for transverse shear strains to occur so that the bending strains take the form:

$$\varepsilon_{x'x'} = \frac{\partial u'}{\partial x'} + z' \frac{\partial \theta_{y'}}{\partial x'} \tag{1.63}$$

where the "prime" denotes that these are coordinates and displacements in local coordinates in the plane and normal to the mid-thickness surface. There are other similar terms for the other bending strains. This definition of strain only requires first derivatives to be found, which greatly simplifies the determination of the Jacobian matrix. In addition, the formulation allows for the transverse displacements w' and the rotations $\theta_{x'}$ and $\theta_{y'}$ to be interpolated independently of each other. It is this which greatly simplifies the definition of the shape functions. Standard shape functions of the form:

$$w' = [N_1 N_2 N_3 ... N_m] \begin{bmatrix} w_1 \\ w_2 \\ . \\ w_m \end{bmatrix} \tag{1.64}$$

and

$$\theta_{x'} = [N_1 N_2 N_3 ... N_m] \begin{bmatrix} \theta_{x1} \\ \theta_{x2} \\ . \\ \theta_{xm} \end{bmatrix} \tag{1.65}$$

can be used, where the shape function for the ith node, N_i, is the standard simple form used for many 2D membrane plate and solid elements.

The Mindlin theory allows shear strains to occur and so these must also be included in the element behaviour and take the typical form (constant through the thickness):

$$\varepsilon_{x'} = \frac{\partial w'}{\partial x'} + \theta_{y'} \tag{1.66}$$

In reality the transverse strains cannot be constant through the thickness since they must be zero on the top and bottom faces of the plate, and they will generally vary in some parabolic form through the thickness. The transverse shears in the Mindlin theory therefore represent average through-thickness values. For thin plates the consequence of the variation through the thickness is second order and this average value is quite sufficient for good accuracy.

1.4 Design optimisation of laminated composites

An advantage of FRC materials over conventional ones is the possibility of tailoring their properties to the specific requirements of a given application. The tailoring is mostly achieved by maximising the mechanical properties as a result of selecting the layer fibre angles optimally.

1.4.1 The optimal design of laminated plates

Various researchers have studied the effect of sandwich panels and the optimisation of sandwich structures. For example, the inplane load carrying capacity of laminates can be enhanced via sandwich construction [24], [25]. Muc and Zuchara [26] discussed thin-walled sandwich plates having laminated composite faces, isotropic cores, and subjected to an axial compression. They discussed the 2-D geometrically nonlinear formulation of the governing equations with the use of the Hamilton and Lagrangian variational principles. This work allowed the authors to compare and verify values of the buckling loads with the use of different variants of sandwich plate theory. The analytical results that were obtained were confronted with finite element computations. The problems of local failure damage of sandwiches based on 3-D finite element analysis were also considered. The aim of their investigations was to study the effects of the normal stresses and their influence on sandwich behaviour.

Anisotropic facesheets affect the buckling properties of sandwiches [27]. It appears that only a few researchers have studied the optimisation of composite sandwich panels under buckling loads. Moh and Hwu [28], for example, examined composite plates with balanced or unbalanced anisotropic laminated faces and an ideally orthotropic core. A closed-form solution of the buckling load was derived for the sandwich plates consisting of cross-ply symmetric laminated faces with all edges simply supported. In addition, a general scheme was developed for the composite sandwich plates with arbitrary layups, boundary and loading conditions. They combined their buckling analysis with Powell's conjugate direction method, and established an optimal algorithm to find the optimal sandwich layup

for resisting biaxial compression and inplane shear loads. Rikards *et al* [29] examined the benefit of selecting the fibre angles of the skins optimally. Walker *et al* [30] discussed the optimisation of symmetric laminates for maximum buckling load including the effects of bending-twisting coupling. Here, optimal designs of symmetrically laminated rectangular plates subjected to a combination of boundary conditions was discussed to maximise the biaxial buckling load.

Researchers have investigated the design of composite structures for minimum mass, deflection, cost or a combination of these three factors. Lucoshevichyus [31] minimised the mass of rectangular plates under bi-directional compression for stability. Shin *et al* [32] investigated the design optimisation of plates for postbuckling performance. Vinson & Shore [33] presented a method for mass optimisation of flat truss-core sandwich panels under lateral loads. Adali *et al* [34] minimised the mass of symmetric angle-ply laminates under multiple uncertain loads. Quian *et al* [35] discussed the maximum stiffness design of rectangular symmetric angle-ply laminates. Kam & Chang [36] researched the optimum layup of thick symmetric and antisymmetric laminates for maximum stiffness. Walker *et al* [37] optimally designed symmetrically laminated plates for minimum deflection and weight. In this paper they used the finite element method using Mindlin plate theory in conjunction with an optimisation routine to obtain optimal designs of symmetrically laminates plates. Adali *et al* [24] minimised both the mass and deflection of thick sandwich laminates via symbolic computation. Adali *et al* [38] investigated the optimal design of hybrid laminates with discrete ply angles for maximum buckling load and minimum cost. Adali & Verijenko [39] presented a minimum cost design for hybrid composite cylinders with temperature dependent properties. Walker *et al* [40] discussed a procedure to select the best material combinations and optimally design hybrid composite plates for minimum mass and cost.

Some researchers have reported the use of genetic algorithms to find the minimum weight of a structure. For example, Walker & Wilson [41] combined the finite element method with a GA to optimise laminated structures for maximum rigidity and minimum weight. Kogiso *et al* [42] presented research on genetic algorithms with local improvement for composite laminate design, while Sivakumar [43] optimised the design of laminated composite plates with cutouts using a genetic algorithm. Nagendra used an improved genetic algorithm for

the design of stiffened composite panels and Haftka & Walsh [44] optimised the stacking sequence for the buckling of laminated plates using integer programming. Nagendra *et al* [45] optimised the stacking sequence of simply supported laminates with stability and strain constraints. Sadagopan & Pitchumani [46] discussed the application of GAs for the optimal tailoring of composite materials, while Crossley *et al* [47] used the two-branch tournament GA for multiobjective design. Some researchers applied optimisation techniques to practical problems. Obayashi *et al* [48] used a multiobjective GA for the multidisciplinary design of a transonic wing planform. Rudenko *et al* [49] used a multiobjective evolutionary algorithm for car front end design. Coello Coello *et al* [50] used a new GA-based optimisation technique for the design of robot arms.

Adali *et al* [51] used multiobjective optimisation of laminated plates for maximum prebuckling, buckling and postbuckling strength using continuous and discrete ply angles. The method of solution involves defining a design index made up of a weighted average of the objective functions, and then selecting the candidate configurations that need to be optimised. Once this is done, the best stacking sequence is determined. Kumar & Tauchert [52] discussed the multiobjective design of symmetrically laminated plates. Soremekun *et al* [53] discussed the stacking sequence design of composite laminates. Park *et al* [54] and Chen & Karunaratne [55] discussed the stacking sequence design of composite laminates for maximum strength, and the optimum stacking sequence of composite laminates, respectively.

1.4.2 The optimal design of laminated cylindrical shells

The optimal design of cylindrical composite shells has been considered by several authors. Optimisation of the stress–strain state of a thick–walled pipe on the basis of Young's modulus of the material was carried out by Kalinnikov & Korlyakov [56]. Walker [57] minimised the mass of composite hybrid shells via symbolic computation and Belingardi *et al* [58] studied optimisation of orthotropic multilayer cylinders and rotating disks using a maximum stress failure criterion. An analytical approach for predicting the probabilistic ultimate strength after initial failure of carbon fibre helical–wound cylinders under internal pressure

was used by Uemura & Fukunaga [59], while Fukunaga & Tsu-Wei Chou [60] considered the use of simultaneous failure and also optimum design of graphite/epoxy laminated composite pressure vessels under stiffness and strength constraints based upon membrane theory [61]. An analysis based on membrane theory of shells of laminated cylindrical pressure vessels subject to strength criterion was also carried out by Adali *et al* [62]. An efficient design method for thick composite cylinders was presented by Roy & Tsai [63] and Byon [64] optimised hybrid thick-walled cylindrical shells under external pressure by using a genetic algorithm.

Not much research has been carried out on the torsional effects of cylindrical shells in the design field. Walker *et al* [65] used multiobjective design to optimise laminated cylindrical shells for maximum torsional and axial loads. Gubran *et al* [66] discussed the stresses developed in composite shafts which were subjected to unbalanced excitations and transmitted torques while Laksimi & Benzeggagh [67]considered the application of the Tsai-Wu criterion for both notched and unnotched composite laminates under torque loading.

Tabakov [68] used a multi-dimensional design optimisation of laminated structures using an improved genetic algorithm. This study demonstrated a new variation of the GA technique, where the proposed selection of the best individuals makes the search more effective for both continuous and discrete design variables. The evaluation of the burst pressure of thick composite pressure vessels based on three-dimensional stress-strain analysis is used as an example. Adali *et al* [69] discussed the multiobjective design of laminated cylindrical shells for maximum pressure and buckling load.

Chapter 2

Optimal design problems and solution procedures

2.1 Problem 1: Design of fibre-reinforced laminated composite structures for a maximum combination of torque and inplane load

A procedure to select the optimal fibre orientations and determine the maximum load carrying capacity of symmetrically laminated fibre-reinforced composite structures is described. Cylindrical shells subject to combinations of torque and inplane forces are used to illustrate the methodology and are optimally designed for maximum strength. Torque tubes are generally used as control mechanisms, for example, in the tail fins of aircraft. The finite element method, based on Mindlin plate and shell theory, is used in this application in conjunction with an optimisation routine in order to obtain the optimal designs. The FEM is used here as it takes the effects of bending-twisting coupling, etc. into account. The methodology consists of two stages; the objective of the first is to maximise the strength of the cylindrical shells by determining the fibre orientations optimally while the objective of the second stage is to maximise the inplane compression loading subject to a failure criterion. The effect of different shell aspect ratios, wall thickness, layer numbers and boundary

conditions on the results is investigated.

2.1.1 Optimal design problem formulation

The objective of the design problem is first to design for maximum strength by selecting the fibre orientations optimally and then to determine the maximum inplane load that the optimised design can sustain. The strength of the shell is reflected by the value of a failure index F; viz. the lower the failure index, the stronger the shell for a given load scenario. A minimum failure index is achieved by optimally determining the fibre orientations given by $\theta_k = (-1)^{k+1}\theta$ for $k \leq K/2$ and $\theta_k = (-1)^k\theta$ for $k \geq K/2+1$. The first part of the design problem may thus be stated as [70]:

$$F_{\min} \triangleq \min_{\theta} \left[F_{\max}(\theta)\right], \ 0^o \leq \theta \leq 90^o \tag{2.1}$$

where

$$F_{\max}(\theta) = \max_{x,\phi,r} F(x,\phi,r) \tag{2.2}$$

The second part of the design problem involves determining $P_{\max}$ subject to the same failure criterion. In this study, the Tsai-Wu failure criterion is used.

The second part of the problem may thus be stated as

$$F_{\min} = \min_{P} F(\theta_{opt}) \tag{2.3}$$

subject to the constraints of Eqn. 1.35, which is evaluated for all plies.

The failure index F is determined from the finite element solution of the problem given by Eqn. 2.10. The first optimisation procedure involves the stages of determining the maximum failure index $F_{\max}(x,\phi,r)$ for a given θ (using Eqn. 1.35) and improving the fibre orientation to minimise $F_{\max}$. The second optimisation stage involves evaluating $F(\theta)$ for a given P and improving the inplane load to maximise P. This step may be described explicitly as

$$\min_{P} | F(\theta_{opt}) - 1 | \tag{2.4}$$

in order to maximise the inplane load. Thus the computational solution consists of successive stages of analysis and optimisation until a convergence is obtained and the optimal angle θ_{opt} and then $P_{\max}$ is determined within a specified accuracy. In both optimisation stages, the Golden Section method is employed (although any optimisation technique may be used), first to determine θ_{opt} and then $P_{\max}$.

2.1.2 Finite element formulation

The finite element formulation [73] of the problem (based on Mindlin type theory) is considered, although any suitable formulation can be substituted. Consider a finite element formulation of the problem. Let the region S of the shell (see Figure 1-8) be divided into n sub-regions S_r ($S_r \in S; r = 1, 2, ..., n$) such that

$$\Pi(u) = \sum_{r=1}^{n} \Pi^{Sr}(u) \tag{2.5}$$

where Π and Π^{Sr} are potential energies of the shell and the element, respectively, and u is the displacement vector. Using the same shape functions associated with node j ($j = 1, 2, ..., n$), $S_j(x, y)$, for interpolating the variables in each element, it can be written that:

$$u = \sum_{j=1}^{n} S_j(\phi, r) u_j \tag{2.6}$$

where u_j is the value of the displacement vector corresponding to node j, and is given by

$$u = \{u^{(j)}, v^{(j)}, w^{(j)}, \phi_1^{(j)}, \phi_2^{(j)}\}^T \tag{2.7}$$

The displacements $\{u, v, w, \phi_1, \phi_2\}$ are approximated as:

$$u = \sum_{j=1}^{n} u_j \psi_j(\phi, r) \ , \ v = \sum_{j=1}^{n} v_j \psi_j(\phi, r) \ , \ w = \sum_{j=1}^{n} w_j \psi_j(\phi, r) \tag{2.8}$$

$$\phi_1 = \sum_{j=1}^{n} S_j^1 \psi_j(\phi, r) \ , \ \phi_2 = \sum_{j=1}^{n} S_j^2 \psi_j(\phi, r)$$

where ψ_j are Lagrange family of interpolation functions. From the equilibrium equations of the first order theory, and Eqn. 2.8, the finite element model of the first-order theory is obtained:

$$\sum_{\beta=1}^{5} \sum_{j=1}^{n} K_{ij}^{\alpha\beta} \Delta_j^{\beta} - F_i^{\alpha} = 0 \ , \ (\alpha = 1, 2, ..., 5) \tag{2.9}$$

or

$$[K]\{\Delta\} - \{F\} = \{0\} \tag{2.10}$$

where K and F are the stiffness and force coefficients respectively, and the variable Δ denotes the nodal values of w and its derivatives.

2.2 Problem 2: The optimisation of laminated composite structures for minimum mass using the finite element method and genetic algorithms

A technique for using GAs together with finite element analysis to minimise the mass of fibre-reinforced symmetrically laminated structures with several discrete design variables is described. The design constraint implemented here is based on the Tsai-Wu failure criterion, although any suitable failure criterion can be implemented. Rectangular plates are used to demonstrate the method, have eight layers, and are symmetric about the midplane. Thus, the four fibre orientations and laminae thicknesses are to be determined optimally. To determine the best configuration, optimal ply angles for each layer are selected from amongst a predefined set of fibre orientations, commonly used in industry. This approach leads to cost-effective (and easier to construct) designs by virtue of allowing the use of standard composite plies. The most common orientations are 0^o, $\pm 30^o$, $\pm 45^o$, $\pm 60^o$and 90^o which are the ones used in the present study. Also, the laminae thicknesses must be multiples of a standard ply, thickness; eg. $0.001m$. Previous work on discrete optimisation of composite laminates include Ref. [33], [43], [44] and [64].

2.2.1 Optimal design problem formulation

The objective of the design problem is to minimise the mass W of the laminated structure, subject to a failure criterion. Here a rectangular plate under a transverse bending load $q(x, y)$ is used to illustrate the methodology. The minimum mass is achieved by optimally determining the fibre orientations and the laminae thicknesses, given by $[\theta_1/\theta_2/... \ /\theta_i \ || \ t_1/t_2/... \ /t_i]_s$. Thus, the design problem may thus be stated as [71]:

$$W_{\min} \triangleq \min_{\theta,t} [W(\theta_i, t_i)], \qquad \theta_i \in (0^o, \pm 30^o, \pm 45^o, \pm 60^o, 90^o), \ i = 1, 2, ..., \ K \qquad (2.11)$$

where the thickness of each layer must be a multiple of a minimum feasible dimension. For example, if a standard ply thickness is $0.001m$, then each individual layer should have thickness $0.001k$, where $k \in Z$ (and $Z \neq 0$).

Here, the mass is determined from the finite element solution of the problem given by Eqn. 2.10, and is used as the fitness parameter P by the GA. In addition, any laminate that does not comply with the failure criterion of choice is rejected, and no further breeding with it takes place. In this study, the Tsai-Wu failure criterion is used.

Finally, it is important to note that when alternative designs had equal mass, the best was that with the lowest failure index.

Many researchers have done similar work in this area, but the optimisation of laminate structures for minimum mass using genetic algorithms has not yet been performed using the finite element method in this way [72].

2.3 Problem 3: The multiobjective optimisation of laminated composite structures for both minimum mass and deflection using the finite element method and genetic algorithms

This work is a continuation of Problem 2. A technique for using GAs together with finite element analysis to minimise both the mass and deflection of fibre-reinforced symmetrically laminated structures with several discrete design variables is presented. The design constraint implemented is based on the Tsai-Wu failure criterion, although any suitable failure criterion can be implemented. Rectangular plates subject to transverse bending loads are used to demonstrate the method, have eight layers, and are symmetric about the midplane. Thus, the four fibre orientations and laminae thicknesses are to be determined optimally. To determine the best configuration, optimal ply angles for each layer are selected from amongst a predefined set of fibre orientations, commonly used in industry. This approach leads to cost-effective designs by virtue of allowing the use of standard composite plies. The most common orientations are 0^o, $\pm 30^o$, $\pm 45^o$, $\pm 60^o$and 90^o which are the ones used in the present study. Also, the laminae thicknesses must be multiples of a standard ply, thickness; eg. $0.001m$.

2.3.1 Optimal design problem formulation

The objective of the design problem is to minimise a weighted sum, P, of the mass W and deflection w of the laminated structure, subject to a failure criterion. The minimum value of P is achieved by optimally determining the fibre orientations and the laminae thicknesses, given by $[\theta_1/\theta_2/.../\theta_i \mid\mid t_1/t_2/.../t_i]_s$. Thus, the design problem may thus be stated as [74]:

$$P_{\min} \triangleq \min_{\theta,t} [P(\theta_i, t_i)], \qquad \theta_i \in (0^o, \pm 30^o, \pm 45^o, \pm 60^o, 90^o),\ i = 1, 2, ...,\ K \qquad (2.12)$$

The value of P is normalised by introducing the following non-dimensionalised quantities:

$$W^* = W/W_0;\ w^* = w/w_0 \tag{2.13}$$

for mass and deflection. In Eqn. 2.13 the subscript '0' denotes the values of W and w for a $[0^o \mid\mid 0.00075]_8$ laminate.

Thus

$$P(\theta_i, t_i) = \mu_1 W^* + \mu_2 w^* \tag{2.14}$$

with $\mu_1, \mu_2 \geq 0$, $\mu_1 + \mu_2 = 1$. As the weighting factors μ_i are varied, the emphasis of the optimisation is shifted among various objectives resulting in compromise solutions. The single objective designs can be obtained as special cases by setting $\mu_1 = 1, \mu_2 = 0$, etc. The thickness of each layer must be a multiple of a minimum feasible dimension. For example, if a standard ply thickness is $0.001m$, then each individual layer should have thickness $0.001k$, where $k \in Z$ (and $Z \neq 0$).

Here, the mass and deflection is determined from the finite element solution of the problem given by Eqn. 2.10, and is used to determine the value of the fitness parameter by the GA. In this study, the Tsai-Wu failure criterion is used.

2.4 Problem 4: A simple self-design methodology for laminated composite structures for minimum mass

This research presents a very simple self-design methodology for laminated composite structures, subject to any type of loading and boundary conditions, which works in conjunction with the finite element method. Remeshing during each iteration is not carried out, and the original laminae fibre orientations and thicknesses remain constant (for simplicity). Two test cases involving plates are used to illustrate the methodology, and it is shown that large mass savings are possible without affecting the integrity of the structure. In addition, it is also shown that remeshing is unnecessary.

2.4.1 Optimal design problem formulation

The objective of the design problem is to minimise the mass of a laminated plate by reducing the area without affecting the integrity in terms of the boundary conditions and applied loads. A failure criterion is used as the constraint. The plate is modelled using the finite element method with an appropriate laminate shell and plate element. After carrying out the finite element analysis, the element with the least stress (viz. lowest failure index F) is removed and the analysis is re-run. If the maximum plate failure index is not critical, another may be removed. If it is, the element is replaced. The process is repeated until all the elements that can be removed without affecting the integrity are deleted. In addition, connectivity is checked at each step to ensure that 'islands' of elements never result [75], [76].

Self-design algorithm

Overview - The first step of the process is to create a finite element model of the laminated composite plate or shell. The algorithm is then employed, which executes the FEA. If the maximum value of the failure index throughout the structure is less than one, it then finds the element with the least failure index (see Figure 2-1). If any of that element's nodes are

associated with loads or boundary conditions, the element may only be removed if that node will not be affected by the removal of the element in question. In addition, connectivity is also checked (see the next section). If appropriate, the element is then deleted, and the model re-analysed. If the maximum value of the failure index throughout the structure is equal to or greater than one, the element that has just been deleted is replaced, and the element with the next lowest value of F is checked in the same way.

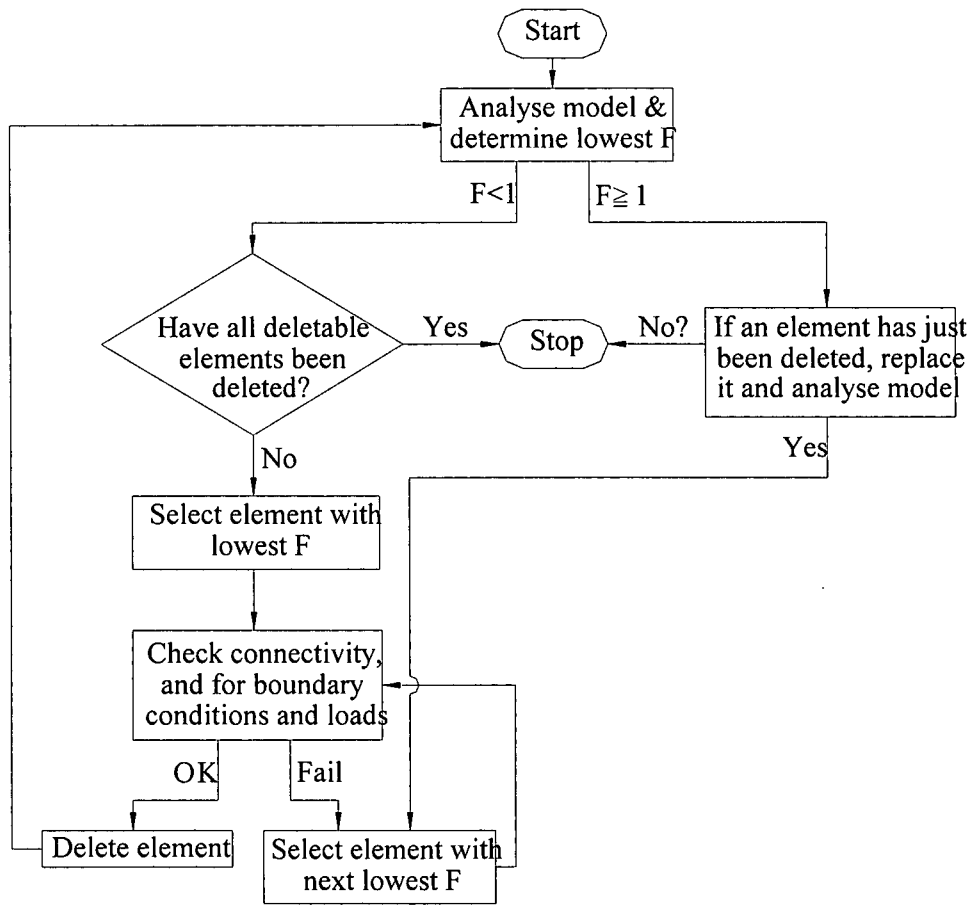

Figure 2-1: Flow diagram of self-design procedure

Although simplistic, the algorithm generally works well. Nonetheless, it has been found that in cases where the shape of the structure or the loading is complex, better results (ie. a lower final mass) can sometimes be found manually using different approaches, but this can be extremely tedious, particularly when the element density is high.

Connectivity - An important part of this methodology is the connectivity checking of the elements. At no stage during the deletion process may any of the elements become detached from the structure, to form 'islands'. This is done by checking that there is always a path running through all the nodes. Once an element is selected for possible deletion, the connectivity check is executed. If, at any stage, a path through the elements might be broken, the element in question is neglected and another possible candidate evaluated.

2.5 Problem 5: The optimal design of composite sandwich panels for minimum cost via the selection of the best material combinations

A procedure to select the best material combination and optimally design sandwich laminates with fibre-reinforced skins and low density cores for minimum cost is described. In this study, the optimal material combination with least cost is determined by admitting different candidates into the design space. This space consists of three continuous variables, viz. the skin fibre angle, and the layer thickness of the skins and core. There is also one discrete variable in the design space; the material combination. The plates are optimised for minimum cost subject to a minimum buckling load and maximum mass constraint. An optimisation procedure with two stages is devised that leads to an optimal design that is chosen from amongst the candidate designs. It should be noted that classical plate theory is used for simplicity, since the focus of this study is an optimisation methodology, and the means by which candidate fitness is assessed is irrelevant here. If more accuracy is desired, a formulation such as that of Reissner - Mindlin should be substituted. It should also be noted that the Love-Kirchhoff hypothesis is implemented here, even though the sandwich cylinders have shear-deformable cores, because it was found in this application that the effect on the results was negligible. A more accurate theory can easily be substituted into the procedure described.

2.5.1 Basic equations

Consider a rectangular sandwich panel with orthotropic FRC skins of thickness t_s and core thickness t_c, as shown in Figure 2-2. The plate lies in the Cartesian x - y plane, and has dimensions of length a, width b and total thickness t. The fibre angle of the skin layers is given by θ_s. The coordinate system x,y,z is located in the midplane, and the plate is subjected to compressive forces N_x in the x direction, and N_y in the y direction with the load-ratio defined as $\lambda = N_y/N_x$. The skin laminae are symmetric with respect to the midplane and the plate is simply supported at all edges.

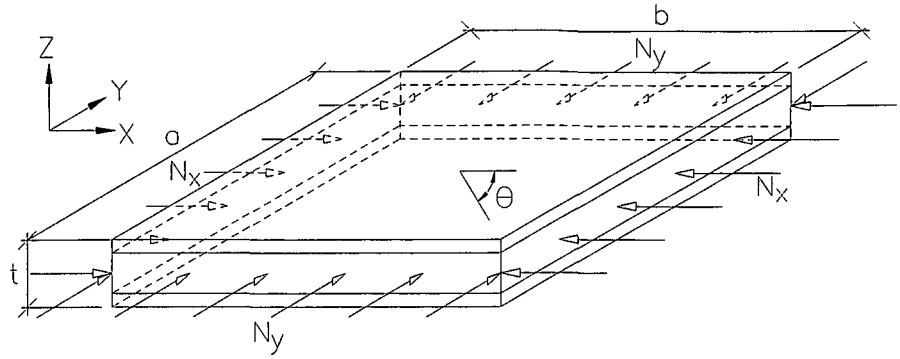

Figure 2-2: Geometry and loading of sandwich panel

The thickness of a sandwich panel is given by $t = 2t_s + t_c$, the mass by $W = ab(2t_s\rho_s + t_c\rho_c)$, and the cost $C = ab(2t_s\rho_s P_s + t_c\rho_c P_c)$ where P_i is the cost per unit mass of the skin and core materials.

2.5.2 Optimal design problem formulation

For a particular buckling load capacity and mass requirement, together with a choice of skin and core material combinations that results in I candidates, the design optimisation procedure consists of two steps [77]:

Step 1. For each candidate, determine the skin fibre angle θ_s optimally by determining the value of θ_s for which the resulting skin and core thicknesses lead to a minimum candidate cost, viz.

$$C_{i_{\min}} = \min_{\theta_s} C(t_s, t_c),\ 0^o \leq \theta_s \leq 90^o \tag{2.15}$$

subject to

$$N_i \geq N_b \text{ and } W_i \leq W,\ i = 1, 2, .., I \tag{2.16}$$

where N_b is the buckling load capacity required, and W the maximum mass allowable.

Step 2. Select the cheapest candidate [78].

2.5.3 Method of solution

Given that the buckling load is dependant on θ_s, t_s and t_c, and the sandwich mass on t_s and t_c, for a particular design buckling load capacity and mass requirement, t_s and t_c can be determined for any value of θ_s. Thus, a suitable optimisation routine can be used to determine $\theta_{s_{opt}}$. Once $\theta_{s_{opt}}$ and the resultant cost have been determined for each candidate, the cheapest is selected. For the optimisation, the *Golden Section* method is employed, and $\theta_{s_{opt}}$ is determined within a prescribed accuracy of 1^o.

2.6 Problem 6: The optimal design of composite sandwich cylindrical shells for minimum mass via the selection of the best material combinations

A procedure to select the optimal fibre orientations and determine the maximum load carrying capacity of symmetrically laminated fibre-reinforced composite structures is described. In this study, the optimal material combination with least mass is determined by admitting different candidates into the design space. This space consists of three continuous variables, viz. the skin fibre angle, and the layer thickness of the skins and core. There is also one discrete variable in the design space; the material combination. The cylindrical shells are optimised for minimum mass subject to a minimum buckling load and maximum cost constraint. An optimisation procedure with two stages is devised that leads to an optimal design that is chosen from amongst the candidate designs. It should be noted that the Love-Kirchhoff hypothesis is implemented here, even though the sandwich cylinders have shear-deformable cores, because it was found in this application that the effect on the results was negligible. A more accurate theory can easily be substituted into the procedure described.

2.6.1 Basic equations

Consider a symmetrically laminated cylindrical shell of sandwich construction with orthotropic FRC skins of thickness t_s and core thickness t_c, as shown in Figure 2-3. The shell lies in the x,y,z coordinate system, where x is the longitudinal, y is the circumferential, and z is the radial direction. It has dimensions of length l, mean radius R and wall thickness t. The displacement components of the midplane are given by u, v and w in the x, y and z directions, respectively. The fibre angle of the skin layers is defined as the angle between the fibre direction and the longitudinal (x) axis and is given by θ_s. The fibre orientations are symmetric with respect to the midplane of the shell and are given by $\theta_k = (-1)^{k+1}\theta$ for $k \leq K_T/2$ and $\theta_k = (-1)^k\theta$ for $k \geq K_T/2 + 1$, where $k = 1, ..., K_T$ with k being the layer number.

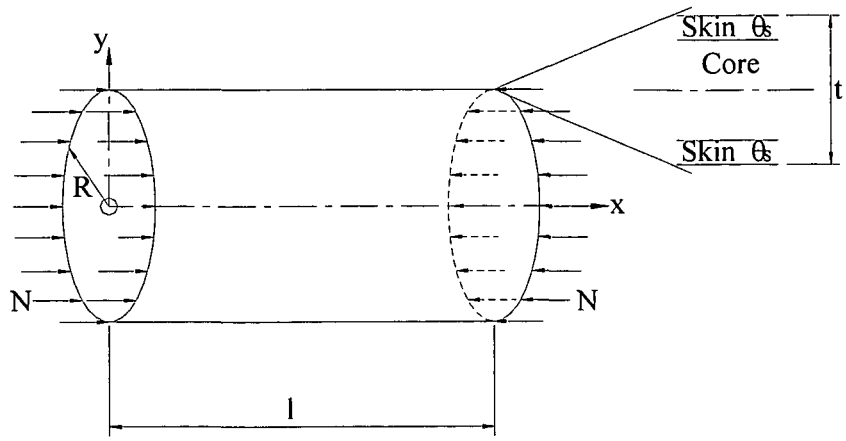

Figure 2-3: Geometry and loading of of cylindrical shell

The thickness of a sandwich panel is given by $t = 2t_s + t_c$, the mass by $W = ab(2t_s\rho_s + t_c\rho_c)$, and the cost, (which should not be confused with C_{ij} in Eqn. (1.25, 1.26)), $C = ab(2t_s\rho_s P_s + t_c\rho_c P_c)$ where P_i is the cost per unit mass of the skin and core materials.

2.6.2 Optimal design problem formulation

For a particular buckling load capacity and cost requirement, together with a choice of skin and core material combinations that results in I candidates, the design optimisation procedure consists of two steps [79]:

Step 1. For each candidate, determine the skin fibre angle θ_s optimally by determining the value of θ_s for which the resulting skin and core thicknesses lead to a minimum candidate mass, viz.

$$W_{i_{\min}} = \min_{\theta_s} W(t_s, t_c),\ 0^o \leq \theta_s \leq 90^o \tag{2.17}$$

subject to

$$N_i \geq N_b \text{ and } C_i \leq C,\ i = 1, 2, .., I \tag{2.18}$$

where N_b is the buckling load capacity required, and C the maximum cost allowable.

Step 2. Select the candidate with least mass [80].

2.6.3 Method of solution

Given that the buckling load is dependant on θ_s, t_s and t_c, and the sandwich cost on t_s and t_c, for a particular design buckling load capacity and cost requirement, t_s and t_c can be determined for any value of θ_s. Thus, a suitable optimisation routine can be used to determine $\theta_{s_{opt}}$. Once $\theta_{s_{opt}}$ and the resultant mass have been determined for each candidate, the least mass option is selected. For the optimisation $\theta_{s_{opt}}$ is determined within a prescribed accuracy of 1^o.

Chapter 3

Results and discussion

3.1 Problem 1: Design of fibre-reinforced laminated composite structures for a maximum combination of torque and inplane load

For the purpose of demonstrating the methodology described, numerical results are given for a typical T300/5208 graphite/epoxy material with properties as in Tables 1.1 and 1.2.

The dependence of F on the fibre angle for both a clamped and simply supported cylindrical shell is given in Figure 3-1, plotted for $P = 2$ x 10^8 N/m (in the clamped case) and $P = 10^9$ N/m (in the simply supported case) while T[1] $= 6.28$ x 10^8 Nm, with $l = 7.5m$, $d = 2m$, $H = 0.01m$, and $K = 8$. Note that *clamped* implies that one end of the shell is completely restrained while the other end is free, and both the inplane load and torque are applied at the free end, whilst *simply supported* implies both ends are simply supported, and half of the torque and inplane load is applied at either end. As can be seen, the optimal fibre orientation (viz. the value of θ that corresponds to minimum F), in the case of the simply supported shell is 90^o, and it is clear that the minimum failure index for a shell can be several times lower than the failure index at other fibre angles. It is evident that $\theta_{opt} = 72.0^o$ in the

[1] A value of $T = \pi d$ x 10^8 is always chosen for the torque loading here, and thus $T = 6.28$ x 10^8 Nm.

case of the clamped shell. It should also be evident that if the fibre orientation is selected optimally, the loading can be maximised.

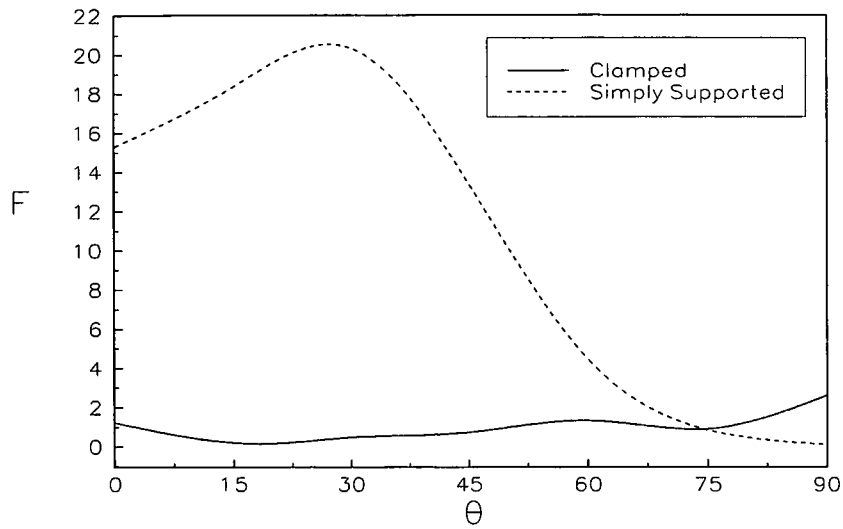

Figure 3-1: Effect of fibre angle on the failure index

Figure 3-2 illustrates the dependance of $P_{F=1}$ (ie. the value of the inplane load for which $F = 1$) on the fibre orientation for the same clamped shell as before, and with $T = 6.28 \text{ x } 10^8$ Nm, $l = 7.5m$, $d = 2m$, $H = 0.01m$, and $K = 8$. Again, it is obvious that $65^o \leq \theta_{opt} \leq 75^o$ and that $P_{\max}$ is approximately 2.1 x $10^8 N/m$. Note that the graph is for $15^o \leq \theta \leq 75^o$ because it is impossible to determine values of P for $F = 1$ at other angles due to the torque loading.

Design optimisation results are now given for shells with different boundary conditions, torque loading, shell length, number of plies and wall thickness.

Example 1. Shells with different boundary conditions

The values of the optimal fibre orientations and maximum inplane loads of the two shells for which trends were given in Figure 3-2/3-3 are shown in Table 3.1. It is obvious that the

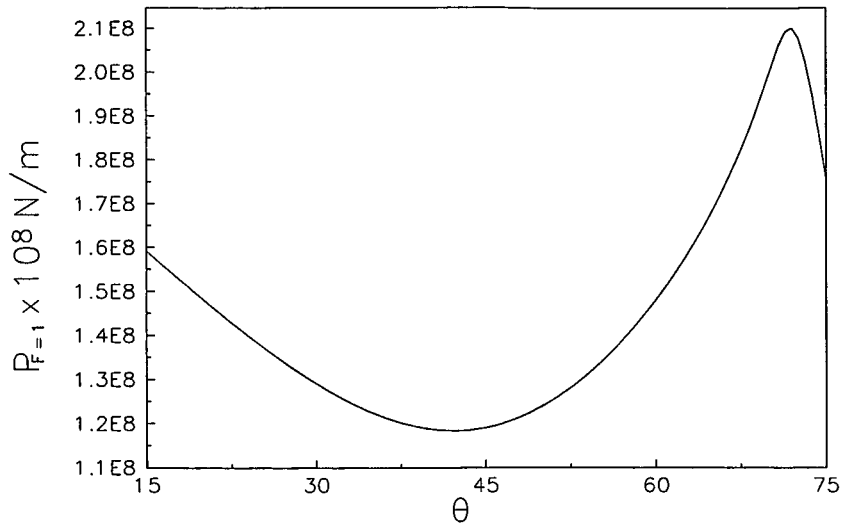

Figure 3-2: Effect of fibre angle on $P_{F=1}$

applied torque and thus the load coupling in the case of the clamped shell has a strength reducing effect (due to the limited degrees of freedom) compared to that of the simply supported shell, evidenced by the large differences in θ_{opt} and $P_{\max}$.

BoundaryCondition	θ_{opt}	$P_{\max}$
Clamped	72.0^o	2.069 x $10^8 N/m$
Simply Supported	90.0^o	2.948 x $10^9 N/m$

Table 3.1: Effect of boundary conditions on the optimal design of shells with $l = 7.5m$, $d = 2m$, $K = 8$, $H = 0.01m$ and $T = 6.28$ x $10^8 Nm$

It should be noted that the value of θ_{opt} and the corresponding magnitude of $P_{\max}$ is independent of the initial choice of P that is used to find θ_{opt} in the first stage of the methodology. Nonetheless, if $P_{\max}/T$ is vastly different to that of $P_{initial}/T$, a fibre angle that appears to be optimal and different in value to θ_{opt} may erroneously result. This is graphically demonstrated in Figure 3-3. The effect of θ on the failure index F is shown for two different values of P for the clamped shell, with $l = 7.5m$, $d = 2m$, $K = 8$, $H = 0.01m$

and $T = 6.28$ x $10^8 Nm$. As can be seen, when $P = 10^8 N/m$, $\theta_{opt} = 18.0^o$, but with $P = 2$ x $10^8 N/m$, the optimal fibre angle is 72.0^o.

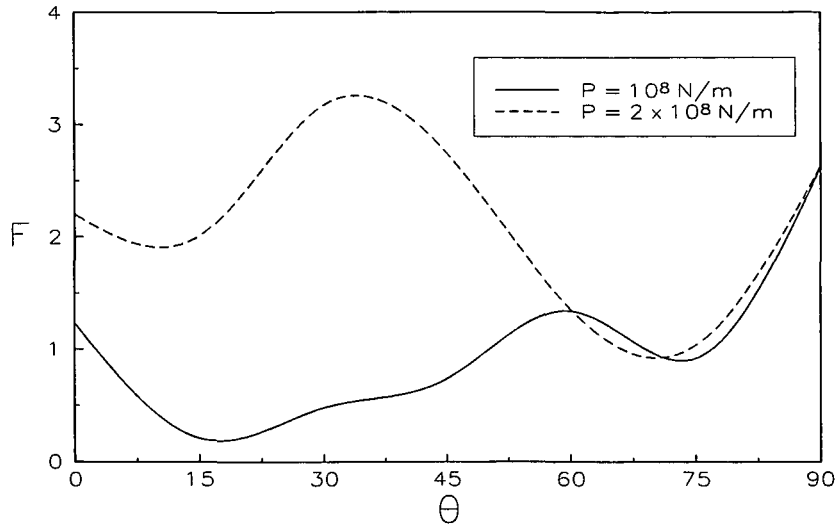

Figure 3-3: Effect of fibre angle on the failure index for different initial choices of P with $T = 6.28$ x $10^8 Nm$

Example 2. Shells with different wall thicknesses

The influence of the wall thickness on the results is shown in Table 3.2. As expected, the allowable inplane load increases as the wall thickness increases. In addition θ_{opt} also gradually increases.

H	θ_{opt}	$P_{\max}$
$0.01m$	72.0^o	2.069 x $10^8 N/m$
$0.025m$	73.0^o	2.790 x $10^8 N/m$
$0.05m$	74.0^o	3.102 x $10^8 N/m$

Table 3.2: Effect of wall thickness on the optimal design of clamped shells with $l = 7.5m$, $d = 2m$, $K = 8$ and $T = 6.28$ x $10^8 Nm$

Example 3. Shells with differing number of layers

The effect of varying the number of layers on the results are given in Table 3.3. $P_{\max}$ is significantly higher for a cylindrical shell with eight layers compared to that with two layers, and this is a result of the bending-twisting coupling effect.

K	θ_{opt}	$P_{\max}$
8	72.0^o	2.069 x $10^8 N/m$
2	68.5^o	1.427 x $10^8 N/m$

Table 3.3: Effect of the number of layers on the optimal design of clamped shells with $l = 7.5m$, $d = 2m$, $H = 0.01m$ and $T = 6.28$ x $10^8 Nm$

Example 4. Shells with different lengths

The influence of the shell length is shown in Table 3.4. The first cylindrical shell has a length of 7.5 metres while the second has a length double that of the first. Although it may have been expected that the shorter shell is capable of carrying a higher inplane load, $P_{\max}$ in either case is not significantly different. This can be explained by the fact that the total strain energy/length ratio in each case is the same.

l	θ_{opt}	$P_{\max}$
$7.5m$	72.0^o	2.069 x $10^8 N/m$
$15m$	72.0^o	2.044 x $10^8 N/m$

Table 3.4: Effect of the length on the optimal design of clamped shells with $d = 2m$, $K = 8$, $H = 0.01m$ and $T = 6.28$ x $10^8 Nm$

3.2 Problem 2: The optimisation of laminated composite structures for minimum mass using the finite element method and genetic algorithms

Results are presented for different load distributions, and various combinations of clamped, simply supported and free boundary conditions are considered. The effect of aspect ratio is also investigated. Initially, the mass of the structure was taken as the GA fitness parameter, but the number of initial genes required for convergence near the global minimum was large, and thus other measures were investigated. Some of these are presented, all demonstrating enhanced efficiency, but introduce problems to the study.

Numerical results are given for a typical T300/5208 graphite/epoxy material. The symmetric plate is constructed of eight layers, viz. $[\theta_1/\theta_2/\theta_3/\theta_4 \parallel t_1/t_2/t_3/t_4]_s$, and is subjected to a uniformly distributed load (UDL) over the entire surface. As already mentioned, the set of fibre orientations available to be used here is $(0^o, \pm 30^o, \pm 45^o, \pm 60^o, 90^o)$, while the set of layer thicknesses is $(0.00075m, 0.001m, 0.00125m, 0.0015m, 0.00175m, 0.002m, 0.00225m)$, leading to a total of $8^4.7^4 = 9834496$ possible design candidates (chromosomes). For expedience, the thickness values will be discussed in terms of their millimeter equivalents; viz. $0.00225m$ will be reported as 2.25. Different combinations of free (F), simply supported (S) and clamped (C) boundary conditions are implemented at the four edges of the plate. In particular, five different combinations are studied, namely, (F,S,F,S), (F,S,C,S), (S,S,S,S) and (C,S,C,S), where the first letter refers to the first plate edge, and the others follow in the anti-clockwise direction.

Boundary condition	layup (thickness values in mm)	W (kg)	F
(F,S,F,S)	$(0^o/0^o/0^o/0^o \parallel 1/1/1/1)_s$	12.8	1
(F,S,C,S)	$(0^o/90^o/0^o/90^o \parallel 1.5/1.75/1.75/1.75)_s$	21.6	0.94
(S,S,S,S)	$(45^o/-45^o/45^o/-45^o \parallel 0.75/1.5/1.5/0.75)_s$	14.4	1
(C,S,C,S)	$(90^o/90^o/0^o/0^o \parallel 0.75/0.75/1/1)_s$	11.2	0.92
(C,C,C,C)	$(0^o/90^o/0^o/90^o \parallel 0.75/2/0.75/0.75)_s$	13.6	0.98

Table 3.5: Effect of boundary conditions on the optimal layup for plates with $a/b = 1$ and UDL $= 100kPa$

Table 3.5 shows the influence of the boundary conditions on the optimal design of a plate with $a/b = 1$ (viz. each side is $1m$ long). Note that F is the value of the Tsai-Wu failure index for each design. Generally, one might expect that as the degrees of freedom are increased, so the mass should increase, but this is not true for the (C,S,C,S) and (F,S,C,S) plates, owing to the minimal number of variables (and thus appropriate combinations that lead to a low mass) available.

3.2.1 Improving the efficiency of the technique

In order to obtain the results given in Table 3.5, at least 60 parent chromosomes were necessary, and generally, at least 20 iterations were required in each case to produce the best design. To improve the efficiency of the technique, a few alternative fitness formulations were investigated. Two are briefly described next.

Alternative 1. P = W.F

Since it is desirable to drive down both the mass and failure index as quickly as possible so that convergence to a global optimal design that meets the failure criterion is achieved efficiently (ie. with a minimum number of parents and generations), the first alternative fitness parameter that was considered was a product of the two, which generally worked very well (viz. the design problem becomes one of minimising P). In many cases, as few as 40 parents (that must be carefully chosen) could be used, and in addition, because of the formulation, it was not necessary to dispose of any genes (design candidates) that did not meet the failure criterion, as long as the final result did. Unfortunately, other problems were introduced by the new fitness formulation. If P was used to select the best design candidate from the list of alternatives after convergence was obtained, sometimes a gene having a greater mass but a fitness value of less than another gene with less mass resulted. Thus, after convergence, it is important to select the best gene from the list based on mass only (after making sure that it complies with the failure criterion).

Table 3.6 shows the influence of the aspect ratio on the optimal layup and thickness for (F,S,C,S) plates with the same loading as before. The results in this table were generated

using the fitness parameter $P = W.F$. As expected, as the aspect ratio increases, so the mass increases. For the plates with aspect ratios of 1.5 and 2, very few candidates had a failure index of 1 or below. Therefore the choice of optimal candidates was minimal.

a/b	layup (thickness values in mm)	W (kg)	F
0.5	$(0^o/45^o/-45^o/90^o \mid\mid 0.75/0.75/0.75/1.25)_s$	5.6	0.88
0.75	$(0^o/90^o/0^o/90^o \mid\mid 0.75/1/1.25/1.75)_s$	11.4	1
1	$(0^o/90^o/0^o/90^o \mid\mid 1.5/1.75/1.75/1.75)_s$	21.6	0.94
1.5	$(60^o/-60^o/60^o/-60^o \mid\mid 2/2/2.25/2.25)_s$	40.8	1
2	$(90^o/60^o/-45^o/60^o \mid\mid 2/2.25/2.25/2.25)_s$	56	0.99

Table 3.6: Effect of aspect ratio on the optimal layup for (F,S,C,S) plates with UDL = $100kPa$

Alternative 2. P = W-F

Because of the problem introduced by the first alternative design formulation, a second was considered. By reformulating the fitness as $P = W - F$ (viz. the design problem is still one of minimising P, but now P can be negative), the frequency with which the problem occurred reduced, but still remained. Nonetheless, as before, as few as 40 parents could be used, and convergence often took place within 4 or 5 generations.

a/b	Load type	layup (thickness values in mm)	W (kg)	F
1	Patch	$(0^o/45^o/-45^o/90^o \mid\mid 0.75/0.75/1/0.75)_s$	10.4	0.85
1	UDL	$(0^o/90^o/0^o/90^o \mid\mid 1.5/1.75/1.75/1.75)_s$	21.6	0.94
2	Patch	$(0^o/0^o/90^o/90^o \mid\mid 0.75/0.75/0.75/1.5)_s$	24	0.83
2	UDL	$(90^o/60^o/-45^o/60^o \mid\mid 2/2.25/2.25/2.25)_s$	56	0.99

Table 3.7: Effect of load type on the optimal layup for square (F,S,C,S) plates, and load magnitude of $100kPa$

Table 3.7 shows the effect of a patch load (which covers only a quarter of the surface) for (F,S,C,S) plates with $a/b = 1$ and $a/b = 2$. The results in this table were generated using the fitness parameter $P = W - F$. As can be seen, the mass of the plates with patch loads (viz. with 1/4 of the total load of the UDL plates) is about half that of the UDL plates.

3.3 Problem 3: The multiobjective optimisation of laminated composite structures for both minimum mass and deflection using the finite element method and genetic algorithms

Results are presented for different load distributions, and various combinations of clamped, simply supported and free boundary conditions are considered. The effect of aspect ratio is also investigated. The weighted sum of both the mass and deflection of the structure was taken as the GA fitness parameter. By using a multiobjective approach, the weighting can be modified to suit the designers requirements. The results presented are for an equally weighted mass and deflection.

Numerical results are given for a typical T300/5208 graphite/epoxy material. The symmetric plate is constructed of eight layers, viz. $[\theta_1/\theta_2/\theta_3/\theta_4 \parallel t_1/t_2/t_3/t_4]_s$, and is subjected to a uniformly distributed load (UDL) over the entire surface. As already mentioned, the set of fibre orientations available to be used here is $(0^o, \pm 30^o, \pm 45^o, \pm 60^o, 90^o)$, while the set of layer thicknesses is $(0.00075m, 0.001m, 0.00125m, 0.0015m, 0.00175m, 0.0025m, 0.00225m)$, leading to a total of $8^4.7^4 = 9834496$ possible design candidates (chromosomes). For expedience, the thickness values will be discussed in terms of their millimeter equivalents; viz. $0.00225m$ will be reported as 2.25. Different combinations of free (F), simply supported (S) and clamped (C) boundary conditions are implemented at the four edges of the plate. In particular, five different combinations are studied, namely, (F,S,F,S), (F,S,C,S), (S,S,S,S), (C,S,C,S) and (C,C,C,C), where the first letter refers to the first plate edge, and the others follow in the anti-clockwise direction.

Boundary condition	layup (thickness values in mm)	W (kg)	F	w (m)
(F,S,F,S)	$(0^o/0^o/0^o/0^o \parallel 1/1/1/1)_s$	12.8	1	0.174
(F,S,C,S)	$(0^o/90^o/0^o/90^o \parallel 2.25/2.25/1.5/0.75)_s$	21.6	0.99	0.053
(S,S,S,S)	$(45^o/-45^o/45^o/-45^o \parallel 0.75/1.5/1.5/0.75)_s$	14.4	1	0.069
(C,S,C,S)	$(90^o/90^o/0^o/0^o \parallel 1/1/0.75/0.75)_s$	11.2	0.97	0.058
(C,C,C,C)	$(0^o/90^o/0^o/90^o \parallel 0.75/2/0.75/0.75)_s$	13.6	0.98	0.032

Table 3.8: Effect of boundary conditions on the optimal layup for plates with $a/b = 1$, $UDL = 100kPa$ and $P = 0.5W^* + 0.5w^*$

Table 3.8 shows the influence of the boundary conditions on the optimal design of a plate with $a/b = 1$ (viz. each side is $1m$ long) and with an applied uniformly distributed load of $100kPa$. Note that F is the value of the Tsai-Wu failure index for each design and that candidates with failure indices greater than one are discarded. Generally, one might expect that as the degrees of freedom are increased, so the mass should increase, but this is not true for the (C,S,C,S) and (F,S,C,S) plates, owing to the minimal number of variables (and thus appropriate combinations that lead to a low mass) available.

a/b	layup (thickness values in mm)	W (kg)	F	w (m)
0.5	$(0^o/0^o/0^o/0^o \mid\mid 1/1/1/1)_s$	6.4	0.90	0.011
0.75	$(0^o/90^o/0^o/90^o \mid\mid 1.25/1.25/1.25/1.25)_s$	12	0.92	0.042
1.0	$(0^o/90^o/0^o/90^o \mid\mid 2.25/2.25/1.5/0.75)_s$	21.6	0.99	0.053
1.5	$(60^o/-60^o/60^o/-60^o \mid\mid 2/2/2.25/2.25)_s$	40.8	1	0.111
2	$(90^o/60^o/-45^o/60^o \mid\mid 2/2.25/2.25/2.25)_s$	56	0.99	0.152

Table 3.9: Effect of aspect ratio on the optimal layup for (F,S,C,S) plates with UDL = $100kPa$, $P = 0.5W^* + 0.5w^*$

a/b	Load Type	layup (thickness values in mm)	W (kg)	F	w (m)
1	UDL	$(0^o/90^o/0^o/90^o \mid\mid 2.25/2.25/1.5/0.75)_s$	21.6	0.99	0.053
1	Patch	$(0^o/30^o/-45^o/90^o \mid\mid 0.75/0.75/1.25/1.75)_s$	12	0.67	0.028
2	UDL	$(90^o/90^o/0^o/0^o \mid\mid 2.25/2.25/2.25/2.25)_s$	57.6	1	0.157
2	Patch	$(0^o/30^o/-60^o/45^o \mid\mid 1.25/1.25/1/0.75)_s$	27.2	0.96	0.065

Table 3.10: Effect of load type on the optimal layup for square (F,S,C,S) plates, and load magnitude of $100kPa$, $P = 0.5W^* + 0.5w^*$

Table 3.9 shows the influence of the aspect ratio on the optimal layup and thickness for (F,S,C,S) plates with the same loading as before. The design index, P, uses an equal weighting for both mass and deflection (ie. $\mu_1 = \mu_2 = 0.5$). As expected, as the aspect ratio increases, so the mass increases. The most interesting result is that for the smallest plate, where almost any arrangement of fibre angles would suffice when used with the choice of layer thicknesses shown, without failure occurring. The combination shown in the table yields the least F.

Table 3.10 shows the effect of a patch load (which covers only a quarter of the surface) for (F,S,C,S) plates with $a/b = 1$ and $a/b = 2$. The design index is again formulated with an equal weighting for both mass and deflection (ie. $\mu_1 = \mu_2 = 0.5$). As can be seen, the mass of the plates with patch loads (viz. with 1/4 of the total load of the UDL plates) is about half that of the UDL plates.

3.4 Problem 4: A simple self-design methodology for laminated composite structures for minimum mass

In order to illustrate the methodology, two simple plate examples are discussed. Consider a symmetrically laminated rectangular plate of length a, width b and thickness h under a transverse bending load $q(x,y)$, as shown in Figure 3-4. The plate is located in the $x-y$ plane and constructed of an arbitrary number K of orthotropic layers of thickness h and fibre orientation θ_k where $k = 1, 2, ..., K$. Different combinations of free (F), simply supported (S) or clamped (C) boundary conditions are implemented at the four edges of the plate. In particular, two different combinations are studied, namely, (F,S,C,S) and (C,C,C,C), where the first letter refers to the first plate edge, and the others follow in the anti-clockwise direction.

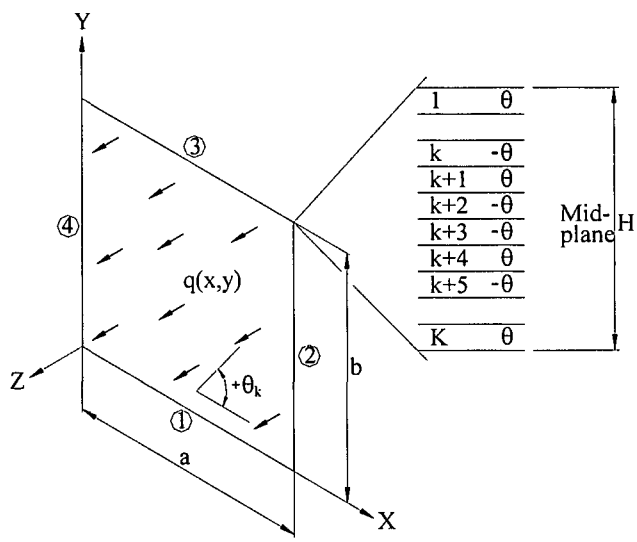

Figure 3-4: Geometry and loading of plate

The first example is a square ($a = b = 1m$) composite plate with (C,C,C,C) boundary conditions, a single 0^o layer, a thickness of $0.01m$ and a point load of 20 kN applied as shown in Figures 3-5. The plate is constructed from a typical T300/5208 graphite/epoxy. The mesh density chosen was 8 x 8 square elements, which proved adequate in convergence

testing. In addition, this density ensured that a node was in the correct position to allow the point load to be correctly located. The formulation of the composite element used was based on Mindlin theory. After the FEA was completed with the virgin plate, the value of the maximum Tsai-Wu failure index was reported as 0.9. The self-design methodology was executed, and the effect after 10, 20, 30 and 40 iterations is shown in Figures 3-6 to 3-9. Note that spaces with crosses in them highlight areas that have been removed, and this has been done to aid clarity where necessary. The process was complete after 47 iterations, and the end result was the same as shown in Figure 3-9. The maximum failure index upon completion was 0.986, and the weight saving was 39%. Finally, to check the integrity of the mesh, the geometry was remeshed with 335 elements. The difference in the result was 3.3%, but it should be noted that, practically, a finer mesh should have been used to begin with.

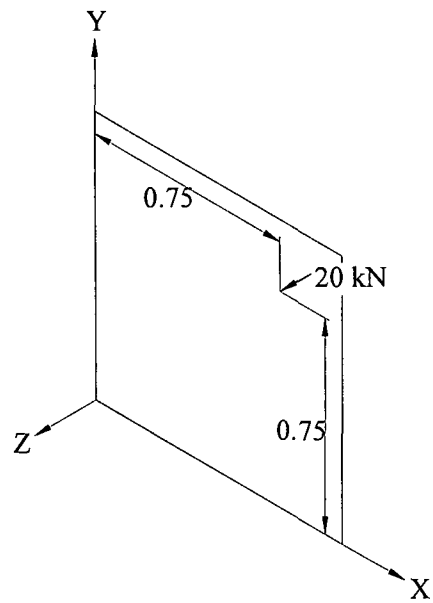

Figure 3-5: Geometry and loading of plates

The second example is also a square plate with $a = b = 1m$, and $H = 0.01m$, but having 8 symmetric layers with $(0^o/45^o/-45^o/90^o)_s$ and (F,S,C,S) boundary conditions (which implies that the first edge could be removed). The point load of 20 kN is in the same place as before. The same number of elements was used in modelling this plate, and the virgin

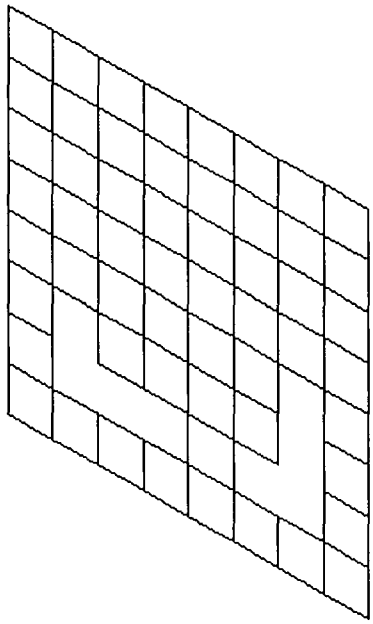

Figure 3-6: Effect of self-design methodology after various stages for square (C,C,C,C) plate with single 0^o layer after 10 iterations.

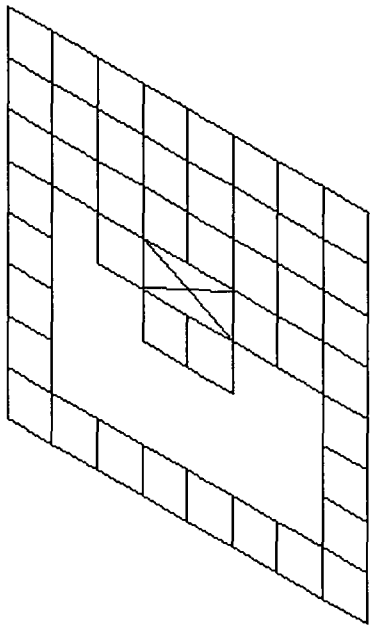

Figure 3-7: Effect of self-design methodology after various stages for square (C,C,C,C) plate with single 0^o layer after 20 iterations.

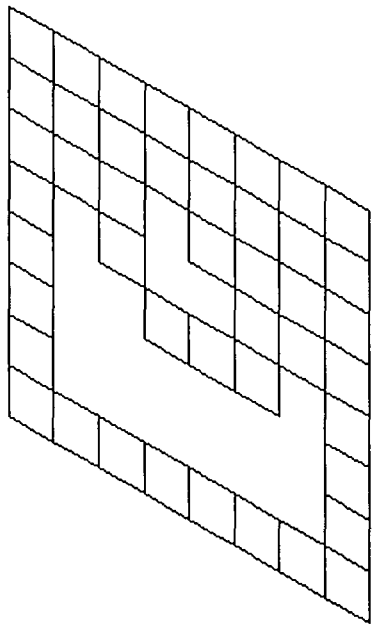

Figure 3-8: Effect of self-design methodology after various stages for square (C,C,C,C) plate with single 0^o layer after 30 iterations.

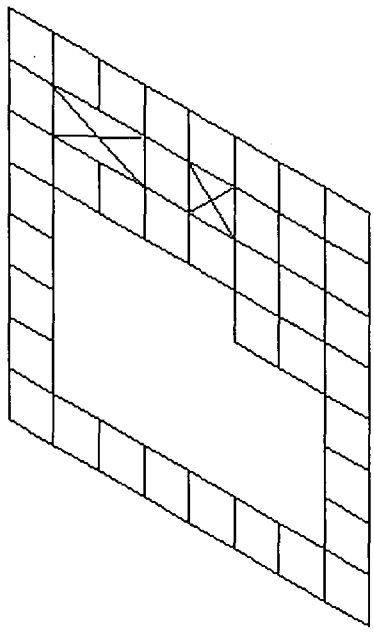

Figure 3-9: Effect of self-design methodology after various stages for square (C,C,C,C) plate with single 0^o layer after 40 iterations.

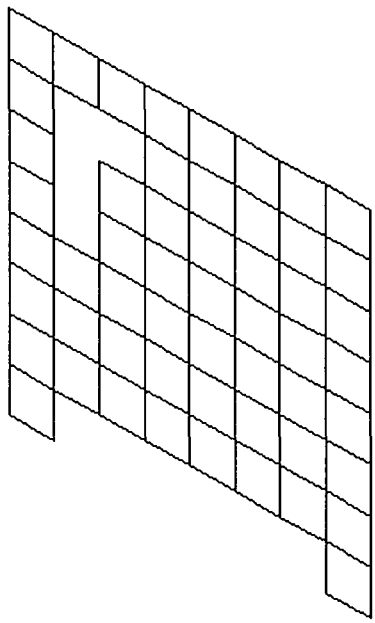

Figure 3-10: Effect of self-design methodology after various stages for square (F,S,C,S) plate with $(0^o/45^o/-45^o/90^o)_s$ layup after 10 iterations.

plate had a maximum F value of 0.79. The effect of the self-design methodology after 10, 20, 30 and 40 iterations is shown in Figures 3-10 to 3-13. The process was complete after 43 iterations, and the end result was the same as shown in Figure 3-13. The maximum failure index upon completion was 0.993, and the weight saving was 42%. When the mesh density was increased, the difference in the result was 1.4%. It should be noted that had deflection been an issue, it is easy to include a maximum deflection constraint together with the failure criterion constraint.

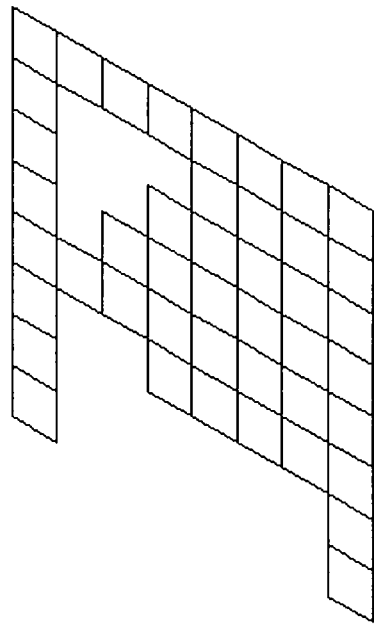

Figure 3-11: Effect of self-design methodology after various stages for square (F,S,C,S) plate with $(0^o/45^o/-45^o/90^o)_s$ layup after 20 iterations.

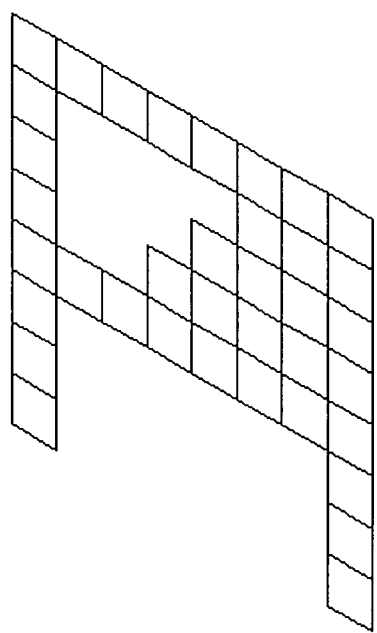

Figure 3-12: Effect of self-design methodology after various stages for square (F,S,C,S) plate with $(0^o/45^o/-45^o/90^o)_s$ layup after 30 iterations.

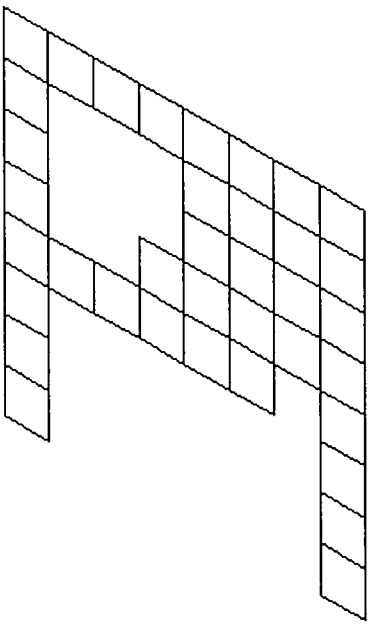

Figure 3-13: Effect of self-design methodology after various stages for square (F,S,C,S) plate with $(0^o/45^o/-45^o/90^o)_s$ layup after 43 iterations.

3.5 Problem 5: The optimal design of composite sandwich panels for minimum cost via the selection of the best material combinations

In order to demonstrate the procedure, results are given for three choices of skin material, viz. T300/5208 Graphite/Epoxy (C), S-2 Glass/Epoxy (G) & Kevlar 49/Epoxy (K), and two core materials, viz. D-100 Balsa (B) & B-2.5 PVC (PVC). Thus, six candidates result from the combinations, viz. C/B, C/PVC, G/B, G/PVC, K/B & K/PVC, where the first letter indicates the skin material, and the second that of the core. The material properties are given in Table 1.1. In this table, the cost factors P_i are calculated as p_i/p_G where p_G is the cost per unit mass of Glass/Epoxy.

Figure 3-14 demonstrates the effect of the choice of the fibre angle of the FRC skins on the resulting cost for each of the six candidates with $a/b = 1.75$, $N_b = 10^6$ N, $W = 50$ kg and $\lambda = 1$. Obviously, all data points on each of the trend lines are design solutions, and

there is a large difference between the cheapest and most expensive of the six candidates. In this particular instance, the best candidate is G/B with $\theta_{s_{opt}} = 0^o$. Table 3.11 gives the optimal values of the skin fibre angles for each of the six candidates along with their respective costs. In addition, the last column gives the ratio of $C_{\min}$ (determined at $\theta_{s_{opt}}$) to $C_{\max}$ (determined at the value of the skin fibre angle that results in the highest cost). In this case, the worst is that for K/B, with $C_{ratio} = 0.896$. This emphasises the need to select θ_s optimally (for each candidate).

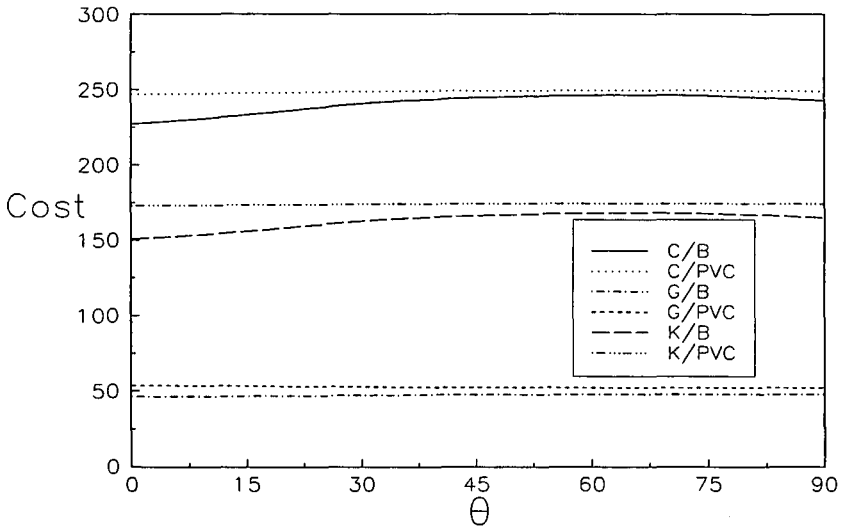

Figure 3-14: Effect of skin fibre angle on the cost of the six candidates

Candidate	$\theta_{s_{opt}}$	$C_{\min}$	C_{ratio}
C/B	0^o	227.1	0.920
C/PVC	0^o	246.8	0.989
G/B	0^o	46.3	0.969
G/PVC	75^o	50.0	0.998
K/B	0^o	150.7	0.896
K/PVC	0^o	172.9	0.991

Table 3.11: Optimal fibre angle and cost of the six candidates, with $a/b = 1.75$, $N_b = 10^6$ N, $W = 50$ kg, and $\lambda = 1$

The influence of the design mass criterion on the choice of the best candidate is shown in Table 3.12 when $a/b = 1.75$, $N_b = 10^6$ N, and $\lambda = 1$. For $W = 100$ kg, 50 kg and 15 kg, the cheapest candidate is G/B. For $W = 5$ kg, the best candidate is C/B, whereafter no design solutions can be found. It can also be seen that $C_{\min}$ and t_s decrease with mass.

W (kg)	Best Candidate	t_s (m)	t_c (m)	$\theta_{s_{opt}}$	$C_{\min}$
100	G/B	0.0138	0.0141	0^o	98.5
50	G/B	0.0058	0.0352	0^o	46.3
15	G/B	0.00008	0.0551	90^o	9.2
5	C/B	0.00006	0.0178	56^o	4.4

Table 3.12: Influence of mass on the results, with $a/b = 1.75$, $N_b = 10^6$ N and $\lambda = 1$

It may be obvious from the above that a designer should set the mass objective to 5 kg when dealing with the loading and plate geometry requirements stated previously, because the candidate that results (C/B) costs the least, but until various mass criterion have been studied, the cut-off point cannot be identified.

Figure 3-15 shows the effect of increasing mass on the ratio t_c/t_s for all six candidates and the same design constraints used for Table 3.12 (viz. $a/b = 1.75$, $N_b = 10^6$ N, and $\lambda = 1$). Generally (except when the mass objective is low), the skin (viz. the higher density material) thickness increases faster than the core thickness. The corresponding costs are shown in Figure 3-16, and it can be seen once again that the cost outcome increases as the mass increases in a generally linear fashion.

Table 3.13 demonstrates the effect of setting $\lambda = 0$ on the results. At $W = 100$ kg, no design solutions that met the criteria could be found, viz. the load requirement (with $\lambda = 0$) is too low / the mass requirement is too high. For $W = 50$, 15 and 5 kg, G/B is the optimal candidate. It is interesting to note that when $W = 50$ kg and 15 kg, the cost of the optimal candidate (viz. G/B) for $\lambda = 1$ (Table 3.12) is less than that when $\lambda = 0$ (Table 3.13).

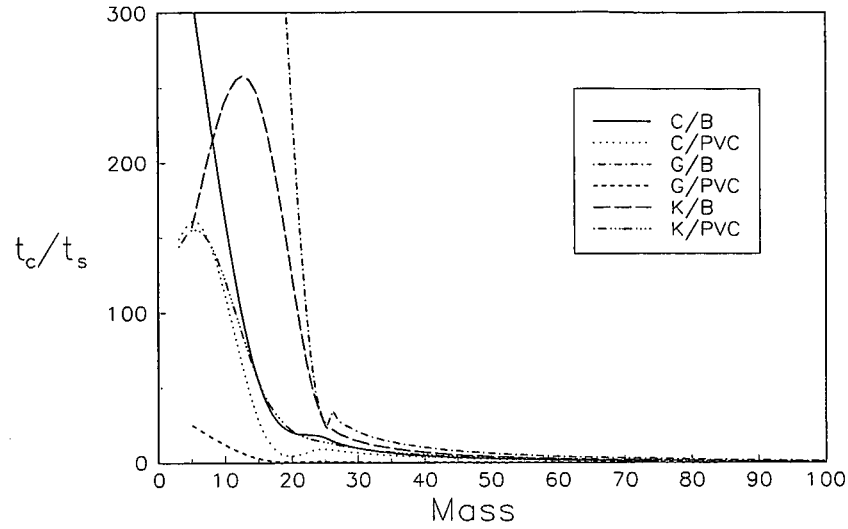

Figure 3-15: Effect of increasing mass on the thickness ratio

W (kg)	Best Candidate	t_s (m)	t_c (m)	$\theta_{s_{opt}}$	$C_{\min}$
100	None	-	-	-	-
50	G/B	0.0063	0.0137	90^o	48.6
15	G/B	0.0007	0.0398	90^o	10.8
5	G/B	0.00006	0.0175	86^o	3.2

Table 3.13: Results for $a/b = 1.75$, $N_b = 10^6$ N and $\lambda = 0$

Table 3.14 shows the difference to the results that a change in the aspect ratio makes. Thus, the results are tabulated for $a/b = 1.0$, $\lambda = 1$ with $N_b = 10^6$ N. At $W = 100$ kg, no design solutions could be found. For $W = 50$ kg, 15 kg and 5 kg, the optimal candidate is once again G/B. Note that in the cases where a solution could be found, $\theta_{s_{opt}}$ is 0^oor 90^o, because the plate is square and the loading symmetric. In addition, the cost of the best candidates when $W = 50$ kg and 15 kg is less than their larger (viz. $a/b = 1.75$) counterparts of Table 3.12, except when the mass objective is 5 kg. In these cases, the core (which is relatively cheaper than the skin material) is thicker for the larger plates in order to carry the applied load.

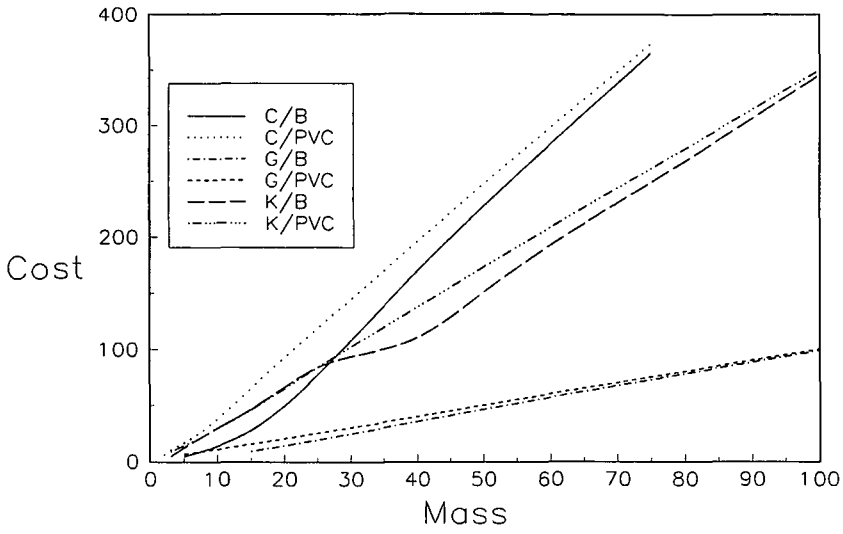

Figure 3-16: Corresponding mass/cost results

W (kg)	Best Candidate	t_s (m)	t_c (m)	$\theta_{s_{opt}}$	$C_{\min}$
100	None	-	-	-	-
50	G/B	0.0122	0.0074	$0^o/90^o$	49.6
15	G/B	0.0023	0.0384	$0^o/90^o$	12.7
5	G/B	0.00005	0.0317	$0^o/90^o$	3.1

Table 3.14: Results for $a/b = 1, N_b = 10^6$ N and $\lambda = 1$

3.6 Problem 6: The optimal design of composite sandwich cylindrical shells for minimum mass via the selection of the best material combinations

In order to demonstrate the procedure, results are given for three choices of skin material, viz. T300/5208 Graphite/Epoxy (C), S-2 Glass/Epoxy (G) & Kevlar 49/Epoxy (K), and two core materials, viz. D-100 Balsa (B) & B-2.5 PVC (PVC). Thus, six candidates result from the combinations, viz. C/B, C/PVC, G/B, G/PVC, K/B & K/PVC, where the first letter indicates the skin material, and the second that of the core. The material properties are given in Table 1.1. In this table, the cost factors P_i are calculated as p_i/p_G where p_G is the cost per unit mass of Glass/Epoxy.

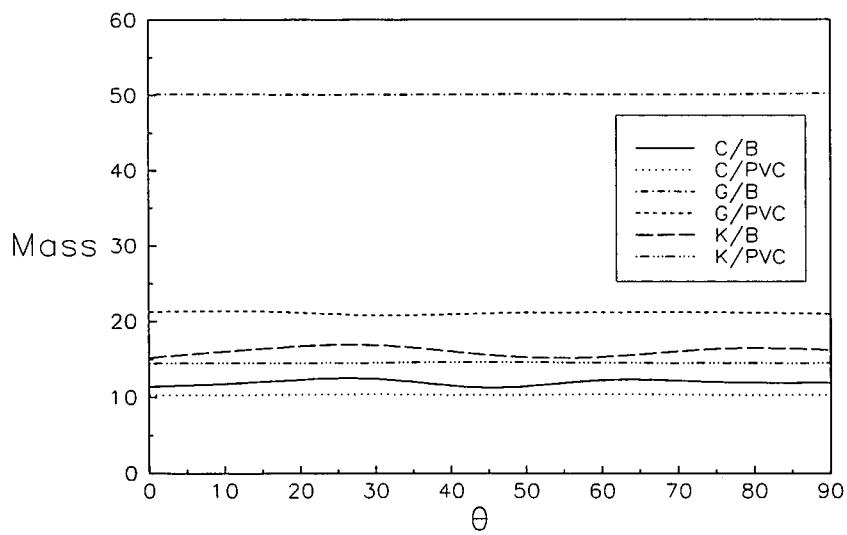

Figure 3-17: Effect of skin fibre angle on the mass of the six candidates

Figure 3-17 demonstrates the effect of the choice of the fibre angle of the FRC skins on the resulting mass for each of the six candidates with $L/R = 1$, $N_b = 10^6$ N and $C = 50$. Obviously, all data points on each of the trend lines are design solutions, and there is a large difference between the lightest and heaviest of the six candidates. In this particular

instance, the best candidate is C/PVC with $\theta_{s_{opt}} = 42°$. Table 3.15 gives the optimal values of the skin fibre angles for each of the six candidates along with their respective masses. In addition, the last column gives the ratio of $W_{\min}$ (determined at $\theta_{s_{opt}}$) to $W_{\max}$ (determined at the value of the skin fibre angle that results in the highest mass). In this case, the worst is that for C/B, with $W_{ratio} = 0.833$. This emphasises the need to select θ_s optimally (for each candidate).

Candidate	$\theta_{s_{opt}}$	$W_{\min}$	C_{ratio}
C/B	$18°$	10.87	0.833
C/PVC	$42°$	10.17	0.974
G/B	$25°$	50.09	0.995
G/PVC	$47°$	20.49	0.929
K/B	$3°$	14.86	0.860
K/PVC	$81°$	14.45	0.989

Table 3.15: Optimal fibre angle and mass of the six candidates, with $R = 1m$, $L = 1m$, $N_b = 10^6$ N and $C = 50$

The influence of the design cost criterion on the choice of the best candidate is shown in Table 3.16 when $L/R = 10$ and $N_b = 10^6$ N. For $C = 200$ the optimal candidate is C/PVC. When the cost is set at 100 the optimal candidate is K/PVC and when the cost is 50 no solutions could be found, viz. the load requirement is too high / the cost requirement is too low. It can be seen that as C decreases, so too does $W_{\min}$.

C	Best Candidate	t_s (m)	t_c (m)	$\theta_{s_{opt}}$	$W_{\min}$ (kg)
200	C/PVC	0.000362	0.002760	$0°$	43.47
100	K/PVC	0.000223	0.004501	$25°$	31.80
50	-	-	-	-	-

Table 3.16: Influence of cost on the results with $R = 1m$, $L = 10m$ and $N_b = 10^6$ N

It may be obvious from the above that a designer should set the cost objective to 100 when dealing with the loading and cylindrical shell geometry requirements stated previously,

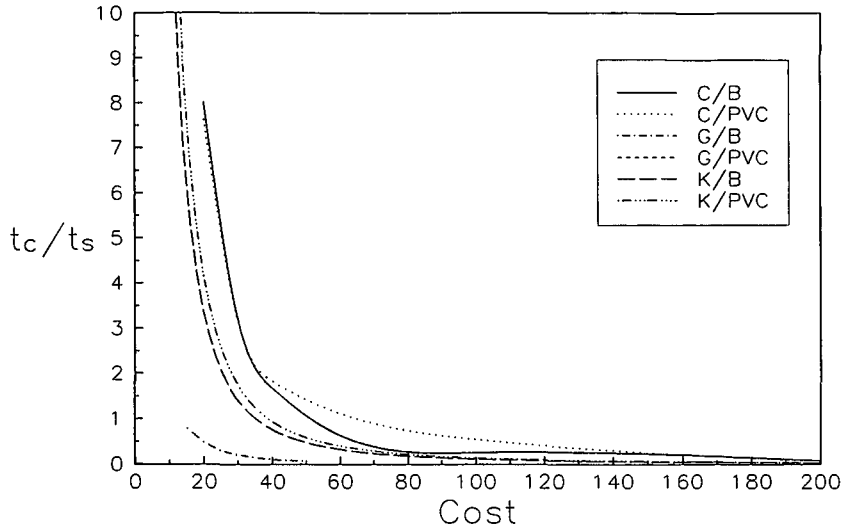

Figure 3-18: Effect of increasing cost on the thickness ratio

because the candidate that results (K/PVC) weighs the least, but until various cost criterion have been studied, the cut-off point cannot be identified.

Figure 3-18 shows the effect of increasing cost on the ratio t_c/t_s for all six candidates and the same design constraints used for Table 3.15 (viz. $L/R = 1$, $N_b = 10^6$ N). The curve for G/PVC has been omitted due to the scale of the graph chosen (viz. the y-axis is limited to $t_c/t_s = 10$). Whereas all the curves show a decreasing thickness ratio with increasing cost, the curve for G/PVC has an increasing trend (for the lowest values of C, t_c/t_s is greater than 10). This is due to the cost factors that were chosen for the analysis. The skins of all of the candidates are more expensive than the corresponding core materials except for that of G/PVC, and thus as the cost constraint increases, so t_c increases while t_s decreases. The corresponding cylinder masses are shown in Figure 3-19, and it can be seen once again that the cost outcome increases as the mass increases in a generally linear fashion.

Table 3.17 shows the influence of cost on the results with $L/R = 5$ and $N_b = 10^6$ N. At $C = 200$ and 100 the optimal candidates are C/PVC. For $C = 50$ the optimal candidate is K/PVC. In general, as the cost constraint increases, so too does t_s and W, while t_c

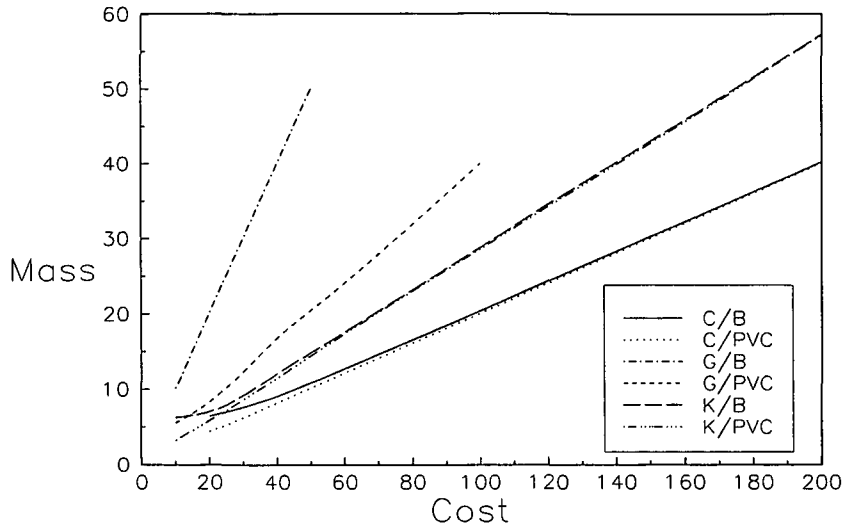

Figure 3-19: Corresponding cost/mass results

decreases.

C	Best Candidate	t_s (m)	t_c (m)	$\theta_{s_{opt}}$	$W_{\min}$ (kg)
200	C/PVC	0.000779	0.001309	66^o	40.82
100	C/PVC	0.000363	0.002768	64^o	21.74
50	K/PVC	0.000223	0.004502	47^o	15.90

Table 3.17: Influence of cost on the results with $R = 1m$, $L = 5m$ and $N_b = 10^6$ N

Table 3.18 shows the influence of cost on the results with $L/R = 1$ and $N_b = 10^6$ N. The optimal candidate is C/PVC for the three cost constraints ($C = 200, 100$ and 50). As for Table 3.17, as the cost constraint increases, so too does t_s and W, while t_c decreases.

C	Best Candidate	t_s (m)	t_c (m)	$\theta_{s_{opt}}$	$W_{\min}$ (kg)
200	C/PVC	0.003975	0.000256	89^o	40.0321
100	C/PVC	0.001982	0.000505	18^o	20.06
50	C/PVC	0.000977	0.001388	42^o	10.17

Table 3.18: Influence of cost on the results with $R = 1m$, $L = 1m$ and $N_b = 10^6$ N

Chapter 4

Conclusions

Fibre-reinforced laminated composites have great advantages over conventional isotropic materials due to their excellent strength and stiffness characteristics combined with low mass. The main disadvantage of using these materials is the associated costs involved with purchasing the raw materials, designing the structure and materials and manufacturing the required components. If these costs could be minimised, laminated composites would certainly increase in popularity.

One method of minimising the cost is through using efficient optimisation techniques during the design phase. If an optimal structure could be designed in minimal time, the costs would decrease. At the same time, the efficiency of the structure could be maximised. This, in turn, leads to reduced life-cycle costs and improved performance. Combining various optimisation techniques with analysis methods such as the FEM is one way to create efficient methodologies for the optimisation of laminated composite structures.

The work presented in this thesis employed various different search routines and optimisation strategies and combined them with design methods, like the FEM, to develop six new methodologies to minimise the mass, deflection and cost, or maximise the load bearing capacity of laminated structures. Four of these procedures were independent of the structure and were tested on simple rectangular plates or cylindrical shells. The fifth and sixth procedures were specific to rectangular sandwich plates (in the fifth case) and cylindrical

sandwich shells (in the sixth case). Each problem that was investigated is summarised below.

Problem 1: *Design of fibre-reinforced laminated composite structures for a maximum combination of torque and inplane load.* A procedure for optimally designing fibre-reinforced laminated composite structures for maximum load carrying capacity was presented to illustrate the methodology. The design variables were the laminae fibre orientations, and once these were optimally selected, the ultimate load the structure could withstand was determined. The finite element method was used in conjunction with a search routine to achieve this, and the finite element formulation implemented here was based on Mindlin laminated plate and shell theory. This approach allows for the inclusion of effects like bending-twisting coupling to be accounted for in the design process. During the first stage of the methodology the structural strength was maximised by selecting the fibre orientations optimally in order to minimise the Tsai-Wu failure index and in the second stage, the maximum load capacity was determined using the Tsai-Wu failure criterion. In order to illustrate the procedure, the design of torque tubes, which were subject to combined torque and inplane compressive loads, were optimised. It should be noted that different finite element formulations, optimisation techniques and failure theories could be selected and should be done so as necessary.

Problem 2: *The optimisation of laminated composite structures for minimum mass using the finite element method and genetic algorithms.* A technique for using genetic algorithms together with finite element analysis to design for manufacture and minimise the mass of fibre-reinforced symmetrically laminated structures with several design variables was described. The design constraint implemented was based on the Tsai-Wu failure criterion, although any suitable one could be substituted. The present study adopts a numerical approach to include the effects of bending-twisting coupling etc., and the finite element formulation used was based on Mindlin theory, although any suitable formulation could be substituted. Composite rectangular plates with eight layers were used to demonstrate the technique. Thus, the four fibre orientations and laminae thicknesses were determined optimally. In addition, the fibre orientations and layer thicknesses were selected from a set of discrete (and commercially available) values. Also, variations of the technique which

enhance efficiency were mentioned.

Problem 3: *The multiobjective optimisation of laminated composite structures for both minimum mass and deflection using the finite element method and genetic algorithms.* A technique for combining genetic algorithms with the finite element method to minimise both the mass and deflection, using a multiobjective approach, of fibre-reinforced structures with several design variables has been described. The design constraint implemented was based on the Tsai-Wu failure criterion, although any suitable one could be substituted. This study adopts a numerical approach to include the effects of bending-twisting coupling, and the finite element formulation used was based on Mindlin theory, although, any suitable formulation could be substituted. Composite symmetrically laminated rectangular plates with eight layers were used to demonstrate the technique. Thus, the four fibre orientations and laminae thicknesses were determined optimally. In addition, the fibre orientations and layer thicknesses were selected from a set of discrete (and commercially available) values. Results were presented for different load distributions, and various combinations of clamped, simply supported and free boundary conditions were considered. The effect of aspect ratio was also investigated. The weighted sum of both the mass and deflection of the structure was taken as the GA fitness parameter. By using a multiobjective approach, the weighting could be modified to suit the designer's requirements. The results presented were for an equally weighted mass and deflection.

Problem 4: *A simple self-design methodology for laminated composite structures for minimum mass.* A simple methodology, based on the finite element method, was presented for the self-design of laminated composite structures. The objective was to minimise the mass, and the design constraint implemented was based on the Tsai-Wu failure criterion, although any suitable one could be substituted. Suitable elements from the finite element model of the structure were deleted until all the elements that could be deleted without affecting the structural (or mesh) integrity had been. In addition, because the study adopted a numerical approach, the effects of bending-twisting coupling etc. were included. The finite element formulation used was based on Mindlin theory, although, any suitable formulation could be substituted. Simple composite rectangular plates with one and eight layers were used to demonstrate the technique and results were presented for plates with (C,C,C,C)

and (F,S,C,S) boundary conditions. In both cases, the average weight saving was 40.5%.

Problem 5: *The optimal design of composite sandwich panels for minimum cost via the selection of the best material combinations.* Optimal designs of sandwich panels with FRC skins and low-density cores for minimum cost were obtained by the use of a procedure described in this study. The objective of the optimisation was to minimise the laminate cost by selecting the skin and core material combination, layer thicknesses and skin fibre angles optimally, subject to load and mass constraints. The procedure consisted of two stages; in the first, the skin and core thicknesses and the skin fibre angles were determined optimally for each candidate. Thereafter, the cheapest candidate was selected. The methodology and its benefits were demonstrated using Graphite, Glass or Kevlar/Epoxy facings, and Balsa or PVC cores. It was shown that the best candidate could be several magnitudes cheaper than the most expensive rival, and that the cost was dependant on the skin fibre angle. The tables of results present the best candidate for different mass constraints under various loading and geometry requirements. In some cases, when the mass constraint was set too high or low, no design solutions could be found. Generally, the G/B candidate appeared to meet most of the design requirements and offer the most cost effective solution. The effect of varying the load ratio and plate aspect ratio on the results was also presented.

Problem 6: *The optimal design of composite sandwich cylindrical shells for minimum mass via selection of the best material combinations.* Optimal designs of sandwich panels with FRC skins and low-density cores for minimum mass were obtained by the use of a procedure described in this study. The objective of the optimisation was to minimise the laminate mass by selecting the skin and core material combination, layer thicknesses and skin fibre angles optimally, subject to load and cost constraints. The procedure consisted of two stages; in the first, the skin and core thicknesses and the skin fibre angles were determined optimally for each candidate. Thereafter, the candidate with least mass was selected. The methodology and its benefits were demonstrated using Graphite, Glass or Kevlar/Epoxy facings, and Balsa or PVC cores. It could be shown that the mass of the best candidate could be several magnitudes lower than the heaviest rival, and that the mass was dependent on the skin fibre angle. The tables of results presented the best candidate for different cost constraints under various loading and geometry requirements. In some cases, when the

cost constraint was set too low, no design solutions could be found. Often, the C/PVC candidate appeared to meet most of the design requirements and offer the best solution. The effect of varying the load ratio and cylindrical shell aspect ratio on the results was also presented.

Bibliography

[1] Gürdal, Z., Haftka, R. T. & Hajela, P. (1999). Design and optimisation of laminated composite materials. Wiley-Interscience, New York.

[2] Tsai, T. W. & Hahn, H. T. (1980). Introduction to composite materials. Technomic Publishing Company. Westport, Connecticut.

[3] Tsai, S. W. & Wu, E. M. (1971). A general theory of strength for anisotropic materials, *Journal of Composite Materials,* **5**, 58 - 80.

[4] Herakovich, C. T. (1998). Mechanics of fibrous composites. John Wiley & Sons, Inc. USA.

[5] Tsai, S. W. & Pagano, N. J. (1968). Invariant properties of composite materials. In *Composite Materials Workshop*, 233 - 253.

[6] Matthews, F. L., Davies, G. A. O., Hitchings, D. & Soutis, C. (2000). Finite element modelling of composite materials and structures. Woodhead Publishing Limited. Cambridge, England.

[7] Cook, R. D. (1995). Finite Element Modelling for Stress Analysis. John Wiley & Sons, Inc., USA.

[8] Jones, R. M. (1975). Mechanics of composite materials, McGraw-Hill, New York.

[9] Nemeth M. P. (1986). Importance of anisotropy on buckling of compression-loaded symmetric composite plates, *AIAA*, **24**, 1831 - 1835.

[10] Gibson R. F. (1994). Principles of Composite Material Mechanics, McGraw Hill, New York.

[11] Vinson, J. R. and Sierakowski, R. L. (1986). The behavior of structures composed of composite materials, Martinus Nijhoff, Dordrecht.

[12] Press, W. H., Teukolsky, S. A, Vetterling, W. T. & Flannery, B. P. (1988). Numerical Recipes in C. Press Syndicate of the University of Cambridge.

[13] Gen. M & Cheng. R. (1997). Genetic algorithms & engineering design. Wiley-Interscience. New York.

[14] Goldberg, D. E. (1989). Genetic algorithms in search optimisation and machine learning. Addison-Wesley Publishing Company, Inc., New York.

[15] Eschenauer, H. A., Koski, J. & Osyczka, A. (1990). Multicriteria design optimization: procedures and applications. Springer, Berlin.

[16] Bull, J. W. & Pitouras, Z. (2001). A review of the self-designing approach on the optimisation of engineering structures. *Proc. Eighth Int. Conf. Civil and Structural Computing*, Eisenstadt, Austria, Paper 96.

[17] Bull, J. W., Christie, W. C., Betress, P. & Fielding, R. (1999). Product optimisation using the concept of self-designing structures. *Design Optimisation, Int. Journ. for Product & Process Improvement*, **1**(2), 220 - 234.

[18] Reynolds, D., Christie, W. C., Betress, P., McConnachie, J., Bull, J. W. (2001). Evolutionary material translation: a tool for the automatic design of low weight, low stress structures. *Int. Journ. Num. Meth. in Eng.*, **50**, 147 - 167.

[19] Bull, J. W., Woodford, C. H., Christie, W. C., Neau, E. & James, M. N. (2000). The low stress design of welded plates using the self-designing structures approach. *Computers & Structures*, **78**, 487 - 496.

[20] Christie, W. C., Bettress, P. & Bull, J. W. (1999). Through depth profiling for reduced stress concentrations of optimal stiffness. *First ASMO UK/ISSMO Conf. on Eng. Design Optimisation*, 111 - 118.

[21] Reynolds, D., McConnachie, J., Bettress, P. Christie, W. C. & Bull, J. W. (1999). Reverse adaptivity - A new evolution tool for structural optimisation. *Int. Journ. Num. Meth. in Eng.*, **45**, 529 - 552.

[22] Zahavi, E. (1992). The finite element method in machine design. Prentice Hall, New Jersey.

[23] Rao, S. R. (1999). The finite element method in engineering. Butterworth-Heinemann, USA.

[24] Adali, S., Summers, E. B. and Verijenko, V. E. (1994). Minimum weight and deflection design of thick sandwich laminates via symbolic computation. *Composite Structures*, **29**(2), 145 - 160.

[25] Hao, B. (2000). Buckling and Postbuckling of soft-core sandwich plates with composite facesheets, *Computational Mechanics*, **25** (5), 421.

[26] Muc, A. & Zuchara, P. (2000). Buckling and failure analysis of FRP faced sandwich plates, *Composite Structures*, **48** (1), 145 - 150.

[27] Hause, T., Johnson, T. F. & Librescu, L. (2000). Effect of face-sheet anisotropy on buckling and postbuckling of sandwich plates, *Journal of spacecraft and rockets*, **37** (3), 331 - 341.

[28] Moh, J. S. & Hwu, C. (1997). Optimisation for buckling of composite sandwich plates, *AIAA*, **35** (5), 863 - 868.

[29] Rikards, R., Barkanov, E., Chate, A. & Korjakin, A. (1997). Modelling, damping analysis and optimisation of sandwich and laminated composite structures, *Pitman Research Notes in Mathematics Series*, Wiley, New York, 374, 149 - 154.

[30] Walker, M., Adali, S. & Verijenko, V. (1996). Optimisation of symmetric laminates for maximum buckling load including the effects of bending-twisting coupling. *Computers & Structures*, **58** (2), 313 - 319.

[31] Lucoshevichyus, R. S. (1976). Minimising the mass of reinforced rectangular plates compressed in two directions in a manner conductive toward stability. *Polymer Mechanics*, **12**, 929 - 933.

[32] Shin, D. K., Gürdal, Z. and Griffin, O. H. (1991). Minimum weight design of laminated plates for postbuckling performance. *Proc. 32nd AIAA/ASME/ASCE/AHS/ASC Structures, Structural dynamics and materials Conf.*, Baltimore, Maryland, 267 - 274.

[33] Vinson, J. R. and Shore, S. (1967). A method for weight optimisation of flat truss-core sandwich panels under lateral loads. *U.S. Naval air engineering centre technical report NAEC-ASL-1111.*

[34] Adali, S., Richter, A., & Verijenko, V. E. (1995). Minimum weight design of symmetric angle-ply laminates under multiple uncertain loads. *Structural Optimisation*, **9**, 89 - 95.

[35] Quian, B., Reiss, R. & Aung, W. (1990). The maximum stiffness design of rectangular symmetric angle-ply laminates, Proc. *2nd Int. Conf. on Computer Aided Design in Composite Material Technology*, Free University of Brussels/Wessex Institute of Technology, computational Mechanics Publications, Southampton, 1990, 451 - 464.

[36] Kam, T. Y. & Chang, R. R. (1992). Optimum layup of thick laminated composite plates for maximum stiffness. *Engineering Optimisation*, **19**, 237 - 249.

[37] Walker, M., Reiss, T. & Adali, S. (1997). Optimal design of symmetrically laminated plates for minimum deflection and weight. *Composite Structures*, **39** (3 - 4), 337 - 346.

[38] Adali, S., Richter, A., Verijenko, V. E. & Summers, E. B. (1995). Optimal design of hybrid laminates with discrete ply angles for maximum buckling load and minimum cost. *Composite structures*, **32**(1-4), 409 - 415.

[39] Adali, S. and Verijenko, V. E. (1997). Minimum cost design of hybrid composite cylinders with temperature dependent properties. *Composite Structures*, **38**(1-4), 623 - 630.

[40] Walker, M., Reiss, T. & Adali, S. (1997). A procedure to select the best material combinations and optimally design hybrid composite plates for minimum weight and cost. *Engineering Optimisation*, **29**, 65 - 83.

[41] Walker, M. & Wilson, M. (1997). The use of Genetic Algorithms and the FEM to optimise laminated structures for maximum rigidity and minimum weight. *Proc. 2nd South African Conf. Applied Mechanics*, 13 - 15 Jan. 1998, 2, 1115 - 1125.

[42] Kogiso, N., Watson, L. T., Gürdal, Z. & Haftka, R. T. (1994) Genetic algorithms with local improvement for composite laminate design. *Structural Optimization*, **7**, 207 - 218.

[43] Sivakumar, K. (1998). Optimum design of laminated composite plates with cutouts using a genetic algorithm. *Composite Structures*, **42** (3), 265.

[44] Haftka, R. & Walsh, J. (1992). Stacking sequence optimisation for buckling of laminated plates by integer programming. *AIAA*, **30**, 814 - 819.

[45] Nagendra, S., Haftka, R. & Gürdal, Z. (1992). Stacking sequence optimization of simply supported laminates with stability and strain constraints. *AIAA*, **30**, 2132 - 2137.

[46] Sadagopan, D. & Pitchumani, R. (1998). Application of genetic algorithms to optimal tailoring of composite materials. *Composites Science and Technology*, **58** (3/4), 571.

[47] Crossley, W. A., Cook, A. M., Fanjoy, D. W. & Venkayya, V. B. (1999). Structural mechanics and materials - Using the two-branch tournament genetic algorithm for multiobjective design, *AIAA*, **37** (2), 261.

[48] Obayashi, S., Yamaguchi, Y. & Nakamura, T. (1997). Multiobjective genetic algorithm for multidisciplinary design of transonic wing planform. *Journal of Aircraft*, **34** (5), 690.

[49] Rudenko, O., Schoenauer, M., Bosio, T. & Fontana, R. (2002). A multiobjective evolutionary algorithm for car front end design. *Lecture notes in computer science*, **2310**, 205 - 218.

[50] Coello Coello, C. A., Christiansen, A. D. & Aguirre, A. H. (1998). Using a new GA-based multiobjective optimisation technique for the design of robot arms. *Robotica*, **16** (4), 401 - 414.

[51] Adali, S., Walker, M. & Verijenko, V. E. (1996). Multiobjective optimisation of laminated plates for maximum prebuckling, buckling and postbuckling strength using continuous and discrete ply angles. *Composite Structures*, **35**, 117 - 130.

[52] Kumar, N. & Tauchert, T. R. (1992). Multiobjective design of symmetrically laminated plates. *Trans. ASME*, **114**, 620 - 625.

[53] Soremekun, G., Gürdal, Z., Kassapoglou, C. & Toni, D. (2002). Stacking sequence blending of multiple composite laminates using genetic algorithms. *Composite Structures*, **56** (1), 53.

[54] Park, J. H., Hwang, J. H., Lee, C. S. & Hwang, W. (2001). Stacking sequence design of composite laminates for maximum strength using genetic algorithms. *Composite Structures*, **52** (2), 217.

[55] Chen, H. P. & Karunaratne, R. (2002). Optimum stacking sequence design of composite laminates using genetic algorithms. *International SAMPE Symposium and Exhibition: [proceedings]*, **47**, 1402-1414.

[56] Kalinnikov, A. E. & Korlyakov, S. V. (1988). Optimization of the stress–strain state of a thick–walled pipe on the basis of Young's modulus of the material. *Problemy Prochnosti*, **2**, 88 – 91. (English translation: Plenum Publishing Corporation).

[57] Walker, M. (1997). Minimum weight design of composite hybrid shells via symbolic computation, *Journal of the Franklin Institute.* **334B**(1), 47 - 56.

[58] Belingardi, G., Genta, G. & Gola, M. (1979). Optimization of orthotropic multilayer cylinders and rotating disks. *AMR (J'Aerotecnica Missili E Spazio)*, **4**, 204 – 209.

[59] Uemura, M. & Fukunaga, H. (1981). Probabilistic burst strength of filament–wound cylinders under internal pressure. *Composite Materials*, 462 – 479.

[60] Fukunaga, H. & Tsu-Wei Chou (1988). On laminated configurations for simultaneous failure. *Composite Materials*, 271 – 286.

[61] Fukunaga, H. & Tsu-Wei Chou (1988). Simplified design techniques for laminated cylindrical pressure vessels under stiffness and strength constraints. *Composite Materials*, 1156 – 1169.

[62] Adali, S., Summers, E. B. & Verijenko, V. (1993). Optimisation of laminated cylindrical pressure vessels under strength criterion. *Composite Structures*, 305 – 312.

[63] Roy, A. K. & Tsai, S. W. (1988). Design of thick composite cylinders, *Journal of Pressure Vessel Technology*, 255.

[64] Byon, O. (1998). Optimizing lamination of hybrid thick-walled cylindrical shell under external pressure by using a genetic algorithm. *Journal Thermoplastic Composite Materials*, **11** (5), 417.

[65] Walker, M., Reiss, T. & Adali, S. (1997). Multiobjective design of laminated cylindrical shells for maximum torsional and axial buckling loads. Computers & Structures. **62** (2), 237.

[66] Gubran, H. B., Singh, S. P. & Gupta, K. (1998). Stresses in composite shafts subjected to unbalance excitation and transmitted torque. *Shock and Vibration Digest.* **30** (5).

[67] Laksami, A. & Benzeggagh, M. L. (2000). Application of Tsai-Wu criterion notched and unnotched composite laminates under torque loading. Journal of Composite Materials. **34** (6). 460 - 478.

[68] Tabakov, P. Y. (2001). Multi-dimensional design optimisation of laminated structures using an improved genetic algorithm. *Composite Structures*, **54** (2), 349.

[69] Adali, S., Richter, A. & Verijenko, V. E. (1995). Multiobjective design of laminated cylindrical shells for maximum pressure and buckling load. *Microcomputers in Civil Eng.*, **10**, 269 - 279.

[70] Walker, M. & Smith, R. E. (2001). A methodology to design laminated composite structures for maximum strength. *Composites Part B.* To appear.

[71] Walker, M. & Smith, R. E. (2002). A technique for using genetic algorithms and finite element analysis to minimise the mass of laminated structures. Submitted to *Finite Elements in Analysis and Design.*

[72] Walker, M. & Smith, R. E. (2003). A procedure for using GAs and the FEM to minimise the weight of composite structures. Accepted for the *Proc. Seventh Int. Conf. The Application of Artificial Intelligence to Civil and Structural Eng.*, Egmond-aan-Zee, The Netherlands.

[73] Ochoa, O. O. & Reddy, J. N. (1992). *Finite Element Analysis of Composite Laminates: Solid Mechanics and its Applications*, Kluwer Academic Publishers, Dordrecht.

[74] Walker, M. & Smith, R. E. (2002). A technique for the multiobjective optimisation of laminated composite structures using genetic algorithms and finite element analysis. To appear in *Composite Structures.*

[75] Walker, M. & Smith, R. E. (2002). A simple self-design methodology for laminated composite structures to minimize mass. Submitted to *Advances in Engineering Software.*

[76] Walker, M. & Smith, R. E. (2003). A simple self-design procedure for laminated composite structures to minimize mass. *Proc. Fourth Int. Conf. Composite Science and Technology, ICCST/4*, Durban, South Africa.

[77] Walker, M. & Smith, R. E. (2002). A computational methodology to select the best material combinations and optimally design composite sandwich panels for minimum cost. *Computers and Structures*, **80**, 1457 - 1460.

[78] Walker, M. & Smith, R. E. (2001). A computational methodology to select the best material combinations and optimally design composite sandwich panels for minimum cost. *Proc. of the 8th Int. Conf. on Civil and Struct. Eng. and Computing*, Eisenstadt, Austria.

[79] Walker, M. & Smith, R. E. A procedure to select the best material combination and optimally design composite sandwich cylindrical shells for minimum mass. Submitted to *Computers & Structures.*

[80] Walker, M. & Smith, R. E. (2002). A methodology to select the best material combinations and optimally design composite sandwich cylindrical shells for least mass. *Proc. of the 6th Int. Conf. on Comp. Struct. Tech.*, Eisenstadt, Austria.